

**PLACE IN RETURN BOX** to remove this checkout from your record.  
**TO AVOID FINES** return on or before date due.  
**MAY BE RECALLED** with earlier due date if requested.

DATE DUE	DATE DUE	DATE DUE

HYDROPEROXIDE SUBSTRATE SPECIFICITY,  
CYCLOOXYGENASE ACTIVATION AND PARTNERING  
BETWEEN THE TWO MONOMERS OF PROSTAGLANDIN  
ENDOPEROXIDE H SYNTHASE

By

Jiayan Liu

A DISSERTATION

Submitted to  
Michigan State University  
in partial fulfillment of the requirements  
for the degree of

DOCTOR OF PHILOSOPHY

Department of Biochemistry and Molecular Biology

2007

## ABSTRACT

# HYDROPEROXIDE SUBSTRATE SPECIFICITY, CYCLOOXYGENASE ACTIVATION AND PARTNERING BETWEEN THE TWO MONOMERS OF PROSTAGLANDIN ENDOPEROXIDE H SYNTHASE

By

Jiayan Liu

The cyclooxygenase (COX) activity of prostaglandin endoperoxide H synthases (PGHSs) converts arachidonic acid and  $O_2$  to prostaglandin  $G_2$  ( $PGG_2$ ). PGHS peroxidase (POX) activity reduces  $PGG_2$  to  $PGH_2$ . The first step in POX catalysis is the formation of an oxyferryl heme radical cation (Compound I). Compound I undergoes intramolecular electron transfer forming Intermediate II with an oxyferryl heme and a Tyr385 radical required for COX catalysis. The PGHS POX is unusual in preferring hydrophobic primary and secondary peroxides but the basis for this specificity is unresolved. The distal surface of the PGHS POX site is open to solvent, except for large hydrophobic amino acids that form a “dome” over part of the heme. This suggested that dome residues facilitate the binding of alkyl hydroperoxides. However, substitutions of dome residues with alanine had no significant effect on Compound I formation from 15-hydroperoxy-eicosatetraenoic acid (15-HPETE) or hydrogen peroxide ( $H_2O_2$ ). Moreover, *ab initio* calculations of heterolytic bond dissociation predicted that the stabilities of the peroxy groups of 15-HPETE and  $H_2O_2$  are the same. Molecular Dynamics simulations suggest that  $PGG_2$  binds the POX site through a peroxy-iron bond, a hydrogen bond with His207 and van der

Waals interactions involving methylene groups adjoining the carbon bearing the peroxyl group and the protoporphyrin IX. We speculate that these latter interactions, which are not possible with H<sub>2</sub>O<sub>2</sub>, are major contributors to PGHS POX specificity.

The distal Gln203 four residues away from His207 has been thought to be essential for stabilizing the transition state in Compound I formation. However, Q203V PGHS mutant catalyzed rapid heterolytic cleavage of 15-HPETE and exhibited native COX activity; whereas, Q203V PGHS showed no spectral intermediate with H<sub>2</sub>O<sub>2</sub>. Thus, we hypothesize that Gln203 is not essential for alkyl hydroperoxide catalysis by PGHS, but may be critical for H<sub>2</sub>O<sub>2</sub>.

PGHSs are homodimers with each monomer having a POX site and COX site. No cross-talk between the POX and COX sites of partner monomers was observed in a heterodimer comprising a Q203R monomer having an inactive POX site and a G533A monomer with an inactive COX site.

*To Yang Long*

## ACKNOWLEDGMENTS

I would like to express my sincere gratitude to my advisor, Dr. William L. Smith, for his patient guidance and generous support throughout these years. His dedication to science, diligence in work and outstanding leadership always inspired me to be the best.

I would like to acknowledge our collaborators Drs. Robert I. Cukier and Steve A. Seibold for their work on modeling enzymatic reactions. It has been a happy scientific and personal experience. I am grateful for their advice and our numerous stimulating discussions. Their beautiful models were instrumental in developing a hypothesis for my thesis project.

I also want to thank all my research committee members, Drs. William L. Smith, Robert I. Cukier, Robert Hausinger, R. Michael Garavito, Honggao Yan and Shelagh M. Ferguson-Miller, for their invaluable suggestions during the course of my doctoral work. I am grateful to them for teaching me the art of critical thinking, writing, and presenting.

I thank all my lab members, past and present, Drs. Chong Yuan, Dmitry Kuklev, Christine Harman, Cynthia DeLong, Masayuki Wada, Holly Hong, Ranjinder Sidhu, Insork Song and Yeon-Joo Kang, Ms. Caroline J Rieke and Katie Mason, Mr. Uri Mbonye and Terry Ball for an active, helpful, creative and friendly atmosphere. Their help with the cell maintenance, protein purification, structure visualization, technique training and lab management is of great value for my research.

I want to extend my gratitude to Drs. David DeWitt, Dave Ballou, Bruce Palfey, Shelagh M. Ferguson-Miller, Yoichi Osawa and their lab members at both Michigan State University and the University of Michigan for their helpful discussions and sharing equipment. I appreciate all my friends at the Michigan State University and the University of Michigan not only for help, but also for their precious friendship. Particularly I would like to thank Bhramara Tirupati for her heartwarming encouragements, brilliant ideas and careful critique of my writings.

I am indebted to my family for teaching me to be mentally strong and independent. And a special thank you for my friend and husband, Yang Long. Without his love, kindness, patience and support, I would never have reached this far.

Life is a journey. For all the love, happiness, excitement, trust, understanding, sympathy, disappointment, frustration and grief that has happened and is yet to come, I am truly grateful.

# TABLE OF CONTENTS

<b>LIST OF TABLES</b>	<b>ix</b>
<b>LIST OF FIGURES</b>	<b>x</b>
<b>LIST OF ABBREVIATIONS</b>	<b>xii</b>
<b>Introduction</b>	<b>1</b>
<b>1 Literature Review</b>	<b>3</b>
1.1 Biology and Enzymology of Prostaglandin Endoperoxide H Synthase (PGHS)	3
1.1.1 Biological Roles of PGHS	3
1.1.2 Reaction Mechanism of PGHS	5
1.2 PGHS Structures	12
1.2.1 Crystal Structures of PGHS-1 and PGHS-2	12
1.2.2 The Structure of the POX Active Site	15
1.2.3 The Structure of the COX Active Site	20
1.3 The COX Activity is Regulated by the POX Reaction	21
1.3.1 Catalytic Mechanism of PGHS COX	21
1.3.2 Tyrosyl Radicals	24
1.3.3 COX Inhibition by NSAIDs	26
1.4 Regulation of PGHS POX by Oxidizing and Reducing Substrates	27
1.4.1 Hydroperoxide Initiates PGHS Reaction	27
1.4.2 Regulation of PGHS Catalysis by Reductants	31
1.4.3 PGHS and Other Peroxidases	32
1.5 Hypothesis	36
<b>2 Hydroperoxide Dome Residues and Substrate Specificity</b>	<b>38</b>
2.1 Introduction	38
2.2 Materials And Methods	40
2.3 Results	46
2.3.1 Hydroperoxide Substrate Specificity of the POX Activity of OvPGHS-1	46
2.3.2 Compound I Formation with Different Hydroperoxides	47
2.3.3 COX Activation by Different Hydroperoxides	54
2.3.4 Mutations of Hydrophobic Residues in the POX Dome	57
2.3.5 Compound I Formation of Fe <sup>3+</sup> -PPIX OvPGHS-1 from Different Hydroperoxides	59
2.3.6 Compound I Formation of Mn <sup>3+</sup> -PPIX OvPGHS-1 from Different Hydroperoxides	60
2.3.7 Cyanide Binding to the POX Active Site	64

2.3.8	COX Activation of OvPGHS-1 by Compound I Formation . . . . .	67
2.4	Discussion . . . . .	68
<b>3</b>	<b>The Role of Q203 in PGHS Peroxidase Catalysis</b>	<b>77</b>
3.1	Introduction . . . . .	77
3.2	Materials and Methods . . . . .	81
3.3	Results . . . . .	83
3.3.1	The POX Activities of Gln203 Mutant OvPGHS-1s . . . . .	83
3.3.2	The Formation of Compound I for Gln203 Mutant PGHSs . . . . .	84
3.3.3	Cyanide Binding to the Active Site . . . . .	85
3.3.4	Product Analysis of Guaiacol Peroxidase Assays . . . . .	86
3.3.5	COX Activation Influenced by Q203V Substitution . . . . .	87
3.4	Discussion . . . . .	89
<b>4</b>	<b>Cross-talk between POX and COX Active Sites of PGHS Homodimer</b>	<b>92</b>
4.1	Introduction . . . . .	92
4.2	Materials and Methods . . . . .	95
4.3	Results . . . . .	96
4.3.1	Construct, Expression and Purification of HuPGHS-2 Homodimers and Heterodimer . . . . .	96
4.3.2	POX Activities of HuPGHS-2 Homodimers and Heterodimer . . . . .	98
4.3.3	COX Activities of HuPGHS-2 Homodimers and Heterodimer . . . . .	98
4.4	Discussion . . . . .	100
<b>5</b>	<b>Conclusions and Future Directions</b>	<b>102</b>
	<b>BIBLIOGRAPHY</b>	<b>105</b>

## LIST OF TABLES

1.1	Alkyl Hydroperoxides Have Higher $k_1$ Values for Compound I Formation	29
2.1	Peroxidase Activities of Native ovPGHS-1 with Different Hydroperoxides	48
2.2	Alkyl Hydroperoxides Have Higher $k_1$ Values for Compound I Formation	53
2.3	Oxygen Consumption and Lag Times in COX Activation . . . . .	56
2.4	Side Chain Substitutions of Hydrophobic Residues in the POX Distal Dome Altered POX Activities . . . . .	58
2.5	Rate Constants for Compound I Formation of Fe <sup>3+</sup> -PPIX OvPGHSs . .	59
2.6	Activities of Fe <sup>3+</sup> - and Mn <sup>3+</sup> -PPIX ovPGHS-1s . . . . .	62
2.7	Rate Constants for Compound I Formation by Mn <sup>3+</sup> -PPIX OvPGHS-1s	64
2.8	Effect of Val291 and Leu294 on CN <sup>-</sup> Binding to the Heme Group of OvPGHS-1 . . . . .	65
2.9	Lag Times and Specific COX Activities of Fe <sup>3+</sup> -PPIX ovPGHS-1s . . . .	67
2.10	Bond Dissociation Energies of Different Hydroperoxides . . . . .	70
3.1	Gln203 Mutations in the PGHS Distal Active Site Altered POX Activities	84
3.2	Rate Constants for Compound I Formation from Q203V Mn <sup>3+</sup> -PPIX OvPGHS-1 . . . . .	85
3.3	Effect of Gln203 on CN <sup>-</sup> Binding to the Heme Group of OvPGHS-1 . .	86
3.4	Lag Times and Specific COX Activities of Gln203 Mutant Fe <sup>3+</sup> -PPIX OvPGHS-1s . . . . .	89

## LIST OF FIGURES

1.1	Pathway of Prostanoid Biosynthesis . . . . .	6
1.2	Proposed Reaction Mechanism of PGHS. . . . .	8
1.3	“Push and pull” Mechanism for PGHS POX Catalysis . . . . .	11
1.4	PGHS Structure. . . . .	14
1.5	Structure of the POX Active Site . . . . .	17
1.6	Comparison of the POX Active Sites of PGHS-1 and PGHS-2 . . . . .	18
1.7	Structure of Heme <i>b</i> . . . . .	19
1.8	Structure of the COX Active Site . . . . .	22
1.9	COX Reaction Mechanism. . . . .	23
1.10	Hydroperoxide Substrate Specificity of PGHS Peroxidase . . . . .	28
2.1	Comparison of Fe- and Mn-PPIX PGHS-I Heme Intermediates . . . . .	48
2.2	POX Activities of Native OvPGHS-1 with Different Hydroperoxides . . . . .	49
2.3	UV/Visible Spectra of Intermediates of Fe-PPIX OvPGHS-1 . . . . .	50
2.4	Kinetic Traces of Fe-PPIX OvPGHS-1 Intermediates . . . . .	51
2.5	Effect of 15-HPETE Concentrations on the Rate Constants for Fe-PPIX OvPGHS-1 Intermediate Formation . . . . .	52
2.6	COX Activation and Lag Time . . . . .	55
2.7	COX Activation by Different Hydroperoxides . . . . .	56
2.8	UV/Visible Spectrum of Mn-PPIX PGHS-1 Intermediates . . . . .	61
2.9	Effect of Hydroperoxide Concentrations on the Rate Constants for Mn- PPIX OvPGHS-1 Intermediate Formation . . . . .	63

2.10	UV/Visible Absorbance of Fe <sup>3+</sup> -PPIX native ovPGHS-1 with CN <sup>-</sup> titration	66
2.11	Molecular Dynamics Simulations with PGG <sub>2</sub> or H <sub>2</sub> O <sub>2</sub>	72
2.12	Surface Model of the POX Active Site.	74
3.1	Proposed Mechanism for the Formation of Compound I.	79
3.2	Gln203 is not Essential for Heterolytic Cleavage of the O-O Bond of 15-HPETE by Fe <sup>3+</sup> -PPIX OvPGHS-1	88
4.1	Models of PGHS-2 Homodimer and Heterodimer	94
4.2	Construct of PGHS-2 Heterodimer and Protein Purification Strategy	97
4.3	Expression and Identification of PGHS-2 Homodimers and Heterodimer	99
4.4	Normalized POX Activities of Native/native, G533A/G533A, Q203R/Q203R and G533A/Q203R HuPGHS-2s	100
4.5	Specific COX Activities of HuPGHS-2 Enzymes	101

## LIST OF ABBREVIATIONS

<b>AA</b>	arachidonic acid
<b>BDE</b>	bond dissociation energy
<b>C<sub>10</sub>E<sub>6</sub></b>	Polyoxyethylene(6)-decyl ether
<b>CcP</b>	cytochrome <i>c</i> peroxidase
<b>COX</b>	cyclooxygenase
<b>CPO</b>	chloroperoxidase
<b>DHA</b>	docosahexaenoic acid
<b>EGF</b>	epidermal growth factor
<b>EPA</b>	eicosapentaenoic acid
<b>EPO</b>	eosinophil peroxidase
<b>ER</b>	endoplasmic reticulum
<b>EtOOH</b>	ethyl hydroperoxide
<b>H<sub>2</sub>O<sub>2</sub></b>	hydrogen peroxide
<b>HETE</b>	hydroxyeicosatetraenoic
<b>His<sub>6</sub></b>	hexa-histidine
<b>HPETE</b>	hydroperoxyeicosatetraenoic acid
<b>HPLC</b>	high performance liquid chromatography
<b>HRP</b>	horseradish peroxidase
<b>hu</b>	human
<b>KETE</b>	keto-eicosatetraenoic acid
<b>LPO</b>	lactoperoxidase
<b>MBD</b>	membrane binding domain

**MOI** multiplicity of infection  
**MP2** Møller-Plesset perturbation method  
**MPO** myeloperoxidase  
**mu** murine  
**NF- $\kappa$ B** nuclear factor kappa B  
**NE** nuclear envelope  
**NSAID** non-steroidal anti-inflammatory drug  
**ov** ovine  
**POX** peroxidase  
**PG** prostaglandin  
**PGHS** prostaglandin endoperoxide H synthase  
**cPLA<sub>2</sub>** phospholipase A<sub>2</sub>  
**PPA** 5-phenyl-4-pentenyl-alcohol  
**PPAR** peroxisomal proliferator activated receptors  
**PPHP** 5-phenyl-4-pentenyl-hydroperoxide  
**PPIX** protoporphyrin IX  
**QM** quantum mechanical  
**ROOH** hydroperoxide  
**ROS** reactive oxygen species  
**SVD** singular value decomposition  
***t*-BuOOH** *t*-butyl hydroperoxide  
**TPO** thyroid peroxidase

## INTRODUCTION

Insights into the mechanisms of inflammation, pain and fever have shed light on our current understanding of lipid biology. Prostaglandin endoperoxide H synthase (PGHS) has emerged as playing a critical role [1, 2]. PGHS generates prostaglandin  $H_2$  ( $PGH_2$ ), from which is derived a group of oxygenated, lipid signaling molecules called prostanoids. These local hormones that include prostaglandins, thromboxanes and prostacyclin, regulate a broad range of physiological functions, as well as being involved in pathophysiologies. There are two PGHS isoforms referred to as PGHS-1 and PGHS-2, both of which are important pharmaceutical targets of non-steroidal anti-inflammatory drugs (NSAIDs). Recent studies indicate that PGs play roles in cardiovascular diseases, brain disorders and tumor formation [3, 4].

Both PGHSs are integral membrane proteins that are embedded in the luminal side of the endoplasmic reticulum (ER) and nuclear envelope (NE) [5, 6, 7, 8, 9]. The expression and degradation of PGHS-2 is controlled differently from PGHS-1 [10, 11]. PGHS-1 is expressed constitutively in nearly all mammalian cells, and is responsible for basal prostanoid synthesis and considered to be a housekeeping gene, except in a few cases (e.g. brain and kidney), PGHS-2 is inducible and is important in replication and differentiation [12].

The formation of  $PGH_2$  involves two different enzymatic functions of PGHS: (a) conversion of arachidonic acid (AA) to prostaglandin  $G_2$  ( $PGG_2$ ) by a cyclooxygenase

(COX) activity and (b) reduction of PGG<sub>2</sub> to PGH<sub>2</sub> by a peroxidase (POX) activity [13, 14, 15]. Both the COX and POX activities depend on a heme prosthetic group in the POX site. PG formation via PGHS-1 or PGHS-2 pathways is differentially modulated perhaps because of their different sensitivities to cellular hydroperoxide levels [16]. Subcellular compartments are enriched in enzyme or reactive oxygen species (ROS) derived hydroperoxides [17, 18]. Investigations of the regulation of PGHS activity by hydroperoxides is of both theoretical and practical interests. I have used mutagenic and kinetic approaches to gather information on the hydroperoxide requirements for PGHS functions.

My dissertation research has focused on determining the structural basis for the unique hydroperoxide substrate specificity of PGHS-1 and the influence of different hydroperoxide initiators on COX activation. I have characterized the role of hydrophobic residues on the distal surface of the POX heme group in alkyl hydroperoxide catalysis. In addition, I have evaluated the importance of distal glutamine 203 in PGHS POX catalysis; the results are important in understanding how mammalian POXs function. Finally, my work has explored the putative relationship between the POX and COX sites on the two monomers comprising a PGHS homodimer.

# Chapter 1

## Literature Review

### 1.1 Biology and Enzymology of Prostaglandin Endoperoxide H Synthase (PGHS)

#### 1.1.1 Biological Roles of PGHS

The introduction of aspirin or acetylsalicylic acid in the late nineteenth century was a landmark in the modern pharmaceutical industry. Aspirin, along with other non-steroidal anti-inflammatory drugs (NSAIDs), has analgesic, antipyretic and anti-inflammatory functions. Recently it was also found to be anti-thrombogenic. All of these functions are related to the inhibition of protein targets called prostaglandin endoperoxide H synthases (PGHSs, also well known as cyclooxygenases or COXs) [19].

PGHSs catalyze the committed step in the formation of an important class of lipid mediators called prostanoids [1]. Prostanoids, including prostaglandins, throm-

boxanes and prostacyclins originated from  $\omega$ 3- or  $\omega$ 6- $C_{20}$  and  $C_{22}$  polyunsaturated fatty acids which are mobilized from the sn-2 position of glycerophospholipids by cytosolic phospholipase  $A_2$  (cPLA<sub>2</sub>) and secretory PLA<sub>2</sub> (sPLA<sub>2</sub>). Different prostanoids are formed in a cell-type specific fashion, and their release from cells is transporter dependent [2]. They are autocrine and paracrine hormones involved in inflammatory and anaphylactic reactions (prostaglandins), vasoconstriction (thromboxanes) and the resolution phase of inflammation (prostacyclins).

There are two PGHS isoforms, PGHS-1 and PGHS-2, both of which are of considerable interest for their physiological and pathological roles. PGHS-1 and PGHS-2 act coordinately in homeostasis, inflammation, gastric ulceration and carcinogenesis [12]. They also play unique roles in distinct physiological pathways and disease development. PGHS-1 is responsible for platelet aggregation and parturition. PGHS-2 is mainly involved in reproduction, inflammation, pain, fever, various cancers and Alzheimer's disease.

Immunocytochemical approaches have revealed that PGHS-1 and PGHS-2 are both located on the luminal side of endoplasmic reticulum (ER) and nuclear envelope (NE) in murine NIH 3T3 cells, human monocytes and human umbilical vein endothelial cells [5, 6, 7, 8, 9]. A similar distribution of PGHS-1 and PGHS-2 is also shown in subcellular fractions. The expression and degradation of the two isoforms are differentially regulated [10, 11]. PGHS-1 exists constitutively in most cells. Like many housekeeping genes, the PGHS-1 gene does not contain a TATA box in the promoter region[20]. It is induced early in development and PGHS-1 mRNA is stable. PGHS-1 protein levels are relatively constant level in cells in which the enzyme is expressed.

Upregulation of PGHS-1 is required in reproduction and immune cell differentiation [21, 22, 23]. PGHS-2 is expressed in a rapid and transient manner. The primary sequences of PGHS-1 and PGHS-2 are 60% identical. A unique 19-amino acid cassette near to the C terminus of PGHS-2 appears to be one of the most significant differences determining the different protein stabilities of the two isoforms in cells [24]. This polypeptide was identified to be critical in mediating ER-associated degradation of PGHS-2. Constitutively expressed PGHS-2 is essential for normal functions of brain and kidney as suggested by immunostaining and studies with PGHS-2 knockout mice, respectively [25, 26].

### 1.1.2 Reaction Mechanism of PGHS

Most of our current understanding of the catalytic mechanism comes from extensive studies on PGHS-1, the isoform first isolated in the mid-1970s from bovine and ovine vesicular glands [13, 14, 15]. PGHS-2 was discovered in the early 1990's. Both isoforms are bi-functional, heme-containing proteins, catalyzing the same transformation of AA to  $\text{PGH}_2$  via two enzymatic reactions (Fig. 1.1). A COX activity converts one molecule of arachidonic acid and two molecules of oxygen to a hydroperoxide intermediate  $\text{PGG}_2$ , and the POX activity reduces the hydroperoxyl group of  $\text{PGG}_2$  to  $\text{PGH}_2$  which is the precursor of downstream prostanoids.

The POX can operate *in vitro* independent of the COX. In contrast, the COX of PGHS is driven by a protein-based radical formed during the reaction of hydroperoxide with the heme in the PGHS POX site [27]. This protein radical is located on a ty-

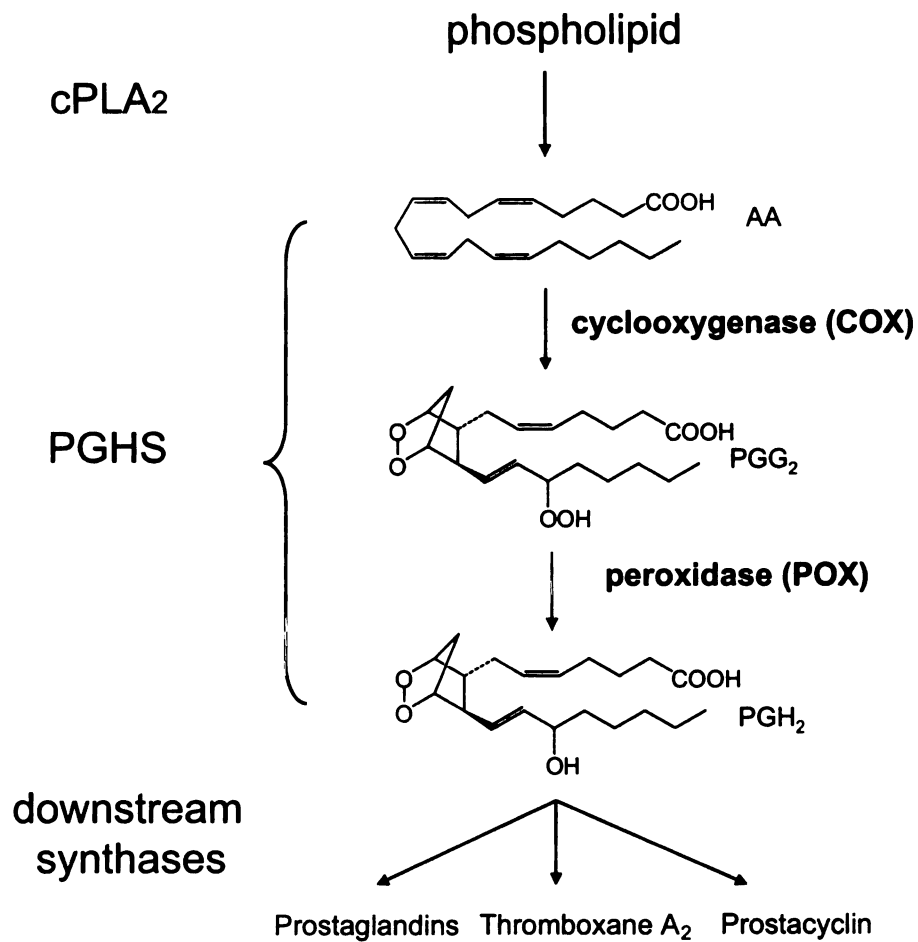


Figure 1.1: **Pathway of prostanoid biosynthesis.** PGHS catalyzes the committed step of prostanoid formation from arachidonic acid, involving the COX and POX reactions. This diagram is adapted from [1].

rosine. Ruf and coworkers detected an intermediate with a low spin ferryl state ( $S=1$ ) after mixing PGHS-1 with PGG<sub>2</sub> or AA [28]. It was later recognized as tyrosine 385 radical in a species called Intermediate II [29, 28]. Intermediate II is spectroscopically similar to Compound II of horseradish peroxidase (HRP) [30, 31, 32, 33]. Derivation of Intermediate II of PGHS results in a spectroscopic analog of Intermediate ES of cytochrome *c* peroxidase (CcP) [34, 35].

PGHS catalysis involves a branched chain mechanism linking the POX and COX activities (Fig. 1.2). The overall reaction is initiated by the reduction of hydroperoxide in the PGHS POX active site. The peroxidase containing a ferric protoporphyrin IX (Fe<sup>3+</sup>-PPIX or heme *b*) co-factor reduces a hydroperoxide to an alcohol. An oxyferryl intermediate, Fe<sup>4+</sup>=O coupled with a porphyrin radical  $\pi$ -cation (Fe<sup>4+</sup>=O PPIX<sup>•+</sup>), is referred to as Compound I. Compound I is two oxidative equivalents above the resting enzyme. Compound I can either be reduced by endogenous or exogenous reductants to an oxyferryl heme form containing Compound II, or it can undergo intramolecular reduction, involving transfer of an electron from Tyr385, forming a Compound II-like spectral intermediate and a tyrosyl radical. This latter complex is designated as Intermediate II. When AA is present in the COX site, the tyrosyl radical removes a hydrogen atom from C13 of AA, triggering a di-oxygenation reaction [36]. Intermediate II is regenerated within the COX site when PGG<sub>2</sub> is produced and released from the COX site.

The O-O bond of hydroperoxides can undergo either homolytic or heterolytic cleavage as depicted in Equations 1.1 and 1.2.

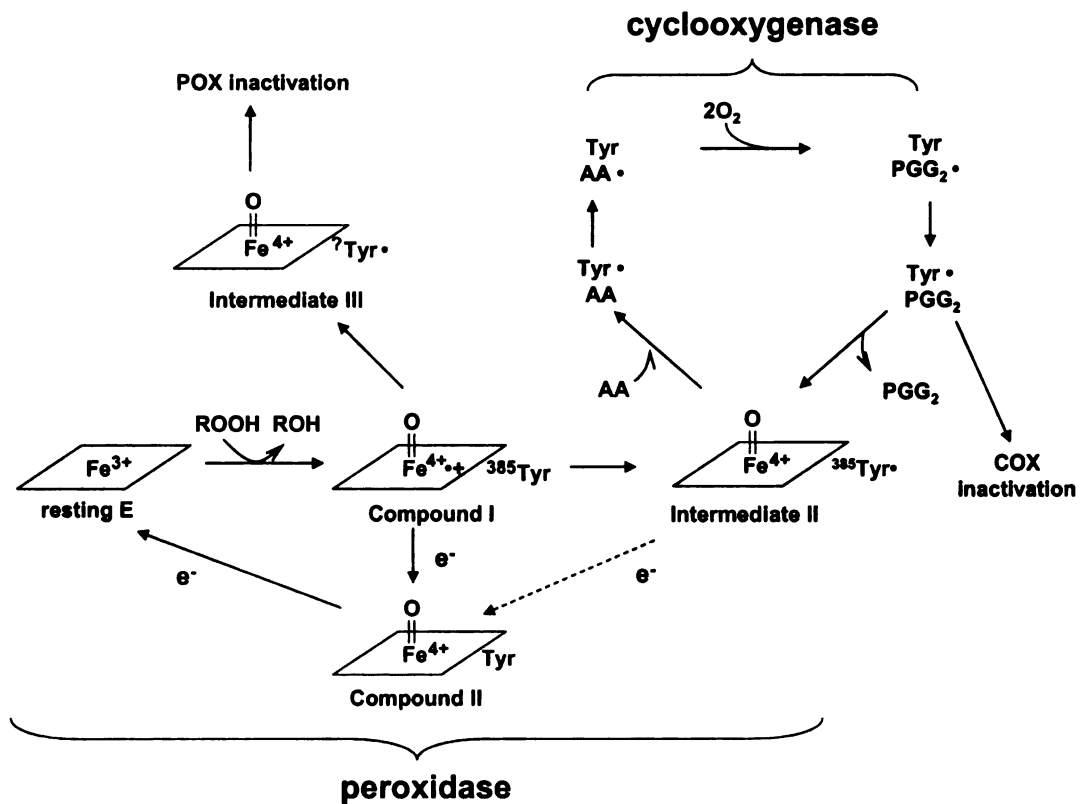
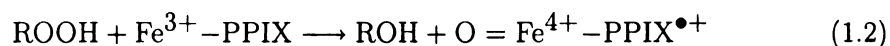
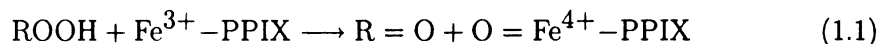


Figure 1.2: **Proposed reaction mechanism of PGHS.** Resting enzyme containing  $\text{Fe}^{3+}$ -PPIX reduces a hydroperoxides ( $\text{ROOH}$ ) to the corresponding alcohol ( $\text{ROH}$ ) and generates an oxo-ferryl heme radical intermediate (Compound I). An electron is transferred from Tyr385, producing a protein radical that initiates the COX reaction. Alternatively, in the presence of endogenous or exogenous reducing co-substrate the heme radical can be reduced to Compound II and then to resting enzyme. The COX and POX activities also undergo suicide inactivations as shown in the figure. Adapted from Ref. [37].



The type of cleavage is sensitive to the heme environment [38]. Free  $\text{Fe}^{3+}$ -PPIX only catalyzes homolytic cleavage and at low rates. Addition of a fifth heme ligand in peroxidases dramatically increases peroxidase turnover and the proportion of heterolysis rises depending on the different distal ligands. A histidine on the distal side of PGHS is essential for the reduction of hydroperoxides. The proximal and distal histidines along with heme iron is thought to carry out O-O cleavage in a “push and pull” manner (Fig. 1.3) [39]. The proximal histidine is usually involved in a hydrogen bond network involving polar residues or water molecules. These interactions make the axial nitrogen of the histidine “push” electrons toward the heme. On the other hand, the distal histidine functions as a general base, deprotonating the  $\alpha$ -oxygen of the incoming hydroperoxide substrate. And then it switches hydrogen bond to the  $\beta$ -oxygen, forming a strong electrophilic center (pull). The O-O bond collapses with the pair of electrons transferred to the  $\beta$ -oxygen atom. The corresponding alcohol is produced as the leaving group obtains a proton from the distal histidine. 15-hydroperoxyeicosatetraenoic acid (15-HPETE) can undergo heterolytic or homolytic cleavage by PGHS POX activity leading to an alcohol (15-hydroxyeicosatetraenoic, 15-HETE) or a ketone (15-ketoeicosatetraenoic acid, 15-KETE), respectively [40]. In an investigation of the POX activity using 50  $\mu\text{M}$  15-HPETE, PGHS-1 catalyzes

95% heterolytic cleavage of the O-O bond, while heterolysis only accounts for 60% of hydroperoxide reduction by PGHS-2 [40]. These differences reflect structural diversity between the POX active sites of the two isozymes.

Similar to many heme and radical involving enzymes, both the PGHS POX and COX activities undergo suicide inactivation by processes that are not fully understood. PGHS activities are measured by monitoring O<sub>2</sub> consumption in COX assays and oxidized product formation in POX assays. Neither of the reactions presents a steady state even with sufficient substrate provided [37]. Indeed, the rate of substrate consumption decreases immediately after a maximum value is reached, following a first-order process [41].

The loss of the POX activity on a millisecond time scale is detectable colorimetrically using guaiacol (2-methoxyphenol) as a chromophore in sequential stopped-flow measurements [41]. POX inactivation is induced by different hydroperoxides used at various concentrations for a fixed time, and the amount of POX activities remaining is quantified with a hydroperoxide-reductant mixture. The inactivation rate constant is about  $0.4 \text{ s}^{-1}$  regardless of the substrate structure and concentration, suggesting a unimolecular process. Rapid mixing and scanning approaches identified a spectroscopic species having a shorter UV absorption and followed by a decay of the whole spectrum. This species, designated Intermediate III, is believed to be the inactive intermediate and to contain a ferrous heme. Electron paramagnetic resonance (EPR) experiments show that a tyrosyl radical other than Tyr385 is generated during suicide inactivation [42]. It is believed that Intermediate III is derived from Intermediate II through an intramolecular transformation pathway, because if it is from Compound

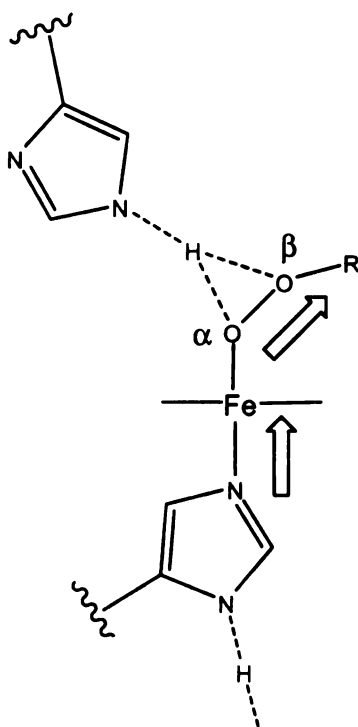


Figure 1.3: **“Push and pull” mechanism for PGHS POX catalysis.** Adapted from [39]. The block arrows indicate electron flow facilitated by axial histidine ligands.

I, inactivation should be substrate independent; however, this conclusion is based on experiments with saturating substrates. An alternative interpretation is that saturating hydroperoxide induces formation of enough of the PGHS Intermediate III precursor(s) [37], either Compound I or Intermediate II or something else, and that the process is pseudo-first order and not necessarily unimolecular. It seems more likely that inactive Intermediate III originates from Compound I. A Y385F mutant PGHS undergoes similar POX inactivation as the native enzyme, supporting that POX inactivation need not proceed via Intermediate II.

Unlike peroxide-induced suicide inactivation of myoglobin which involves cross-linking between heme and protein, the heme group of the inactivation form of PGHS is not covalently linked to the protein [41]. Substrate-induced suicide inactivation of PGHS catalysis may involve radical cross-linking within the protein, and may trigger an ER chaperone-assisted unfolding and degradation process [24]. Substrate induced protein degradation and related mechanistic components have not been well studied. Addition of POX reducing substrates can retard both POX and COX inactivation.

## **1.2 PGHS Structures**

### **1.2.1 Crystal Structures of PGHS-1 and PGHS-2**

Since the first PGHS crystal structure was determined over 10 years ago, we have gained more understanding of how PGHSs and NSAIDs function. PGHS is a homodimer with a subunit molecular weight of 70, 72 or 74 kDa depending on the different

glycosylation levels of PGHS-1 or PGHS-2 (Fig. 1.4A). PGHS monomers have three structural domains (Fig. 1.4B) [43, 44]. The N-terminus starts with an epidermal growth factor (EGF)-like domain, thought to be important for the dimerization. The four disulfide bonds of PGHS are all associated with the EGF-like domain, three within the domain, and another linked to the main body of the monomer. Following the EGF-like domain is a four-helix membrane binding domain (MBD). C-terminal to the MBD is a large catalytic domain in which are located the COX and POX active sites. Crystallographic analysis reveals that although the two sites neighbor each other, they are on opposite sides of the heme. There is no physical channel between the COX and POX sites in any of the crystal structures of PGHSs. Presumably, AA is mobilized from the lipid bilayer and moves through a tunnel in the MBD to the COX site where AA is converted to PGG<sub>2</sub>. It is believed that PGG<sub>2</sub> is then released from the COX site and diffuses through the aqueous solvent to enter the POX pocket. Interestingly, metabolic PGG<sub>2</sub> channelling from the COX site to the POX site was observed in microsomal, but not purified, PGHS-1, suggesting that PGG<sub>2</sub> partitions into the membrane following release from the COX site [45].

PGHS-1 and PGHS-2 are remarkably similar. The primary sequences are 60% identical. The major differences in the primary structure are observed in the N-terminal signal peptide, the loop above the POX sites and a 19-amino acid cassette formed exclusively in PGHS-2. These differences are somehow associated with differences in substrate utilization and protein stabilities. Differences before the signal peptides and MBDs of PGHS-1 and PGHS-2 appear not to affect the subcellular localization of the isoforms within ER (DeWitt and Smith, unpublished data). The

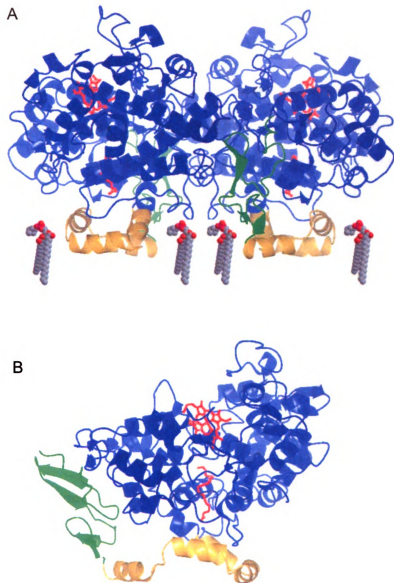


**Figure 1.4: PGHS structure.** (A) A model of PGHS homodimer associated with the lipid bilayer. The protein structure is adapted from ovPGHS-1 (pdb code, 1CQE). A ferric heme (red) is associated in the POX site and a flurbiprofen in the COX site (red molecule close to the gold helices). (B) PGHS monomer structure (ovPGHS-1; PDB code, 1DIY). Green, EGF domain in the N-terminus; gold, membrane binding domain; blue, catalytic domain. The heme group is a cobalt porphyrin analog (red), and the COX site contains arachidonic acid substrate (red). Images in this thesis/dissertation are presented in color.

POX loop of PGHS-1 is susceptible to trypsin digestion and flurbiprofen binding to the COX site protects against trypsin hydrolysis, suggesting an allosteric relationship between the COX and POX active sites. The third difference, the 19-amino-acid cassette in PGHS-2 is a signal for PGHS-2 protein degradation in cells. The tertiary structures of the two isoforms are more than 90% similar. A pharmaceutically important structural difference is that PGHS-2 has a valine at position of 523 in the COX active site instead of an isoleucine in PGHS-1 [46]. This one side chain difference results in a larger side pocket for substrate access and is the basis for the design and development of PGHS-2 specific drugs known as COX-2 inhibitors.

### **1.2.2 The Structure of the POX Active Site**

The PGHS POX active site is largely open to the solvent, exposing a large portion of the heme group including a propionate (Fig. 1.5); in contrast, most peroxidases have buried active sites [47, 48, 49]. In PGHS, the heme iron is coordinately bound to His388. This histidine interacts with tyrosine 504 through a water molecule. The POX reaction occurs on the distal side of the heme. The distal His207 is present in the center of the POX pocket, about 5 Å away from the heme iron. The sixth coordination position is occupied by a weak field ligand, probably a water molecule. The residues in the POX site of PGHS-2 are mostly conserved. PGHS-2 has a relatively closed distal heme dome in that a histidine and a tyrosine take place of Gly214 and Phe409, respectively, at the edge of the POX site in PGHS-1 (Fig. 1.6). This may be a

molecular basis for the fact that resveratrol (a phytoalexin found in grapes) is a peroxidase-dependent inactivator of PGHS-1 but not PGHS-2 [50].

The heme in PGHS POX enzymes is heme *b* (i.e. ferric protoporphyrin IX, Fig. 1.7). It is attached to the surrounding protein matrix through a single coordinate bond between the heme iron and His388 (Fig. 1.5). Heme *b*-containing proteins possess three major biological functions: electron transport, oxygen/nitric oxide transport and catalysis of redox reactions [51]. The differences stem from differences in the ways in which the heme prosthetic group interacts with the protein active site. Except for electron transfer hemoproteins, the other two types have one accessible ligand binding site. Hemoproteins catalyzing redox reactions fall into three families: catalases, heme-thiolate P450s and peroxidases; the fifth coordinated groups are tyrosine, cysteine and histidine, respectively. For the peroxidases, interactions of the fifth ligand with other protein component(s) or water molecule(s) determine the spin state of ferric ion in the heme plane. Mutagenic approaches have demonstrated that a strong, basic proximal histidine is required in most of the peroxidases [52, 53]. However, in PGHS, the proximal ligand is a neutral histidine bridging to Tyr504 through a water molecule [54].

There is a conserved polar residue four amino acids upstream of the distal histidine in all peroxidases (Fig. 1.5). It is an arginine in plant POXs (e.g. HRP and CcP) or a glutamine [e.g. myeloperoxidases (MPO) and PGHSs]. These residues are believed to serve as a polarity “enhancer”, that function together with the distal histidine, to provide a “pull” during heterolysis of the O-O bond stabilizing the developing charge on the  $\beta$ -oxygen (Fig. 1.3).

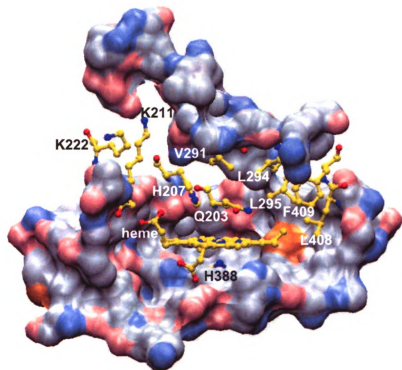


Figure 1.5: **Structure of the POX active site.** His388 is the proximal ligand group. His207 is the distal histidine. Gln203 is the distal glutamine. Val291, Leu294, Leu295, Leu408 and Phe409 are the residues that form the hydrophobic dome. In this surface model of the POX site, carbon is shown in gray, nitrogen in blue and oxygen in red. In the stick-ball model, carbon is yellow, nitrogen is blue and oxygen is red. This figure shows residues comprising the POX active site pocket (1DIY).

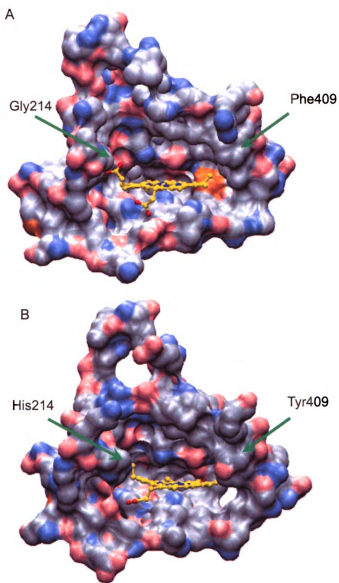


Figure 1.6: Comparison of the POX active sites of PGHS-1 and PGHS-2. (A) ovPGHS-1; PDB code is 1DIY. (B) muPGHS-2; PDB code is 1CVU. Surface presentations of the POX active sites are open to the solvent. Carbon atoms are shown in gray; oxygen, red; nitrogen, blue; sulfur, orange. The heme groups are shown as stick-ball models. Carbon, yellow; oxygen, red; nitrogen, blue; iron, green.

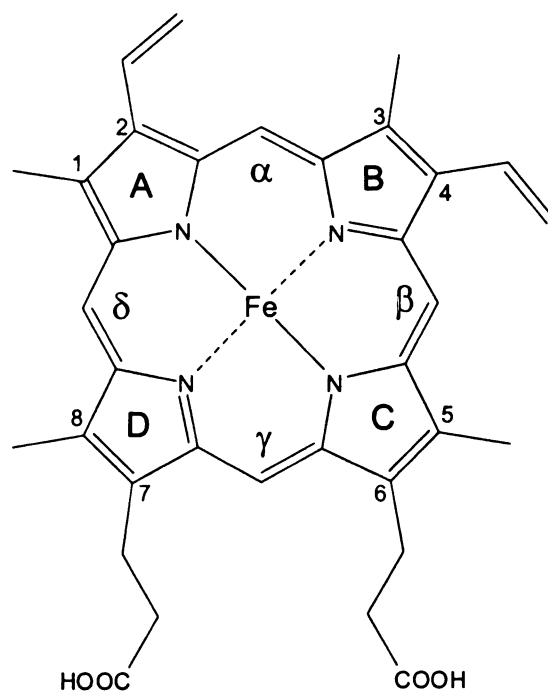


Figure 1.7: **Structure of Heme b.** A-D designate the pyrrole rings of Fe<sup>3+</sup>-PPIX. 1-8 and α-δ indicate carbons at the edge of the heme plane.

An intriguing feature of the distal surface of the PGHS-1 POX active site is a cluster of hydrophobic residues (Fig. 1.5). It involves Val291, Leu294, Leu295, Leu408 and Phe409. Except for a valine to leucine substitution at position 295 and a phenylalanine to tyrosine at 409, these residues are also conserved in PGHS-2. The side chains of the residues protrude from the “dome” of the distal heme active site, facing His207 and Gln203.

On the other side of the POX dome, there are two lysines with side chains forming a small side pocket in the POX active site (Fig. 1.5 and 1.6A). In a PGHS crystal structure it has been observed that a citrate molecule binds in the POX site through these lysines (Harman, CH; unpublished results). There are different possibilities for the role of these polar residues in the POX site. This region may be important for the interaction with the hydrophilic portion of hydroperoxides or reducing substrates. Some molecular dynamics simulations, however, have suggested that the carboxyl groups of hydroperoxy fatty acid substrates may interact with the POX site via salt bridges with these lysines [55].

### **1.2.3 The Structure of the COX Active Site**

The COX active site begins with Arg120 near the C-terminus of the MBD and involves a narrow hydrophobic channel (Fig. 1.8). Arg120 and Tyr355 at the mouth of the channel facilitate the association of the carboxyl end of fatty acid substrates and the moieties of many NSAIDs[56, 57, 58, 59]. Crystallographic analyses clearly show that the carbon tail of AA lies toward the distal end of the COX channel [44]. Tyr385 faces

the pro-S hydrogen at C13 of AA. Other important residues are Gly533 and Tyr348 which are involved in correctly positioning C13 of AA, and Val349, Trp387 and Leu534 which orient AA so that it is converted to PGG<sub>2</sub> and not other oxygenated products [60].

## **1.3 The COX Activity is Regulated by the POX Reaction**

### **1.3.1 Catalytic Mechanism of PGHS COX**

The cyclooxygenase reaction is one of the most intriguing events that occur during prostanoid biosynthesis (Fig. 1.9) [61]. The COX activity is triggered by a hydroperoxide-driven oxidation of the heme iron at the POX active site. The tyrosyl 385 radical of Intermediate II removes the pro-S hydrogen from C13 of AA, forming a carbon-centered radical at C13. The radical can migrate to position 11, where it reacts with molecular oxygen. The resulting transient 11-peroxy radical quickly forms an endoperoxide bridge at C9. A rearrangement occurs with formation of a bond between C8 and C12 and a radical at C15. The radical at C15 reacts with an additional molecule of oxygen, producing a PGG<sub>2</sub> radical. Its one electron reduction to PGG<sub>2</sub> regenerates tyrosyl 385 radical. The abstraction of hydrogen from C13 is the committed step in the COX reactions.

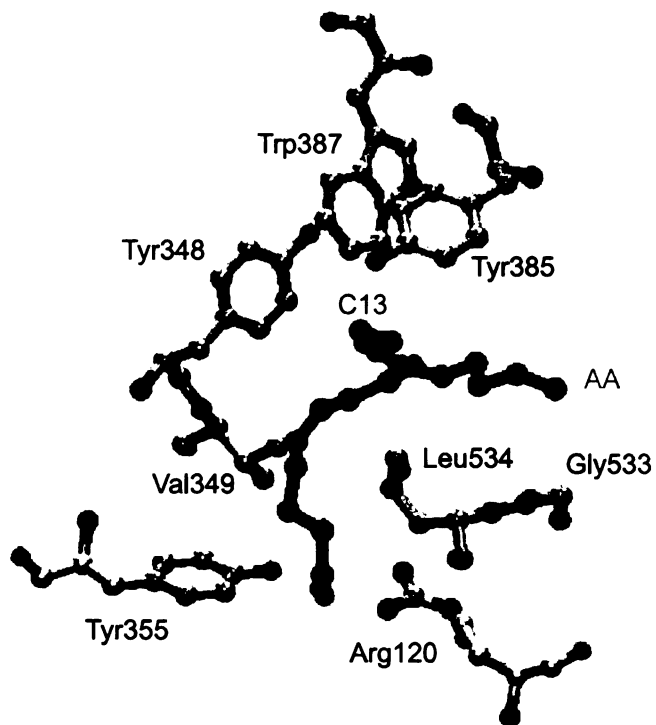


Figure 1.8: **Structure of the COX active site.** Arachidonic acid is shown in a red stick-ball model. Active site residues are shown with Tyr385 facing C13 of AA. PDB code is 1DIY.

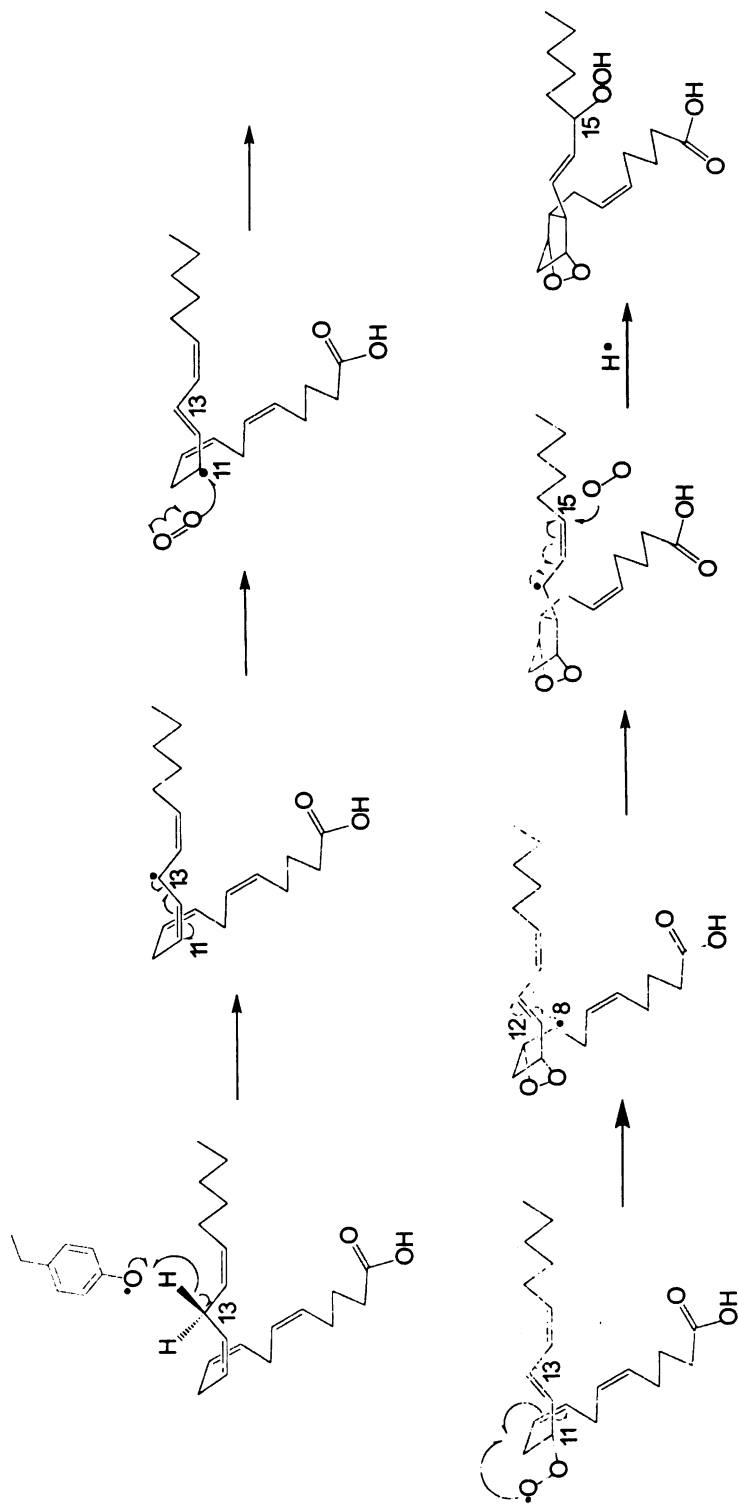


Figure 1.9: COX reaction mechanism. This diagram is adapted from Ref. [61].

Formation of the Tyr385 radical triggered by hydroperoxide in the POX site leads to COX activation [62]. In practice, this is an auto catalytic event and occurs with a kinetic lag as the enzyme generates PGG<sub>2</sub> in a COX reaction activated by hydroperoxides contaminating commercial substrate preparations [63]. Finally, the rate decays because of suicide inactivations. The activation of PGHS-2 COX is slightly faster due to the more rapid formation of Intermediate II [64]. COX activation can be impaired by agents like cyanide ion that bind the heme in the PGHS POX site [65]. The lag can be shorted by addition of an exogenous hydroperoxide.

Intermediate II formation occurs more slowly with PGHS-1 than PGHS-2, accounting for a sigmoidal-shaped kinetic trace of substrate consumption for PGHS-1, but not PGHS-2 [66, 67, 68, 16]. Thus, there is a negative allosteric effect in COX catalysis by PGHS-1. The negative allosterism can be eliminated by adding hydroperoxide to the system. The effect may be in controlling PGHS-1 activity in intact cells. Oxygenation of eicosapentaenoic acid (EPA) and docosahexaenoic acid (DHA) which has a low  $k_{cat}$  value with PGHS-1 is particularly sensitive to hydroperoxide levels [69].

### 1.3.2 Tyrosyl Radicals

The notion that radical chemistry is involved in the COX reaction dates to 1978 when a radical mechanism was proposed for the conversion of AA to PGH<sub>2</sub>[70]. EPR studies identified that the protein radicals as tyrosyl radicals. There are 27 tyrosine residues in a PGHS monomer. Tyrosyl 385 radical is critical for the COX activation. Mutation

of Tyr385 to phenylalanine eliminates COX activity but causes little impairment of the POX reaction [71]. However, two tyrosyl radicals other than Tyr385 have been detected by EPR in both Y385F PGHS-1 and indomethacin-treated PGHS-1 [72, 71]. Although the identification of these two tyrosines are not clear yet, they appear not to impact normal catalytic processes. In PGHS-2, a Y385F mutation also generates a tyrosyl radical in the vicinity of the heme but at an unknown position(s).

Additional studies using hydroperoxide driven PGHS radical and a stoichiometric amount of AA identified an EPR signal derived from fatty acid substrate, clearly supporting the proposed mechanism that the Tyr385 radical is competent for COX activation [70].

Addition of a hydroperoxide increases the rate of tyrosyl radical formation and the number of the COX turnovers as is evidenced when using EPA as the COX substrate. On the other hand, the reducing co-substrate of the POX recycles Intermediate II but increases the COX reaction rate at the same time. This contradiction is interpreted as partial reduction of tyrosyl radicals, with the remaining tyrosyl radicals sufficient for full COX activity. With the increase of reductant level, heme reduction becomes the major event and COX catalysis exhibits a substrate inhibition pattern. Thus, the main function of the POX reductant for the COX reaction is to protect the enzyme from suicide inactivation and prolong protein lifetime, but without interfering with the COX reaction cycle.

### 1.3.3 COX Inhibition by NSAIDs

NSAIDs target the PGHS COX activity and can act through three different mechanisms [1]. The first is simple reversible, competitive inhibition as is the case with ibuprofen (i.e. the active ingredient in Advil<sup>®</sup> and Motrin<sup>®</sup>). Flurbiprofen and indomethacin are classified as time-dependent inhibitors. They bind to the COX site initially in a reversible manner, but apparently induce a protein conformational change, which releases the inhibitor quite slowly. Aspirin is the sole member of the third class of NSAIDs. It acetylates Ser530 in the PGHS-1 COX pocket, irreversibly inhibiting the binding of AA in a catalytically competent conformation. Interestingly, acetylation in Ser530 of PGHS-2 by aspirin converts the enzyme from a di-oxygenase to a mono-oxygenase that converts AA to 15-HPETE [73]. This is due to a larger COX active site in PGHS-2 which accommodates AA even after acetylation. COX inhibition by aspirin is dependent on the heme oxidation state. Aspirin-treated PGHS-2 is still able to generate tyrosyl radical identical to that prior to acetylation modification. In contrast, PGHS-1 treated with aspirin exhibits an EPR signal similar to that from Y385F mutant, suggesting acetylation at Ser530 in PGHS-1 induces a positional or orientation change of Tyr385 and inhibits deprotonation of this tyrosine.

In addition, some NSAIDs bind to the transcription factors nuclear factor kappa B (NF- $\kappa$ B) and peroxisomal proliferator activated receptors (PPARs), which interferes with transcription regulation of some genes responding to cell stimulations by trauma, growth factor and cytokines [2]. But these pathways require very high levels of NSAIDs, well above those likely to occur *in vivo*.

PGHS-2 specific drugs have molecular structures designed to promote tight binding to the COX-2 active site. In general, they have no effect on PGHS-1, and they reduce the gastrointestinal side effects of common NSAIDs. However, administration of a PGHS-2 specific drug (e.g. Vioxx or Rofecoxib, Merck & Co.), increases cardiovascular risk. The mechanism for Vioxx induced cardiovascular events is still not clear. Inhibition of PGHS-2 by Vioxx may unbalance the formation of downstream anti-thrombotic PGI<sub>2</sub> and pro-thrombotic thromboxane A<sub>2</sub> causing thrombosis in some individuals. More cautious applications of all other PGHS-2 specific inhibitors and more mechanistic investigations on the roles of prostanoids and their regulatory mechanisms *in vivo* are required.

## **1.4 Regulation of PGHS POX by Oxidizing and Reducing Substrates**

### **1.4.1 Hydroperoxide Initiates PGHS Reaction**

The overall rate of the PGHS POX reaction is affected by the structure of hydroperoxide substrates as shown many years ago (Fig. 1.10) [74]. PGHS POX preferentially catalyzes the reduction of primary and secondary long chain alkyl hydroperoxides; whereas, it is less active to H<sub>2</sub>O<sub>2</sub> and almost inactive with tertiary hydroperoxides. It is believed that this specificity is determined by the structure of the heme active site in PGHS.

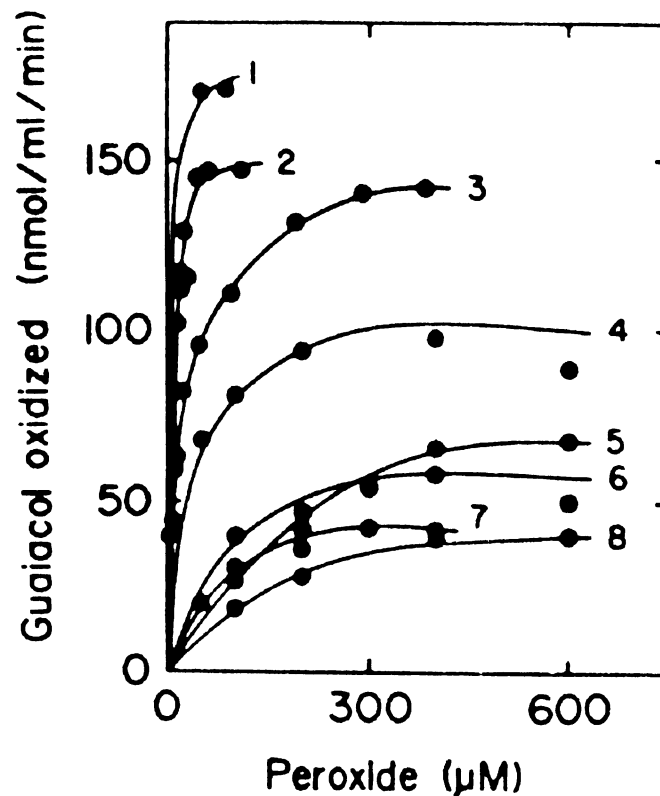


Figure 1.10: **Hydroperoxide substrate specificity of PGHS peroxidase.** Peroxidase activity was measured as guaiacol oxidation in a concentration dependent manner with different hydroperoxides in the peroxidase assay [74]. 1. PGG<sub>1</sub>; 2. 15-hydroperoxy-PGE<sub>1</sub>; 3. 15-hydroperoxyeicosatetraenoic acid; 4. methyl-15-hydroperoxy-15-methyl-PGF<sub>1α</sub>; 5. H<sub>2</sub>O<sub>2</sub>; 6. *t*-butyl hydroperoxide (*t*-BuOOH); 7. *p*-menthane hydroperoxide; 8. cumene hydroperoxide. This figure is cited from [74].

Table 1.1: Alkyl hydroperoxides have higher  $k_1$  values for Compound I formation.

Hydroperoxides	$k_1$ ( $M^{-1}s^{-1}$ )	References
15-HPETE	$7.1 \times 10^7$	[74, 75]
EtOOH	$2.5 \times 10^6$	[75, 76]
H <sub>2</sub> O <sub>2</sub>	$4.4 \times 10^5$	[76]
<i>t</i> -BuOOH	$5.9 \times 10^4$	[77]

Compound I is formed as a result of heterolytic cleavage of hydroperoxide by PGHS POX. The rates of Compound I formation with any given peroxide substrate are similar for PGHS-1 and PGHS-2 [75]. However, there are substantial differences in rates of Compound I formation from different hydroperoxides (Table. 1.1) [74, 75, 76, 77]. The rate constants for Compound I formation from enzyme plus primary and secondary alkyl hydroperoxides are  $\geq 10^7 M^{-1}s^{-1}$ , 2-3 orders of magnitude faster than with *t*-BuOOH or H<sub>2</sub>O<sub>2</sub>. In contrast, for a variety of eukaryotic peroxidases including yeast CcP, HRP and human MPO, the rate constants for Compound I formation with H<sub>2</sub>O<sub>2</sub> are  $10^7$ - $10^8 M^{-1}s^{-1}$ .

The identity of PGHS activator *in vivo* is not known, but may serve as the physiological heme oxidant in some cells (e.g. macrophages) [78]. Lipid peroxidation occurs ubiquitously in cellular and subcellular membrane systems. 5-, 12- and 15-Lipoxygenases and epidermis/platelet-type lipoxygenases are a major group of sources for lipid peroxides. There are studies reporting co-expression of 5- or 12-lipoxygenase with PGHS in the nucleus and ER tissues from stomach, small intestine, colon, lung, thymus, lymph node and spleen. Immunochemical/fluorescent and immunoelectron microscopic approaches have shown that mammalian lipoxygenases are predominately

located in the cytoplasm of hematopoietic cells, and may translocate to the inner side of plasma membrane or the cytosolic side of intracellular vesicles. However, the hydrophobicity of lipid peroxides makes diffusion through membranes and contacts with PGHSs possible. Product analysis of bovine corneal epithelial cells suggested the dominant endogenous HPETE is synthesized by a 12-lipoxygenase. Reactive oxygen species (ROS) including oxygen ions, free radicals and peroxides formed via non-enzymatic lipid peroxidation is another important source of alkyl hydroperoxides.

PGHS-1 and PGHS-2 catalyze the same reactions of PGH<sub>2</sub> formation. However, their activities appear to be tuned delicately by different hydroperoxide levels. PGHS COX activation requires a hydroperoxide to generate a Tyr385 radical-containing Intermediate II during the POX reaction cycle. The rate constants for Compound I formation of PGHS-1 and PGHS-2 are similar, but PGHS-2 conversion of Compound I to Intermediate II appears to be one order of magnitude quicker than PGHS-1. *In vitro*, the COX activity assays indicate that oxygen consumption by PGHS-2 is triggered at a hydroperoxide concentration ten times lower than that required for PGHS-1. This suggests that PGHS-2 can be activated at lower hydroperoxide levels than PGHS-1. This may be important for PGHS functions *in vivo*. PGHS-1 and PGHS-2 are co-expressed at comparable levels and at the same subcellular sites in murine NIH 3T3 cells. However, only PGHS-2 responds to endogenously generated AA while PGHS-1 is latent. A possible explanation for this result is that PGHS isoforms are differentially regulated by cellular hydroperoxide levels.

## 1.4.2 Regulation of PGHS Catalysis by Reductants

The influence of reducing substrates on overall PGHS catalysis depends on their abilities to stabilize the Tyr385 radical and protect against suicide inactivation. Some reductants stimulate the COX activity at lower concentrations but have inhibitory effects at higher levels, because they promote the reduction of oxidized heme intermediates thereby decreasing the levels of the Tyr385 radical. Some reductants are also reasonable COX inhibitors (e.g. acetaminophen).

Marnett and coworkers quantitatively investigated the potentials of various electron donors as reductants for PGHS *in vitro* [79]. Polyhydroxylated compounds (e.g. hydroquinone and epinephrine) and aromatic diamines (e.g. benzidine and tetramethylphenylenediamine) were the best reducing co-substrates, among over 50 compounds tested. The best naturally occurring reductants are epinephrine and uric acid. The compound most likely to be a reductant *in vivo* is uric acid which is present at a fairly high concentration ( $\sim 300 \mu\text{M}$ ). A common reductant in cells, reduced glutathione, is a poor reducing substrate for PGHS POX.

One difficulty in identifying physiological reducing substrates for PGHS is knowing the redox state of the lumen of the ER and nuclear envelope where PGHS isoforms are found. Common reducing compounds are mostly found in the cytosol. The oxidation state of the ER determined as the GSH/GSSG ratio is 1:1 to 1:3, while the ratio is 100:1 in the cytosol [80]. Possible reducing substrate candidates would be compounds that readily diffuse into the ER. For example, it is known that coenzyme Q can be detected in the ER and in subcellular membranes in addition to the inner

membrane of mitochondria [81]. Reduced coenzyme Q is a good anti-oxidant and its phenolic structure suggests it is a good reducing substrate for PGHS as mentioned by Marnett and coworkers [79]. Meanwhile, Coenzyme Q is also capable of generating  $H_2O_2$  [82] which triggers lipid peroxidation spontaneously. Thus, it is possible that coenzyme Q may function as the endogenous reducing reagent for PGHS. Another possibility is an endogenous reductant in that the spontaneous decay of the tyrosyl radicals occurs in the absence of exogenous reductants. And treatment with mild oxidant is not able to neutralize the endogenous reductants which amount to about 10 equivalents per monomer. The endogenous reductants are yet to be determined.

### 1.4.3 PGHS and Other Peroxidases

Peroxidases catalyze one-electron oxidation of micro- and macromolecules at the expense of hydroperoxides. Heme containing peroxidases are composed of two super-families, a) plant and fungal peroxidases including HRP, CcP, and chloroperoxidase (CPO). and b) animal peroxidases including PGHS, MPO, thyroid peroxidase (TPO), eosinophil peroxidase (EPO) and lactoperoxidase (LPO). As described above in “the Structure of the POX Active Site”, they all have heme *b* in the active site. The axial ligands are all histidines in both the proximal and distal positions except for CPO, a nonclassical peroxidase with a thiolate as the proximal heme ligand [83]. But this thiolate contributes to the broad catalytic capabilities of CPO similarly to a histidine as suggested by a mutagenic study [84]. The essential distal catalytic residue is normally a histidine; again, CPO is an exception in that it possesses a

glutamate in the distal active site. The distal histidines are not coordinated to the heme iron directly; instead, they act as general bases in O-O heterolytic cleavage. The reactions of these peroxidases typically follow the similar cycle of PGHS POX: resting enzyme→Compound I→Compound II→resting enzyme. There are four major structural differences between these various peroxidases as described briefly below [51].

The first distinction among peroxidases is the accessibility of the heme active site. This feature of heme peroxidases has been investigated using cross-linking reagents, in particular alkyl- or aryl-hydrazine, as probes [85]. The POX site of HRP and MPO are buried in the proteins, which restricts bulky substrate access to the heme ion. The reaction of HRP with phenylhydrazine results in  $\delta$ -*meso*-phenyl- and 8-hydroxymethyl modified hemes [86]. The distal histidine of HRP appears to serve as a barrier preventing reductants from freely interacting with ferryl oxygen. CcP predominantly produces  $\delta$ -*meso* heme derivatives, but also forms a small amount of iron-phenyl complex [87]. In contrast, cytochrome P450 enzymes with open active sites generate iron-aryl or *N*-alkyl-heme complexes [85]. Thus, the size of the heme active site can determine the reaction specificity of peroxidases. Reducing substrate are generally oxidized at the edge of the heme group at least for HRP. PGHS enzymes have open POX active sites with  $\beta$ -carbon, 5-methyl and 6-propionate groups exposed to the solvent. Reducing reactions could occur conceivably either at the heme edge or the surface of the heme plane.

The second difference among peroxidases involves the nature of the group that interacts with the proximal histidine. In general, the proximal histidines are stabilized

through hydrogen bonds by asparagines in mammalian POXs (e.g. LPO; Singh, A.K, 2006, to be published), or aspartates in plant/fungal/bacterial POXs (e.g. HRP and CcP). There are also exceptions; for example, huMPO has a Asp235 hydrogen bonding the proximal histidine (His336) [88, 89]. Nevertheless, these interactions impart imidazole character to the proximal histidine. The heme plane normally presents a bent conformation in these POX active sites with iron moving toward the proximal histidine which is a strong nucleophile, and thus the resting enzymes are usually five-coordinate species [52, 53]. However, the proximal hydrogen bond network is unique in PGHS in that a tyrosine was found to interact with the proximal histidine (His388) via a water and it is not critical for Compound I formation [54]. The neutral proximal His388 of PGHS makes it a weaker electron donor than those in CcP and HRP. The loose proximal histidine-ferric ion interaction allows water as the sixth ligand when hydroperoxide substrate is absent.

The third difference among peroxidases is in the distal polar components including water molecules and residues other than histidine. The residue 4 amino acids upstream of the distal histidine always has a polar side chain, glutamine in mammalian POXs (e.g. PGHS and MPO) and arginines in plant/fungal/bacterial POXs (e.g. HRP and CcP). This polar residue, the distal histidine, and the heme and proximal ligand are thought to provide the “push and pull” machinery required for heterolytic bond O-O scission, as evidenced by the results of studies using site-directed mutagenesis [40, 90, 91]. The distal arginine in HRP is critical for both of binding and heterolytic cleavage of H<sub>2</sub>O<sub>2</sub>. However, the distal arginine in CcP is not essential for the formation of Compound I. In addition to the distal histidine and upstream

glutamine/arginine, peroxidases can also have other polar, e.g. arginine in MPO and tryptophan in CcP. These residues may interact with distal histidines through hydrogen bonds, modulating the pKa of histidines making them stronger general bases. The distal heme dome in CPO, again, is unique that it does not have a conserved glutamine or arginine upstream to the putative general base, Glu183; but His105 in the vicinity of Glu183 may facilitate deprotonation of H<sub>2</sub>O<sub>2</sub> through Glu183 [92].

The fourth difference is the interaction between the heme group and the active site [93]. The heme prosthetic groups in classic POXs (HRP and CcP) bind in the active sites via the axial coordinations only. Whereas in mammalian POXs, covalent linkages are commonly seen between heme side groups and polar residues in the binding site. The heme group in huMPO has a methylsulfonium bond involving Met243 and two ester bonds with Glu242 and Asp94 [94]. These covalent modifications cause the Soret absorbance to red-shift from around 410 nm for other POXs such as HRP and PGHSs. Along with the strong fifth coordinate His-iron interaction, these heme-protein linkages are responsible for the distortion of the heme group in the huMPO active site. Disruption of these covalent linkages dramatically decreased catalytic activity of huMPO with chloride, H<sub>2</sub>O<sub>2</sub> or hypochlorous acid [95, 96, 97]. Besides, it has been demonstrated that at least one heme-protein covalent bond was required to protect heme peroxidases from modification by highly reactive metabolites of reductants [98].

## 1.5 Hypothesis

*In vitro* studies have demonstrated that PGHS POX prefers alkyl hydroperoxides as opposed to bulky or hydrophilic ones. Alkyl hydroperoxides increase the turnover numbers for the PGHS POX reaction. They also provide more rapid formation of Compound I. Crystallographic analysis shows a cluster of hydrophobic residues in the POX site of PGHS. Glutamine 203 is the distal polar residue instead of the arginine or aspartate observed in other POXs. The hypothesis underlying my work is as follows:

The hydrophobic dome residues of ovPGHS-1 POX facilitate hydrophobic interactions between the alkyl portion of 15-HPETE and the POX active site, which makes 15-HPETE an excellent initiator for the COX activity. Gln203 can be a determinant for substrate discrimination by PGHS.

To test this hypothesis, the following studies were performed and are reported in this thesis:

1. Examination of the potentially critical amino acids that account for the unusual hydroperoxide substrate specificity of PGHS-1
2. Analysis of the hydroperoxide initiator requirements for the cyclooxygenase activity of PGHS-1
- 3) Characterization of the role of conserved glutamine 203 in PGHS catalysis.
- 4) Testing if the COX activity in one monomer can be activated by the POX of the partner monomer of PGHS homodimer.

The outcome of my studies has provided a better understanding of structure-function relationships of PGHS. In addition, it is the first time that Gln203 has been found not to be an essential catalytic residue.

# Chapter 2

## Hydroperoxide Dome Residues and Substrate Specificity

### 2.1 Introduction

Prostaglandin endoperoxide H synthases (PGHS) catalyze the committed step in prostaglandin (PG) formation [1]. There are two PGHS isoforms, PGHS-1 and PGHS-2 (or COX-1 and COX-2). PGHSs catalyze two reactions including a cyclooxygenase (COX) reaction in which arachidonic acid is converted to prostaglandin G<sub>2</sub> (PGG<sub>2</sub>) and a peroxidase (POX) reaction in which PGG<sub>2</sub> is reduced to PGH<sub>2</sub> [13, 14, 15]. Both PGHS-1 and PGHS-2 are located on the luminal side of the endoplasmic reticulum (ER) and nuclear envelope [5, 99, 7, 100]. PGHS-1 is constitutively expressed as a housekeeping gene and PGHS-2 is inducible in most cell types [10, 11].

The COX and POX reactions occur at structurally distinct sites that are functionally connected [27]. In the POX reaction the Fe<sup>3+</sup> protoporphyrin IX (PPIX) is

first oxidized to an oxyferryl heme radical  $\pi$ -cation, referred to as Compound I that is similar to Compound I of horseradish peroxidase (Fig. 1.2) [30, 38, 32, 33]. Compound I can either be reduced by exogenous reductants to an oxyferryl heme form (Compound II), or it can undergo intramolecular reduction, involving transfer of an electron from Tyr385, forming a Compound II-like spectral intermediate and a tyrosyl radical [29, 28]. This latter complex is known as Intermediate II and is analogous to the intermediate ES of cytochrome c peroxidase [34, 35, 101, 102]. Intermediate II is the COX active form of the enzyme. When arachidonic acid is present in the COX site, the Tyr385 radical removes a hydrogen atom from C-13 of arachidonate, triggering a di-oxygenation reaction [103]. Intermediate II is regenerated within the COX site when PGG<sub>2</sub> is produced. PGHS reconstituted with Mn<sup>3+</sup>-PPIX proceeds through a POX catalytic cycle analogous to that of Fe<sup>3+</sup>-PPIX PGHS but formation of the mangano Compound I-like species is much slower [76, 104, 105].

Activation of the COX activity of PGHS-2 is triggered at a hydroperoxide concentration ten times lower than that required for PGHS-1 [75]. This may be important in cells co-expressing PGHS-1 and PGHS-2 where PGHS-2 COX activity can function when PGHS-1 COX activity is latent [106, 16].

Although PGG<sub>2</sub> is considered to be the natural substrate for PGHS POX activity, other peroxides may also be used as substrates. PGG<sub>2</sub> is chemically unstable and not stored but synthesized *de novo* from arachidonic acid released from membrane by cytosolic phospholipase A<sub>2</sub> (cPLA<sub>2</sub>). The identity of COX-initiating peroxide *in vivo* is unknown. PGHS-1 is reported to prefer primary and secondary alkyl hydroperoxides to H<sub>2</sub>O<sub>2</sub> or bulky peroxides like *t*-butyl hydroperoxide (*t*-BuOOH). The molec-

ular basis for this substrate preference is not known. The crystal structures of the POX active sites in ovine (ov) PGHS-1 and murine (mu) PGHS-2 (Fig. 1.6) suggest that the distal surface of the heme group is open to the solvent, and the POX site is sufficiently spacious to accommodate large and linear hydroperoxides coming directly from the aqueous environment [44, 43]. A dome comprised of mostly hydrophobic amino acids lies above the distal surface of the heme (Fig. 1.5) and molecular dynamics modeling suggests that these residues can interact with alkyl chains of alkyl hydroperoxides related to PGG<sub>2</sub> [54, 55]. In addition to the hydrophobic ligands, His388 covalently binds to a high spin state iron in the heme plane as the fifth ligand and a weak field ligand such as a water molecule serves as the sixth ligand for heme.

Here we report an improved method for obtaining steady state catalytic constants for PGHS POX activity that we have used to quantify hydroperoxide substrate specificity. We have also investigated a number of PGHS POX mutants to examine the basis for PGHS POX specificity and COX activation.

## 2.2 Materials And Methods

**Materials:** 15-Hydroperoxyeicosatetraenoic acid (15-HPETE) was synthesized as described previously [107]. Ethyl hydroperoxide (EtOOH) was purchased from Polyscience. *t*-Butyl hydroperoxide (*t*-BuOOH), H<sub>2</sub>O<sub>2</sub>, guaiacol, phenol and NaCN were from Sigma. Polyoxyethylene(6)-decyl ether (C<sub>10</sub>E<sub>6</sub>) was from Anatrace. Fe<sup>3+</sup> protoporphyrin IX (PPIX) and Mn<sup>3+</sup>-PPIX were from Frontier Scientific. Arachidonic

acid was from Cayman Chemical Company. Other chemicals were analytical grade from Sigma.

**Mutagenesis, Protein Expression and Purification:** A cDNA for the ovPGHS-1 gene containing a hexa-histidine (His<sub>6</sub>) tag at the N-terminus [1, 37] was subcloned into pFastBac plasmid (Life Technologies, Inc.). The QuickChange site-directed mutagenesis protocol (Stratagene) was used to construct the mutants. pFastBac plasmids were used for transposition of DH10Bac *Escherichia coli* cells following Bac-to-Bac<sup>®</sup> expression system protocols (Invitrogen). Mutants were identified by antibiotic resistance and blue/white screening. DNA was isolated and used to transfect *Spodoptera frugiperda* (Sf-21) insect cells (Invitrogen) as a CellFectin (Invitrogen) lipid/bacmid DNA complex. Baculovirus was precipitated from media with polyethylene glycol (MW=3,350), and the DNA fragments containing mutant PGHSs were amplified by PCR for further sequence verification. Media containing baculovirus with correctly mutated sites were harvested and used for cell infection. Sf-21 cells were infected with a multiplicity of infection (MOI) of 0.01 and cell pellets were harvested four days later when cell viability had dropped below 85%.

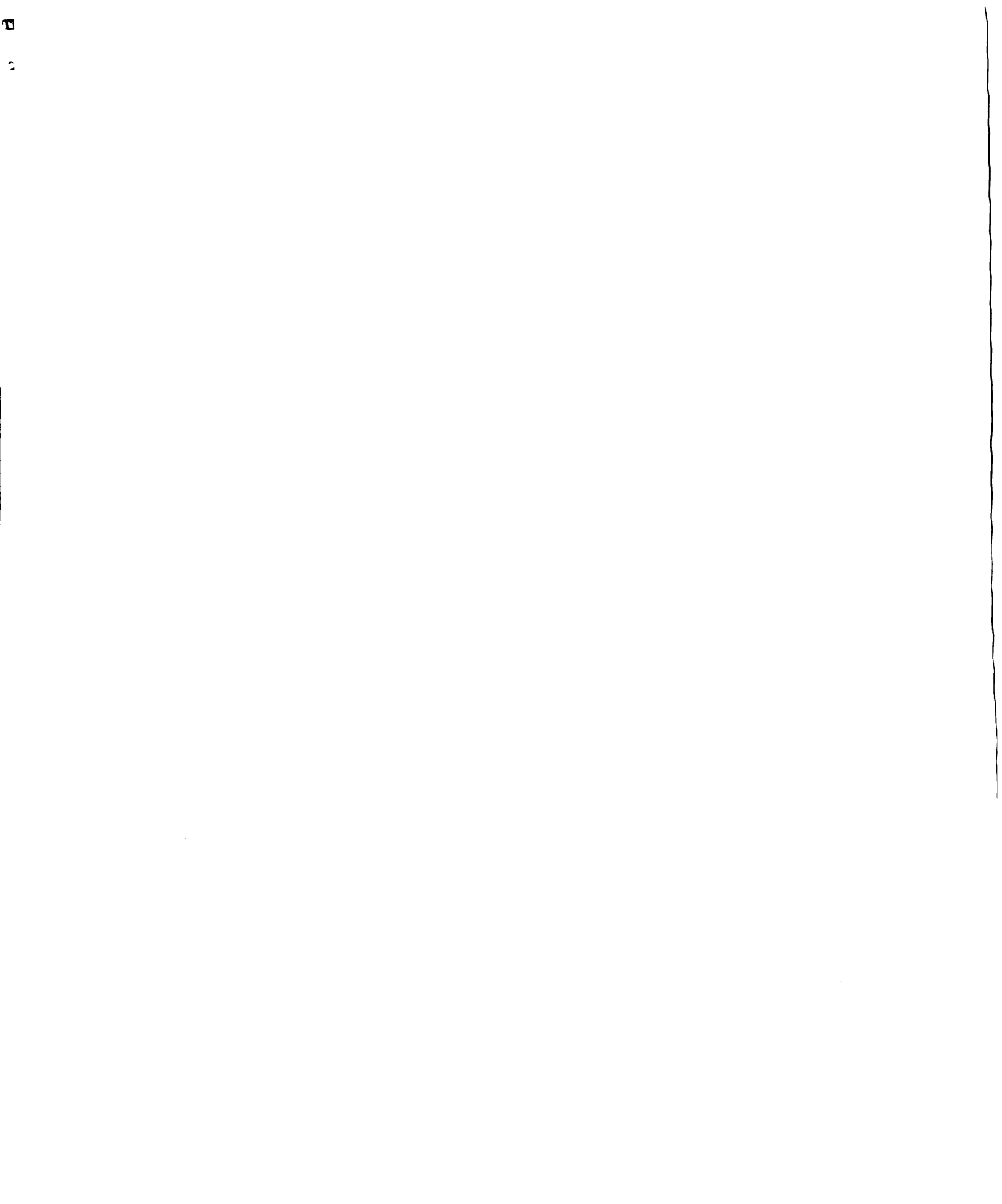
Cell pellets were re-suspended in 20 mM TrisHCl, pH 8.0, and lysed by sonication. Cell lysates were solubilized for 1 hr with 0.8% C<sub>10</sub>E<sub>6</sub>. The supernatant after ultracentrifugation at 158,000×g×2 hr was incubated with 4 ml of Ni-NTA fast-flow agarose (Qiagen) per liter of cell culture in the presence of 5% glycerol, 500 mM NaCl and 5 mM imidazole. The slurry was poured into a column and washed with washing buffer (20 mM TrisHCl, pH 8.0, 5% glycerol, 500 mM NaCl, 20 mM imidazole and 0.1% C<sub>10</sub>E<sub>6</sub>). Bound PGHS was eluted with three column volumes of 250

mM imidazole. These latter eluates were pooled, concentrated, and desalted using a Sephadex G-25 (Sigma) spin-column, which was pre-swollen in desalting buffer (20 mM TrisHCl, pH 8.0, 5% glycerol, 150 NaCl and 0.02% C<sub>10</sub>E<sub>6</sub>).

**POX Activity Assays:** POX reactions were conducted in 100  $\mu$ l of filtered and degassed buffer (100 mM TrisHCl, pH 8.0, and 100 mM NaCl). Heme-reconstituted PGHS (76 nM) containing 9.0 mM guaiacol was mixed with an equal volume of a hydroperoxide substrate solution using a stopped-flow apparatus (SX-60 HiTech Instruments). Formation of the guaiacol oxidation product 3,3'-dimethoxydiphenol-4,4'-quinone was monitored at 436 nm ( $\epsilon_{436}=6,390 \text{ M}^{-1}\text{cm}^{-1}$ ) [108]. The initial velocity  $v$  was determined when guaiacol oxidation was linear with time. Plots of the initial velocities as a function of hydroperoxide substrate concentrations were analyzed by the Michaelis-Menten equation (Equation 2.1) to determine  $V_{max}$  and  $K_m$  values;  $k_{cat}$  is the activity per mole of enzyme.

$$v = \frac{V_{max} \times [S]}{K_m + [S]} \quad (2.1)$$

**COX Activity Assays:** COX reaction mixtures contained 3 ml of 0.1 M TrisHCl, pH 8.0, 100  $\mu$ M arachidonic acid, 1 mM phenol and 5  $\mu$ M hematin equilibrated in a glass chamber at 37 °C. Reactions were initiated by adding enzyme to the assay chamber. A Yellow Springs Instruments Model 53 oxygen monitor was used to monitor O<sub>2</sub> consumption by native or mutant PGHSs with kinetic traces recorded using DasyLab (DasyTec) software. The rates reported are maximal rates occurring after a lag phase. One unit of COX activity is defined as 1  $\mu$ mole of O<sub>2</sub> consumed per min



per mg of enzyme at 37 °C in the assay mixture. The lag time is defined as the time required for the COX activity to reach a maximum after initiating the reaction.

***Identification of POX Spectral Intermediates and Kinetic Analysis:***

Pre-steady-state analysis of the POX reactions was performed with a rapid mixing and scanning technique using a stopped-flow apparatus equipped with double grating monochromators (DX-60 HiTech Instruments). Apo-PGHS was reconstituted with Fe<sup>3+</sup>-PPIX or Mn<sup>3+</sup>-PPIX at a stoichiometry of 0.8 per enzyme monomer. The final heme concentrations were usually 1-2 μM, and substrate concentrations were 2-4 μM 15-HPETE or 50-100 μM H<sub>2</sub>O<sub>2</sub>. In single wavelength experiments at least ten fold higher substrate concentrations were used to ensure steady-state kinetics. Both the enzyme and substrate solutions were prepared in 20 mM TrisHCl, pH 8.0, 150 mM NaCl and 0.02% C<sub>10</sub>E<sub>6</sub>. The enzyme and substrate solutions in individual syringes were mixed rapidly by triggering them into a mixing chamber, driven through an optical cell and stopped with a third syringe.

Different oxidation states of Fe-PPIX or Mn-PPIX were monitored spectroscopically. In the case of Fe<sup>3+</sup>-PPIX, the signal decay at 411 nm is due to the consumption of resting enzyme and the formation of Compound I. The peak shift to 420 nm represents the formation of Compound II and Intermediate II; these two species have the same UV-vis spectral features. There are two isosbestic points in the spectral scans: 427 nm between resting enzyme and Compound I, and 411 nm between Compound I and Compound II/Intermediate II.

The kinetic traces were collected at isosbestic points and fitted to exponential equations to obtain pseudo-first-order rate constants  $k_{obs}$ . For Compound I forma-

tion at 411 nm, a two-step reaction model ( $A \xrightarrow{k_1} B \xrightarrow{k_2} C$ ) was used (Equation 2.2) at low hydroperoxide concentrations. A four-species model was applied at higher concentration because of increases of side reactions such as suicide inactivation.

$$X = A_0 \left[ \varepsilon_Z + \frac{(\varepsilon_A - \varepsilon_C)k_2 + (\varepsilon_B - \varepsilon_A)k_1}{k_2 - k_1} e^{-k_1 t} + (\varepsilon_C - \varepsilon_B) \frac{k_1}{k_2 - k_1} e^{-k_2 t} \right] \quad (2.2)$$

where X stands for the total amount of all the species including intermediates A, B and C;  $A_0$  is the initial amount of species A;  $k_1$  and  $k_2$  are observed rate constants ( $k_{obs}$ ) for the formation of intermediates B and C, respectively.

For the second-order reaction of Compound I formation,  $k_1$  was the slope from the linear part of a plot of pseudo-first-order rate constants  $k_{1(obs)}$  versus hydroperoxide substrate concentrations (Equation 2.3).  $k_{-1}$  is the rate constant for the reverse reaction.

$$k_{1(obs)} = k_1[\text{ROOH}] + k_{-1} \quad (2.3)$$

For the formation of Compound II/Intermediate II at 427 nm, one exponential model ( $A \xrightarrow{k_2} B$ ) was applied as Equation 2.4.

$$[B] = [A]_0 (1 - e^{-k_{2(obs)} t}) \quad (2.4)$$

For Intermediate II formation,  $k_2$  was numerically equal to the maximum  $k_{2(obs)}$  at saturating substrate concentrations for the intramolecular two-species reaction system as calculated using Equation 2.5.

$$k_{2(obs)} = \frac{k_2 \times [ROOH]}{K_m + [ROOH]} \quad (2.5)$$

With ovPGHS-1 reconstituted with  $Mn^{3+}$ -PPIX, the resting enzyme (3  $\mu M$ ) when mixed with 50  $\mu M$  15-HPETE showed decreases in absorbance at 372, 472 and 561 nm, and a new peak at 417 nm, as described in previous reports [76, 104, 105]. As established previously,  $Mn^{3+}$ -PPIX PGHS-1 forms intermediates similar to those from  $Fe^{3+}$ -PPIX PGHS-1 (Fig. 2.1). A consecutive three-species model  $A \rightarrow B \rightarrow C$  (SpecFit, Bio-Logic Science Instruments) based on a singular value decomposition (SVD) algorithm was exploited to resolve intermediates deriving from  $Mn^{3+}$ -PPIX ovPGHS-1. Kinetic traces were collected at 417 nm and fitted to two exponential equations (Equation 2.2). A three-exponential equation was applied for higher substrate concentrations when side reactions (e.g. reduction of oxidized heme intermediates or suicide inactivation) may be involved.

**Cyanide Binding Assay** Purified ovPGHS-1 proteins (1-3  $\mu M$ ) were reconstituted with 0.8 moles  $Fe^{3+}$ -PPIX per protein monomer and incubated at room temperature for 30-60 min. The protein solution was centrifuged at  $10,000 \times g$  for 10 min and 1 ml of the supernatant was transferred to a quartz cuvette. Aliquots of concentrated NaCN stocks solution were added to the protein solution to yield final cyanide concentrations of 0, 0.08, 0.16, 0.24, 0.32, 0.40, 0.65, 1.15, 1.65, 2.90, 4.15,

6.65, 11.65, 16.65, 26.65 mM. The protein-ligand mixture was incubated for 5 min for each concentration of cyanide. The absorbance changes measured at 430 nm where the maximum change occurs were fitted to Eq. 2.6 to calculate a dissociation constant ( $K_d$ ).

$$\Delta AU = \frac{\Delta AU_{max} \times [CN^-]}{K_d + [CN^-]} \quad (2.6)$$

## 2.3 Results

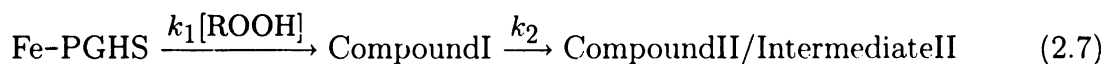
### 2.3.1 Hydroperoxide Substrate Specificity of the POX Activity of OvPGHS-1

Previous studies have established that ovPGHS-1 catalyzes guaiacol oxidation efficiently with several alkyl hydroperoxide substrates (i.e. PGG<sub>2</sub>, 5-phenyl-4-pentenyl-1-hydroperoxide (PPHP) and 15-HPETE) [109, 75, 110, 111]. However, because the POX activity undergoes rapid suicide inactivation [112, 37, 113], it has not been possible to obtain accurate rate constants using conventional steady-state spectroscopic assays. We developed a rapid mixing stopped-flow assay to determine ovPGHS-1 POX activity more precisely. Oxidation of the reducing substrate guaiacol was monitored at 436 nm immediately after the reaction components were mixed. This method permits steady-state product formation to be quantified before enzyme suicide inactivation affects the rates significantly. The initial rates of guaiacol oxidation as a function of substrate concentrations are shown for representative hydroperoxides in Fig. 2.2. The

$k_{cat}/K_m$  values for guaiacol-dependent hydroperoxide reduction by ovPGHS-1 were 2.7, 0.23, 0.01 and 0.0023  $\mu\text{M}^{-1}\text{s}^{-1}$  for 15-HPETE, EtOOH,  $\text{H}_2\text{O}_2$  and *t*-BuOOH, respectively (Table 2.1). Thus, as observed previously [74, 1, 110, 111], primary and secondary lipid hydroperoxides (i.e. 15-HPETE and EtOOH) are much better substrates than  $\text{H}_2\text{O}_2$  or *t*-BuOOH. There was no detectable inhibition of ovPGHS-1 POX activity with a variety of alkyl alcohols including 5-HETE and 15-HETE, even with alcohol to hydroperoxide ratios of more than 100 (Song, I., unpublished data).

### 2.3.2 Compound I Formation with Different Hydroperoxides

Native ovPGHS-1 reconstituted with  $\text{Fe}^{3+}$ -PPIX has a major peak at 411 nm. It forms a spectral intermediate Compound I, when incubated with 15-HPETE or EtOOH also at 411 nm as illustrated in Fig. 2.3A for 15-HPETE. This is followed by an accumulation of a Compound II/Intermediate II spectral intermediate with a peak at 417 nm and two other minor bands in the visible region. Kinetic traces for formation of intermediates are collected at two isosbestic points ( $\lambda=427$  nm for resting enzyme  $\rightarrow$  Compound I transformation and 411 nm for Compound I  $\rightarrow$  Compound II/Intermediate II), which are shown as two phases for Compound I and one single phase for Compound II/Intermediate II (Fig. 2.4). This behavior is consistent with the following mechanism:



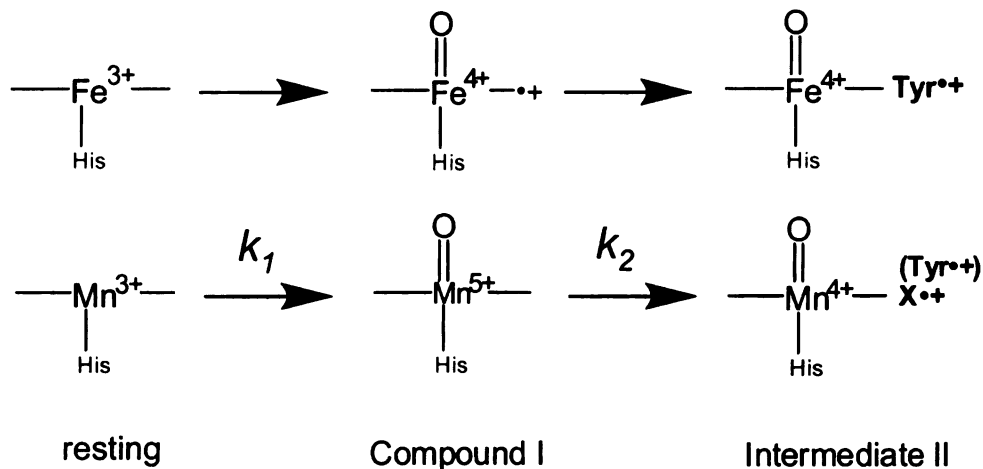


Figure 2.1: Comparison of Fe- and Mn-PPIX PGHS-1 heme intermediates. Mn<sup>3+</sup>-PPIX reconstituted PGHS-1 forms similar intermediates as Fe<sup>3+</sup>-PPIX PGHS-1. The figure is adapted from [76].

Table 2.1: Peroxidase activities of native ovPGHS-1 with different hydroperoxides. The POX activity assays were performed as described in Fig. 2.2. The steady state parameters were calculated following Equation 2.1.

	$k_{cat}$ (s <sup>-1</sup> )	$K_m$ (μM)	$k_{cat}/K_m$ (μM <sup>-1</sup> s <sup>-1</sup> )
15-HPETE	120±21	42±14	2.7
EtOOH	130±14	580±120	2.3×10 <sup>-1</sup>
H <sub>2</sub> O <sub>2</sub>	17±1.6	1700±260	1.0×10 <sup>-2</sup>
<i>t</i> -BuOOH	35±4.2	15000±3000	2.3×10 <sup>-3</sup>

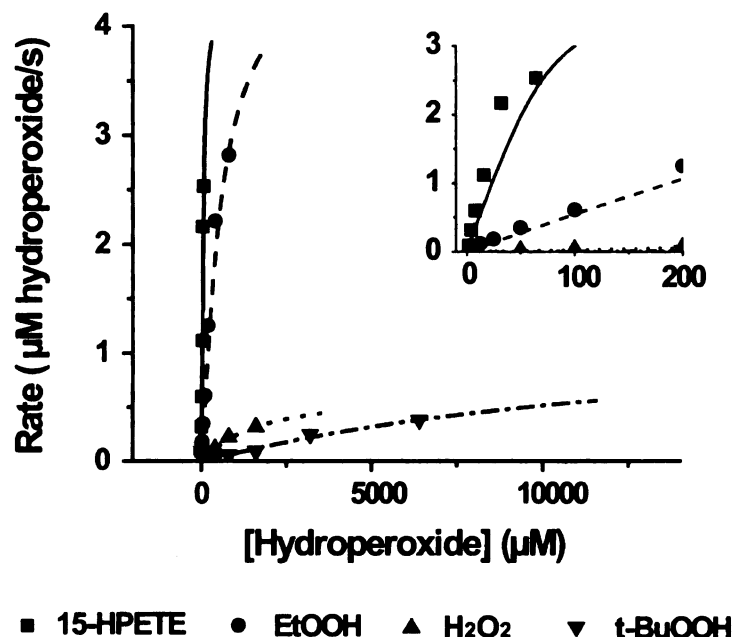


Figure 2.2: POX activities of native ovPGHS-1 with different hydroperoxides. For each reaction, identical volumes ( $50 \mu\text{l}$ ) of solutions containing hexa-His-tagged oPGHS-1 ( $76 \text{ nM}$  plus  $9 \text{ mM}$  guaiacol) or hydroperoxides were mixed rapidly in a stopped flow apparatus and formation of oxidized guaiacol was monitored through a  $1 \text{ cm}$  optical cell spectrophotometrically at  $436 \text{ nm}$ . Final concentrations of components in the  $0.1 \text{ ml}$  reaction mixture were  $38 \text{ nM}$  ovPGHS-1,  $4.5 \text{ mM}$  guaiacol and hydroperoxide as indicated in the figure. The initial rates of hydroperoxide substrate reduction were calculated from the rates of guaiacol oxidation. Each value is derived from the triplicate determinations. Non-linear regression fitting using Equation 2.1, yielded  $V_{max}$  values for hydroperoxide reduction by ovPGHS-1, and first order rate constants were calculated as shown in the lower panel. Inset: lower concentration scale for 15-HPETE and EtOOH dependent ovPGHS-1 peroxidase reaction. Solid line, simulated curve for rate with 15-HPETE; dashed line, EtOOH; dotted line,  $\text{H}_2\text{O}_2$ ; dashed dotted line,  $t\text{-BuOOH}$ .

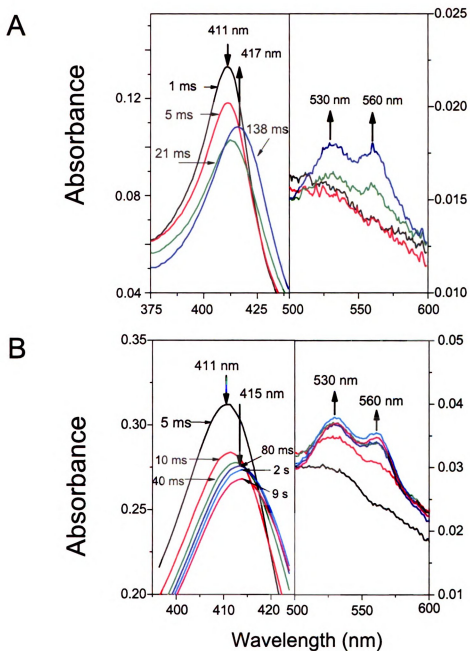


Figure 2.3: UV/Visible spectra of intermediates of Fe-PPIX ovPGHS-1 1 eq  $\text{Fe}^{3+}$ -PPIX reconstituted ovPGHS-1 reacted with 2 eq 15-HPETE (A) or 50 eq  $\text{H}_2\text{O}_2$  (B). Protein concentrations were 0.8 and 2  $\mu\text{M}$  in (A) and (B), respectively. Arrows at top of the peaks indicate the directions of peak migrations after ovPGHS-1 was mixed with hydroperoxide. Images in this thesis/dissertation are presented in color.

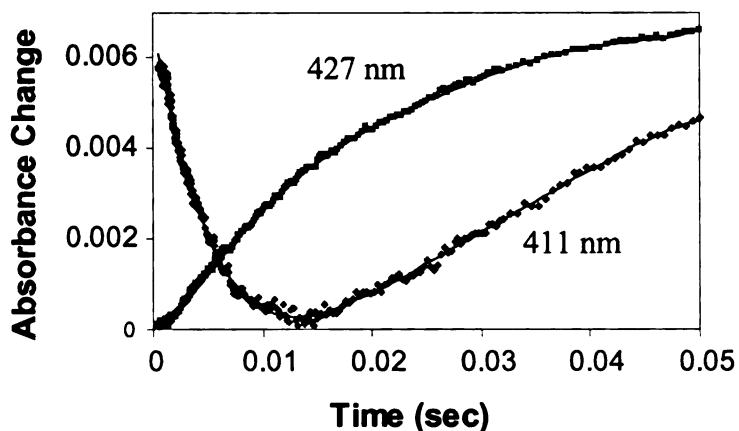


Figure 2.4: **Kinetic traces of Fe-PPIX ovPGHS-1 intermediates.** A kinetic mode of a stopped flow apparatus was used to monitor the formation of Compound I ( $\lambda=411$  nm) and Compound II/Intermediate II ( $\lambda=427$  nm). The dotted curves show absorbance changes of native $\rightarrow$ Compound transition at 411 nm (in blue) and Compound I $\rightarrow$ transition at 427 nm (in pink). Solid lines are fitting results using equations as described in Materials and Methods. Images in this thesis/dissertation are presented in color.

The reverse reaction was omitted in Equation 2.3 because the interception of the linear fitting at  $y$  axis was trivial compared with the value of the slope (Fig. 2.5A).

The values of  $k_{1(obs)}$  and  $k_{2(obs)}$  are dependent on substrate concentration (Fig. 2.5) as per Equations 2.3 and 2.5. Compound I was formed from 15-HPETE and EtOOH with ovPGHS-1 with second-order rate constant of  $10^6$ - $10^7$   $M^{-1}s^{-1}$  (Table 2.2).

Native ovPGHS-1 showed spectral changes only with high concentrations of  $H_2O_2$ . After mixing 50  $\mu M$   $H_2O_2$  and 1  $\mu M$  ovPGHS-1 the Soret peak at 411 nm slowly decreased (Fig. 2.3B). There was a slight red shift ( $\sim 4$  nm) after a short time that occurred concomitant with the appearance of Compound II/Intermediate II-like

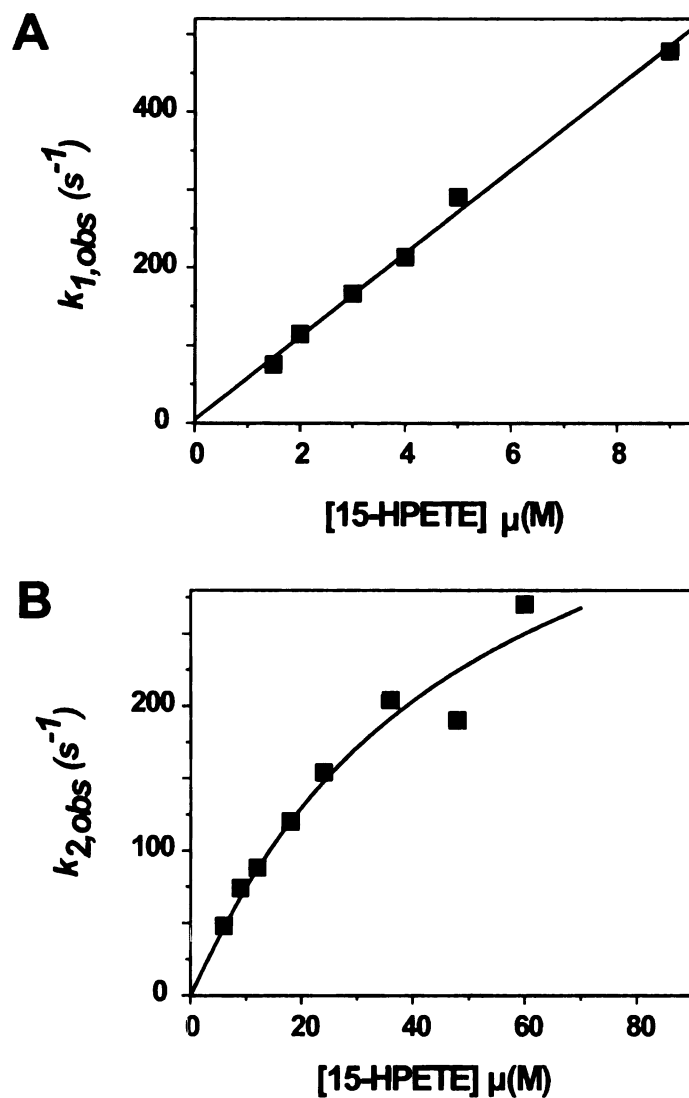


Figure 2.5: **Effect of 15-HPETE concentrations on the rate constants for ovPGHS-1 intermediate formation** . (A) First order rate constant ( $k_{1(obs)}$ ) for the formation of Compound I is a linear function of 15-HPETE concentrations as described in Equation 2.3. (B) Rate constant for the formation of Compound II/Intermediate II shows a saturating pattern over 15-HPETE concentrations following Equation 2.5.

Table 2.2: **Alkyl hydroperoxides have higher  $k_1$  values for Compound I formation.** Second-order rate constants were determined by stopped flow analysis as described in Materials and Methods. Intermediate formation by ovPGHS-1 with 15-HPETE or EtOOH was detected in 10-100 ms scale at 4 °C, with peak shifts between transitions of Compound I→Compound II/Intermediate II or Compound II/Intermediate II→resting enzyme. These intermediates of ovPGHS-1 were not distinguishable in reactions with H<sub>2</sub>O<sub>2</sub> or *t*-BuOOH in the present studies because of bleaching of the heme as described in the text and illustrated in Fig. 2.3B. This table lists previous experimental (a) and simulative results (b).

Hydroperoxides	$k_1$ (M <sup>-1</sup> s <sup>-1</sup> )	References
15-HPETE	$7.1 \times 10^7$	[74, 75]
	$(5.3 \pm 0.2) \times 10^7$	present work
EtOOH	$2.5 \times 10^6$	[75, 76]
H <sub>2</sub> O <sub>2</sub>	<sup>a</sup> $4.4 \times 10^5$	[76]
	<sup>b</sup> $0.9 \times 10^5$	[114]
<i>t</i> -BuOOH	$5.9 \times 10^4$	[77]

spectral features at longer wavelengths (Fig. 2.3B). However, the heme appeared to be decomposing (bleaching) as evidenced by decreased absorbance at later time points. Similar phenomena have been reported previously [28, 41]. Bleaching events are commonly seen with heme proteins in their reactions with peroxides and compromise the resolution of active intermediates [115, 116]. Hence, it was difficult to choose an appropriate model to resolve pure species of Compound I particularly with H<sub>2</sub>O<sub>2</sub>. Listed in Table 2.2 are second order rate constants for Compound I formation from ovPGHS-1 with H<sub>2</sub>O<sub>2</sub> from previous studies [76, 77]; the value was determined by fitting the early phases of the decay of resting enzyme to a two-exponential equation, assuming a consecutive two-step reaction mechanism for H<sub>2</sub>O<sub>2</sub> reduction by ovPGHS-1. Table 2.2 also includes a simulation result for Compound I formation from H<sub>2</sub>O<sub>2</sub> [114]. This indicates that the efficiency of hydroperoxides as heme oxidants follows

the same trend as their steady state activities.  $\text{H}_2\text{O}_2$  and *t*-BuOOH had  $k_1$  values 100-1000 times lower than those of 15-HPETE and EtOOH.

$k_2$  is a macroscopic rate constant for the formation of Compound II/Intermediate II complex which is a parallel reaction (Equation 2.8). It has been reported that aspirin treated PGHS-1 does not form Tyr385 radical. This allows measurements of the formation of Compound II species without a branched reaction to Intermediate II, and the rate constant for Intermediate II can be available.



### 2.3.3 COX Activation by Different Hydroperoxides

$\text{O}_2$  consumption during the COX reaction with AA is sigmoidal (Fig. 2.6A) [65]; i.e. plot of activity vs. time shows a lag time prior to reaching maximal velocity (Fig. 2.6B). In a typical COX assay, the COX activity of PGHS is activated by trace amounts of hydroperoxide contaminants present in commercial fatty acid substrate preparations [63]. The first few COX reaction turnovers then generate sufficient  $\text{PGG}_2$  to support a burst of oxygen consumption. NaCN binds to the heme group of ovPGHS-1 and inhibits 15-HPETE reduction by guaiacol with a  $K_i$  of 0.11 mM (data not shown). The presence of 10 mM cyanide in the COX assays results in considerably longer lag times in the COX reaction (Fig. 2.7) [117]. Lipid hydroperoxides (i.e. 15-HPETE and EtOOH) shortened the lag times that were prolonged by cyanide, but  $\text{H}_2\text{O}_2$  and *t*-BuOOH had little or no effects at the concentrations tested (Table 2.3).

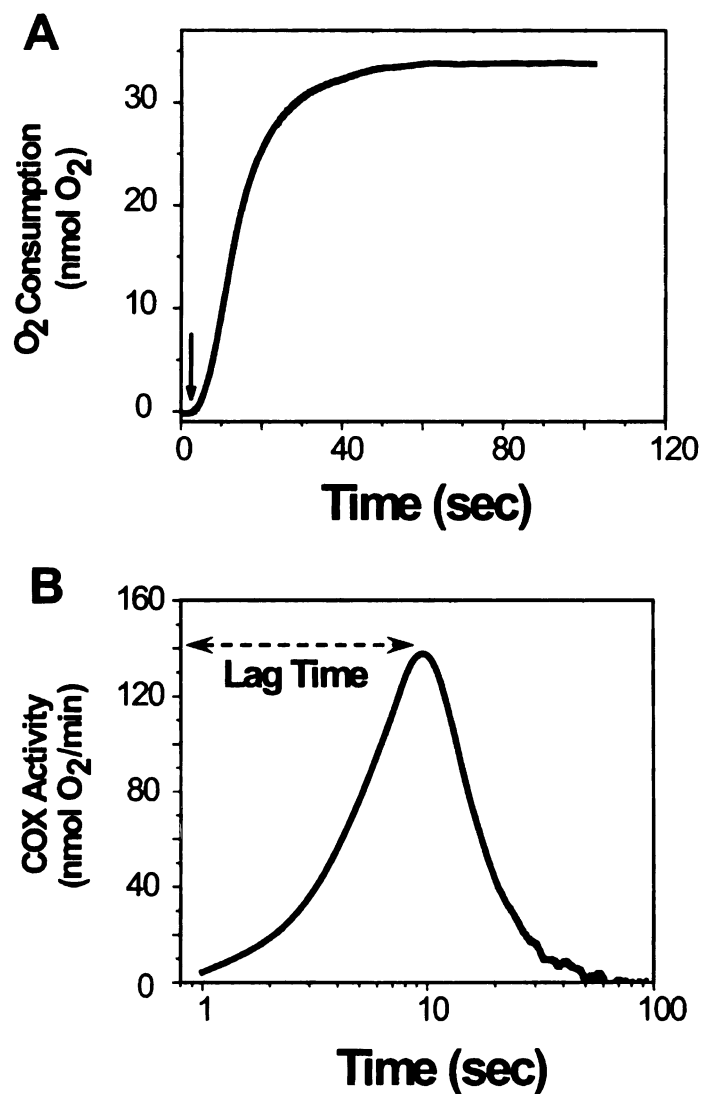


Figure 2.6: **COX activation and lag time** (A) Kinetic trace of O<sub>2</sub> consumption in a typical COX assay. COX assay is carried out in 3 ml TrisHCl, pH 8.0 at 37 °C which contains 1 mM phenol, 1 μM hematin, 100 μM AA and 2 μg ovPGHS-1. The arrow indicates the time to mix the reaction components. (B) Instantaneous COX rates. The rates of O<sub>2</sub> consumption are calculated from (A). The time required to reach the maximum rate after initiating the reaction is defined as the lag time.

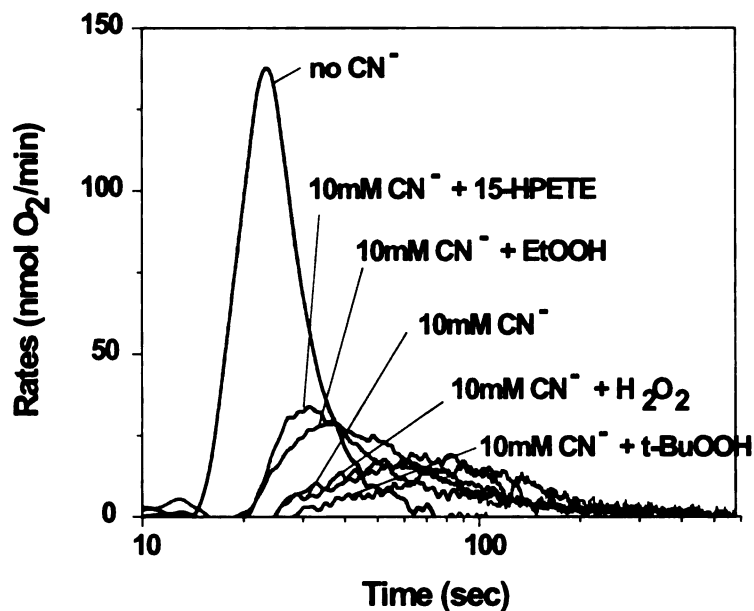


Figure 2.7: COX activation by different hydroperoxides. Cyclooxygenase assays were performed as described in Materials and Methods. Reaction mixtures contained 10 mM  $\text{CN}^-$ , 100  $\mu\text{M}$  AA, 5  $\mu\text{M}$  heme and 50  $\mu\text{M}$  hydroperoxide. Reactions were initiated by injection of 5-10  $\mu\text{g}$  of the indicated enzyme.

Table 2.3: Oxygen consumption and lag times in COX activation. Reaction mixtures contained 100  $\mu\text{M}$  arachidonic acid, 1 mM phenol and 5  $\mu\text{M}$  hematin in 3 ml of 0.1 M TrisHCl, pH 8.0. NaCN (10 mM) present in some of the samples as indicated. The reactions were initiated by injecting 5  $\mu\text{g}$  of ovPGHS-1 and  $\text{O}_2$  consumption measured with an  $\text{O}_2$  electrode. To test for the capability of different hydroperoxides to reverse the cyanide inhibition, 50  $\mu\text{M}$  15-HPETE, 50  $\mu\text{M}$  EtOOH, 100 mM  $\text{H}_2\text{O}_2$  or 100 mM *t*-BuOOH was added to the sample prior to the addition of enzyme. The COX assays were performed in duplicate.

Components	Lag Time (s)	COX Activity (nmol $\text{O}_2$ /min/mg)
No $\text{CN}^-$	10.3	48±1.8
10 mM $\text{CN}^-$	71.7	4.9±2.3
$\text{CN}^-$ + 15-HPETE	23.5	12±0.36
$\text{CN}^-$ + EtOOH	25.7	9.9±0.54
$\text{CN}^-$ + $\text{H}_2\text{O}_2$	66.1	6.1±0.07
$\text{CN}^-$ + <i>t</i> -BuOOH	78.0	15±0.07

### 2.3.4 Mutations of Hydrophobic Residues in the POX Dome

Data on the steady state catalytic efficiencies of PGHS POX activity and the rate constants for Compound I formation with different hydroperoxides along with the abilities of various hydroperoxides to activate PGHS COX functioning are consistent with ovPGHS-1 POX preferring lipid hydroperoxides to hydrophilic or bulky substrates. The molecular basis for this specificity has not been determined. We reasoned that the side chains of leucine, valine and phenylalanine residues (Fig. 1.5) that form a hydrophobic dome over the distal side of the heme of PGHS were important in PGHS POX specificity. Alanine substitutions at some of the sites caused some alterations of POX activity toward 15-HPETE (Table 2.4). However, there was no obvious pattern to the changes in rates. About half of the mutations caused qualitatively similar changes with 15-HPETE vs.  $\text{H}_2\text{O}_2$ . The changes in  $k_{cat}$  values were no more than ten fold and the catalytic efficiencies of mutant enzymes having alanine substitutions expressed as  $k_{cat}/K_m$  values, showed relatively small variations (0.35-1.7 fold).

A second group of mutations involved replacements of residues in the dome with amino acids other than alanine. L294G and L294S mutants had 7-9 fold higher  $k_{cat}$  values with both 5-HPETE and  $\text{H}_2\text{O}_2$ . Substitutions of Leu294 with acidic amino acids (i.e. L294D and L294E) showed much reduced turnover numbers and catalytic efficiencies with 15-HPETE.

Table 2.4: Side chain substitutions of hydrophobic residues in the POX distal dome altered POX activities. POX assays were performed using stopped flow measurements as described in Methods and Materials.  $k_{cat}$  and  $K_m$  values were calculated from the Michaelis-Menten equation. N/A, not applicable. Each value is the average of triplicate determinations. 2.3 nM native ovPGHS-1 was mixed with 100  $\mu$ M AA at 4 °C for 15-HPETE and 25 °C for H<sub>2</sub>O<sub>2</sub>.

Enzyme	15-HPETE				H <sub>2</sub> O <sub>2</sub>		$k_{cat}/K_m$ (mM <sup>-1</sup> s <sup>-1</sup> )
	$k_{cat}$ (s <sup>-1</sup> )	$K_m$ ( $\mu$ M)	$k_{cat}/K_m$ ( $\mu$ M <sup>-1</sup> s <sup>-1</sup> )	$k_{cat}$ (s <sup>-1</sup> )	$K_m$ (mM)		
Native	270±2.7	14±0.5	19	150±13	2.9±0.4	54	
V291A	300±18	31±5	9.8	230±37	7.3±2	32	
L294A	730±28	22±2	33	43±1	2.5±0.09	17	
L295A	230±68	460±170	0.5	160±10	6.4±0.6	25	
L408A	35±0.6	20±1.4	1.7	30±1.3	4.8±0.3	6.7	
F409A	670±32	98±8.4	6.8	180±32	8.0±1.9	23	
V291A/L294A	300±18	28±5	11	540±48	11±1	49	
L294A/L295A	380±39	70±15	5.5	270±34	6.6±1	40	
V291A/L295A	200±16	270±30	0.74	150±12	2.3±0.3	65	
L294A/F409A	480±26	66±7.5	7.3	410±120	7.4±3	55	
L295A/L408A	72±7.8	33±8.0	2.2	93±10	4.6±0.7	20	
V291A/L294A/L295A	290±7	120±5	2.5	610±24	8.9±0.5	68	
L294G	2000±88	140±10	15	1400±110	14±1.4	97	
L294S	2100±170	210±25	10	1200±59	17±1.0	72	
L294D	39±5.6	110±34	0.4	210±48	6.2±2.4	35	
L294E	5.2±0.15	17±1.6	0.3	N/A	N/A	N/A	

### 2.3.5 Compound I Formation of Fe<sup>3+</sup>-PPIX OvPGHS-1 from Different Hydroperoxides

Several alanine-substituted mutant enzymes were selected to examine rates of Compound I formation. Table 2.5 compares the rate constants for Compound I and Compound II/Intermediate II formation by native, V291A, L294A and V291A/L294A ovPGHS-1s with 15-HPETE or H<sub>2</sub>O<sub>2</sub>. These enzymes formed Compound I from 15-HPETE at about the same rate as native ovPGHS-1 when reconstituted with Fe<sup>3+</sup>-PPIX. These results indicate that substituting residues in the dome with a smaller amino acid does not affect Compound I formation; however, as judged by  $k_{cat}$  values the expanded POX active site space does appear in some cases to favor electron transfer from guaiacol to the heme.

Table 2.5: **Rate constants for Compound I formation of Fe<sup>3+</sup>-PPIX ovPGHSs.** Native and V291A ovPGHS-1 enzymes did not form a spectroscopically identifiable Compound I-like intermediate in the presence of H<sub>2</sub>O<sub>2</sub>, so rate constants could not be determined in these cases. N/A, not available. \*, estimated value. Each kinetic constant was calculated from the mean of triplicate determinations.

Enzyme	15-HPETE		H <sub>2</sub> O <sub>2</sub>	
	$k_1$ (10 <sup>7</sup> M <sup>-1</sup> s <sup>-1</sup> )	$k_2$ (s <sup>-1</sup> )	$k_1$ (10 <sup>5</sup> M <sup>-1</sup> s <sup>-1</sup> )	$k_2$ (s <sup>-1</sup> )
native	5.3±0.2	460±50	*0.9	N/A
V291A	6.2±1	460±60	N/A	N/A
L294A	8.5±0.3	290±40	7.0±0.2	42±2
V291A/L294A	7.6±0.9	140±6	3.9±0.6	23±2

L294A-containing mutants of ovPGHS-1 formed spectrally distinct peaks for Compound I and Compound II/Intermediate II with H<sub>2</sub>O<sub>2</sub>, and the rate constants for Compound I formation by these mutants were comparable to the value estimated

previously for native ovPGHS-1 (40); but again, we were unable to obtain  $k_1$  or  $k_2$  values for native enzyme ovPGHS-1 with  $H_2O_2$ .

We also tested L294D and L294E ovPGHS-1 with HPETE and  $H_2O_2$  but observed bleaching of the enzyme.

### **2.3.6 Compound I Formation of $Mn^{3+}$ -PPIX OvPGHS-1 from Different Hydroperoxides**

Because of difficulties in some cases in obtaining kinetic constants for Compound I formation by  $Fe^{3+}$ -PPIX ovPGHS-1 variants, Compound I formation was investigated using  $Mn^{3+}$ -PPIX reconstituted ovPGHSs. The  $Mn^{3+}$ -PPIX prosthetic group is structurally the same as heme *b* except for the metal ion, and it is a reasonable analog with which to study heme behaviors when the iron heme is labile (23,24).  $Mn^{3+}$ -PPIX ovPGHS-1 retains only about 5% of the POX activity of  $Fe^{3+}$ -PPIX ovPGHS-1 but both enzymes have the same COX specific activities (Table 2.6).  $Mn^{3+}$ -PPIX ovPGHS-1 exhibits strong Soret absorption and its oxidized variants can be easily detected spectroscopically (Fig. 2.8A). The slower POX reaction rate of  $Mn^{3+}$ -PPIX ovPGHS-1, and the optical properties of the enzyme facilitate observation of oxidized intermediates.

Kinetic traces were collected at 417 nm where maximum absorbance changes occurred, and fit to two exponential equations to calculate rate constants for formation of the intermediates (Fig. 2.8B).

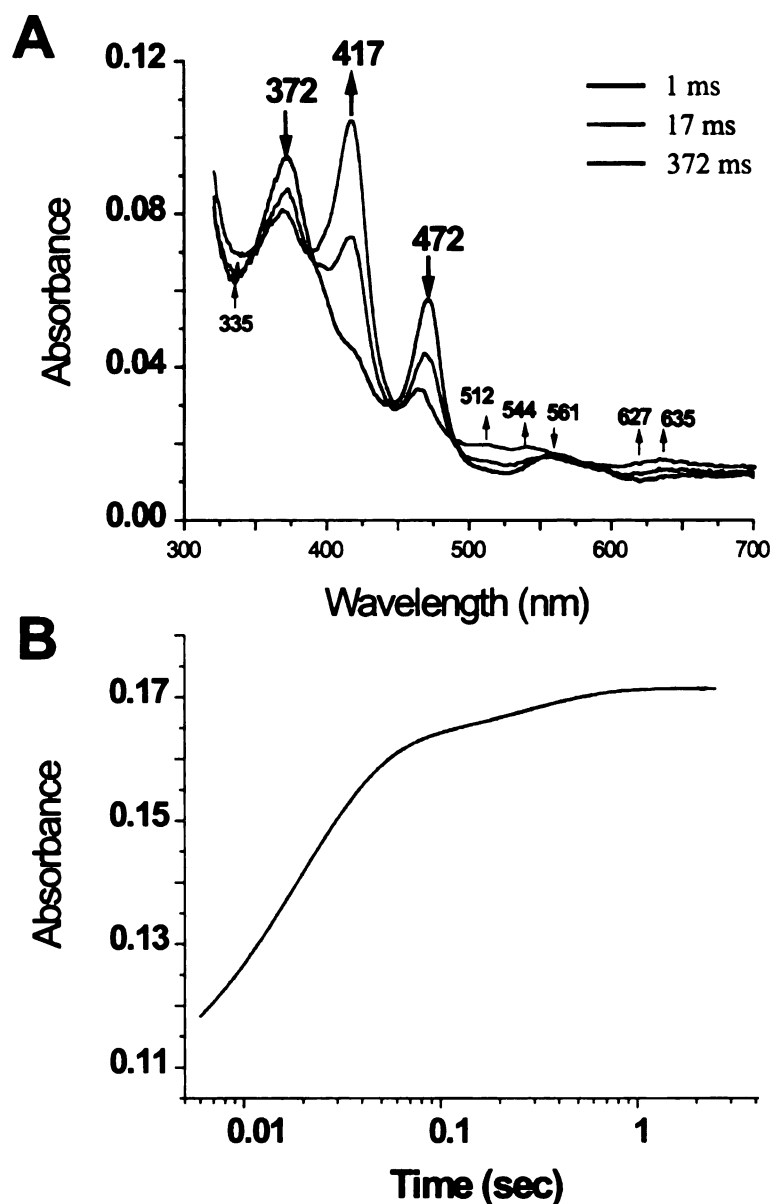


Figure 2.8: UV/Vis spectrum of Mn-PPIX PGHS-1 intermediates. (A) UV/Vis spectra of Mn-PPIX native ovPGHS-1 intermediates produced in the reaction with  $\sim 20$  eq 15-HPETE. Intermediate species were isolated by SVD algorithm-based program (SpecFit). This figure presents intermediates (shown in different colors) with similar spectra to those of the simulations. Arrows indicate the directions of peak abolishment or formation. (B) Kinetic trace (gray cycles) of intermediate formation at 417 nm. Solid line is the fitting results using the equation described in Materials and Methods. (A) and (B) represent two reactions using different protein concentrations.

Table 2.6: **Activities of Fe<sup>3+</sup>- and Mn<sup>3+</sup>-PPIX ovPGHS-1s.** The reactions were performed the same as described in Materials and Methods. % stands for the percentage of Fe<sup>3+</sup>-PPIX ovPGHS-1 activity which is equivalent to the full activity of Mn<sup>3+</sup>-PPIX ovPGHS-1.

prosthetic group	COX Activity ( $\mu\text{mol O}_2/\text{min}/\text{mg}$ )	POX Activity	
		15-HPETE ( $\text{s}^{-1}$ )	H <sub>2</sub> O <sub>2</sub> ( $\text{s}^{-1}$ )
Fe <sup>3+</sup> -PPIX	70	116	17
Mn <sup>3+</sup> -PPIX	57	6.6	1.3
%	81	5.7	7.6

Plotting first order rate constant  $k_{1(obs)}$  versus 15-HPETE concentration (Fig. 2.9A) exhibited saturation, suggesting at least one intermediate was formed before the formation of Compound I for Mn-PGHS-1. This intermediate was probably an enzyme-substrate complex. The second order rate constants were achieved by fitting the linear range of the regression curve to Equation 2.3 (Fig. 2.9A, inset). However, this enzyme-substrate-like species was not likely formed with H<sub>2</sub>O<sub>2</sub>. The plotting of  $k_{1(obs)}$  versus H<sub>2</sub>O<sub>2</sub> showed a linear function (Fig. 2.9B). The first order rate constant  $k_{2(obs)}$  for the formation of Compound II/Intermediate II shows a saturating function of the substrate concentration using 15-HPETE or H<sub>2</sub>O<sub>2</sub> (data not shown) as seen with Fe-PPIX ovPGHS-1 (Fig. 2.5B).

The rate constants for Compound I formation in Mn<sup>3+</sup>-PPIX ovPGHSs and mutant enzymes except for L294E ovPGHS-1 were similar to Fe<sup>3+</sup>-PPIX ovPGHSs. The  $k_1$  value for L294E ovPGHS-1 mutant was two orders of magnitude lower than that of native enzyme. Thus, it appears that the introduction of a longer side chain having a negative charge changes the geometry of the active site significantly. (Table 2.7)

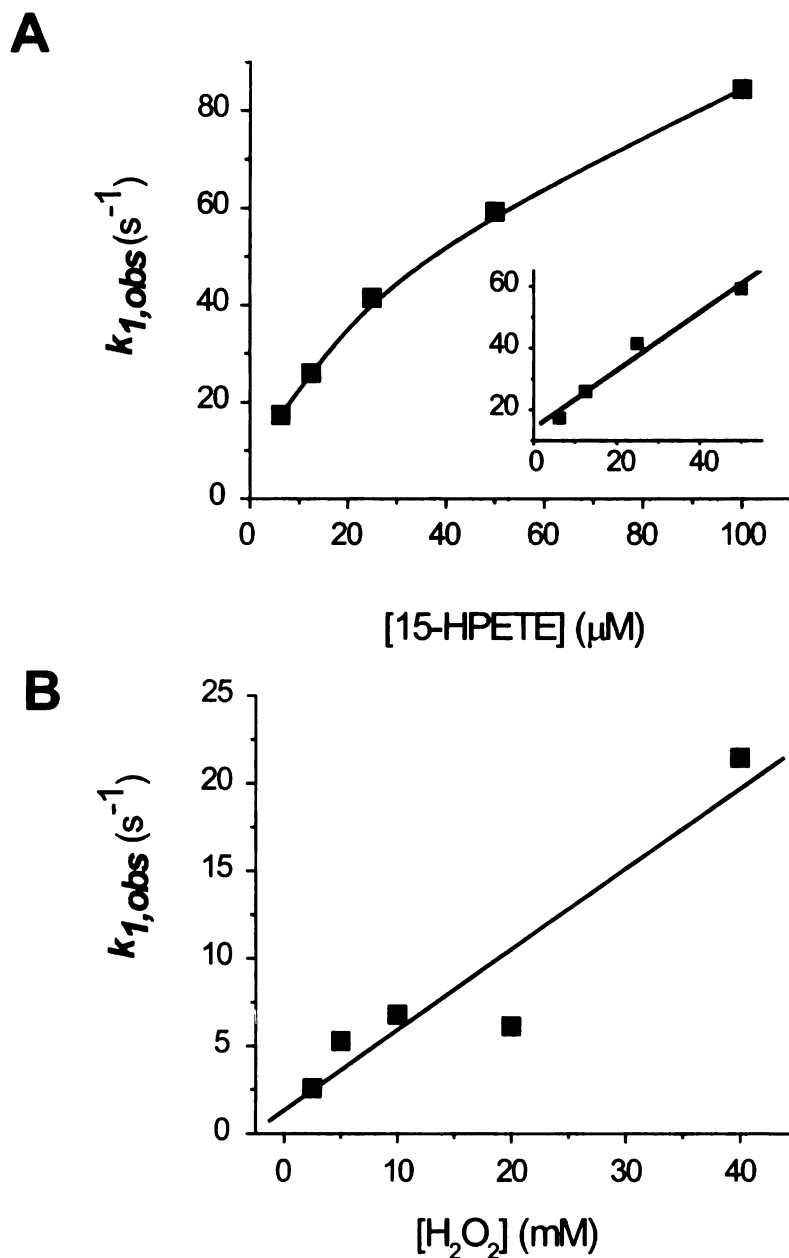


Figure 2.9: **Effect of Hydroperoxide concentrations on the rate Constants for Mn-PPIX ovPGHS-1 intermediate formation.** (A)  $k_{1(obs)}$  levels off at higher concentrations of 15-HPETE. Inset, linear fitting of  $k_{1(obs)}$  at lower 15-HPETE concentrations. (B)  $k_{1(obs)}$  for Compound I formation of Mn-PPIX ovPGHS-1 from H<sub>2</sub>O<sub>2</sub> is a linear function of the hydroperoxide substrate concentration. These two figures show kinetic properties of Mn<sup>3+</sup>-PPIX native ovPGHS-1 as a representative. The behaviors of the other mutant enzymes were similar except for L294D as parameters listed in Table 2.7.

Table 2.7: **Rate constants for Compound I formation by Mn<sup>3+</sup>-PPIX ovPGHS-1s.** Kinetic data were collected at 417 nm where Compound I, Compound II and Intermediate II exhibit increased absorbance upon addition of 15-HPETE or H<sub>2</sub>O<sub>2</sub>. The data were fitted to an A→B→C kinetic model to calculate  $k_{1,obs}$  and  $k_{2,obs}$  values because Compound II and Intermediate II are identical spectroscopically. Second order rate constants were obtained at saturating peroxide substrate concentrations.  $k_2$  values were not available in the case of L294A and L294D Mn<sup>3+</sup>-PPIX ovPGHS-1 with 15-HPETE and V291A Mn<sup>3+</sup>-PPIX ovPGHS-1 with H<sub>2</sub>O<sub>2</sub> because kinetic data fitting yielded decreasing first order rate constants versus hydroperoxide concentrations which could not be used to calculate  $k_{2,obs}$  at saturating concentrations. Rate constants for the reaction of Q203V ovPGHS-1 and H<sub>2</sub>O<sub>2</sub> were not determined for that there was no spectral change at any tested concentrations of H<sub>2</sub>O<sub>2</sub>. Each value was the mean of three duplicates.

Enzyme	15-HPETE		H <sub>2</sub> O <sub>2</sub>	
	$k_1$ (10 <sup>5</sup> M <sup>-1</sup> s <sup>-1</sup> )	$k_2$ (s <sup>-1</sup> )	$k_1$ (M <sup>-1</sup> s <sup>-1</sup> )	$k_2$ (s <sup>-1</sup> )
native	9.3±1.1	5.3±0.0049	510±59	3.6±1.1
L294G	13±2.7	6.7±0.0	140±16	13±6.7
L294A	8.4±0.7	N/A	270±13	18±0.43
V291A	6.6±1.4	14±1.0	24±1.3	N/A
V291A/L294A	6.0±0.47	3.3±7.8	79±3.7	5.5±0.36
L294E	0.097±1.6	0.21±0.050	89±4.4	1.5±0.15
L294D	3.1±0.26	N/A	65±11	4.4±0.65

Based on information in Tables 2.5 and 2.7, we conclude that hydrophobic residues of the distal heme active site are not important determinants of Compound I formation.

### 2.3.7 Cyanide Binding to the POX Active Site

The study of the binding of ligands to HRP c is an important source of information for understanding the structure and reactivity of the heme group and its immediate environment. Azide, in common with cyanide and fluoride, binds to HRP c as the undissociated acid. The interaction with hydrazoic acid results in a change to the

Table 2.8: **Effect of Val291 and Leu294 on  $\text{CN}^-$  binding to the heme group of ovPGHS-1.** Native or mutant ovPGHS-1 (1-2  $\mu\text{M}$ ) reconstituted with 0.8 mol heme/monomer were titrated with NaCN and the effects were examined spectrophotometrically. Shifts in the Soret absorbance peak from 411 to 424 nm (420 nm in case of Q203 mutants) were observed. The maximum absorbance changes at 430 nm were plotted as a function of cyanide concentration to obtain  $K_d$  values.

Protein	$K_{d,\text{CN}^-}$ (mM)
native	$0.41 \pm 0.04$
V291A	$0.06 \pm 0.004$
L294A	$0.33 \pm 0.002$
V291A/L294A	$0.14 \pm 0.03$
L294E	$0.59 \pm 0.05$

electronic properties of the heme iron atom, the extent of which is dependent on the concentration of ligand species present. Although the electronic structure of the azide-ligated state has not been defined precisely, it may be considered as a thermally mixed spin state with high-spin and low-spin character. The proportion of this species present may be increased by decreasing the pH of the azide-containing sample within the range pH 7.0-4.0.

In the present studies, cyanide is used as a probe to explore the electronic environment of the distal dome of the PGHS POX site with different side chain substitutions. Cyanide has outer sphere electrons with high spin state. Binding to high spin state iron in the heme group of PGHS POX causes red shifts of UV/Visible absorbance (Fig. 2.10A). The maximum light absorption changes at 430 nm showed saturation and  $K_d$  was obtained by fitting the data to Equation 2.6 (Fig. 2.10B).

As shown in Table 2.8 dissociation constants ( $K_d$ ) for the binding of  $\text{CN}^-$  to the heme group of native and several mutant PGHS were similar. This is consistent

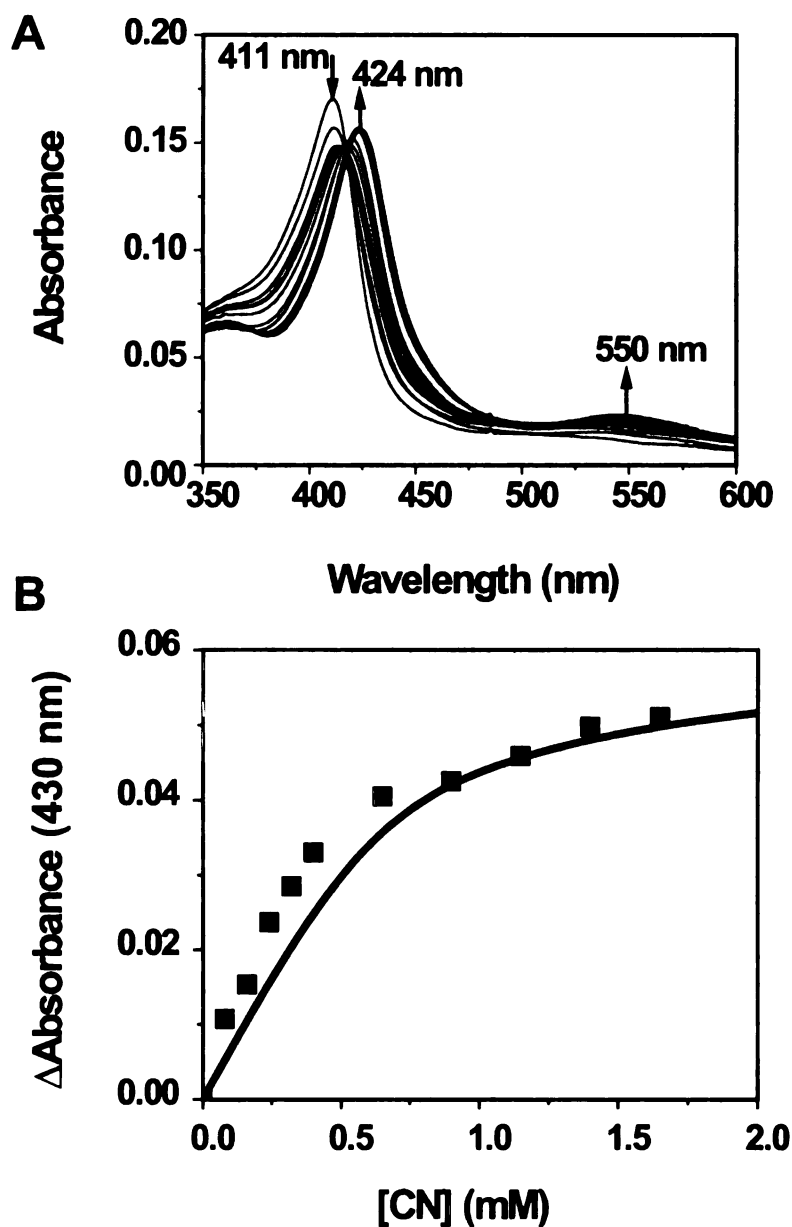


Figure 2.10: UV/Visible Absorbance of  $\text{Fe}^{3+}$ -PPIX native ovPGHS-1 with  $\text{CN}^-$  titration. (A) Titration of the proteins ( $1 \mu\text{M}$ ) with cyanide produces progressive shifts in the Soret absorbance peak from 411 to 424 nm. Arrows indicate the direction of spectral changes with increased  $\text{CN}^-$  concentrations. (B) UV-Visible absorbance changes of  $\text{Fe}^{3+}$ -PPIX native ovPGHS-1 with  $\text{CN}^-$  titration at 430 nm (close squares) and a simulation using Michaelis-Menten equation (solid line).

with the idea that hydrophobic residues of the dome have no major effects on the heme group.

### 2.3.8 COX Activation of OvPGHS-1 by Compound I Formation

At low concentrations of hydroperoxides, the lag time in COX catalysis is determined by the efficiency of Compound I formation and its conversion to Intermediate II. For native ovPGHS-1, a typical lag time in our assays was 10 s at a protein concentration of 23 nM. Side chain substitutions with glycine, alanine or aspartate had no influence on the lag times for oxygen consumption for mutant ovPGHSs (Table 2.9). L294E ovPGHS-1 had a lag three times longer than that for native ovPGHS-1, consistent with L294E ovPGHS-1 having a very low rate of Compound I formation.

**Table 2.9: Lag times and specific COX activities of Fe<sup>3+</sup>-PPIX ovPGHS-1s.** For the COX assays, enzyme protein (5-10  $\mu$ g) was injected into 3 ml of 0.1 M TrisHCl, pH 8.0, 100  $\mu$ M arachidonic acid containing 1 mM phenol and 5  $\mu$ M hematin. O<sub>2</sub> consumption was monitored using an O<sub>2</sub> electrode and recorded using DazyLab software. The specific cyclooxygenase (COX) activities were averaged from multiple ( $\geq 3$ ) independent protein preparations except for V291A/L294A ovPGHS-1 where only one enzyme preparation was analyzed.

Enzyme	Lag Time (s)	Specific COX Activity ( $\mu$ mol O <sub>2</sub> /min/mg)
native	10	34 $\pm$ 15
V291A	10	37 $\pm$ 19
L294A	10	25 $\pm$ 3
V291A/L294A	10	47
L294E	35	91 $\pm$ 38

## 2.4 Discussion

It is well established that lipid hydroperoxides are required for the COX activity of PGHSs [27, 118, 117, 1, 110, 111]. Peroxides function by oxidizing the heme group at the POX site of PGHSs which, in turn, leads to oxidation of Tyr385 in the COX site, and the Tyr385 radical abstracts a hydrogen from AA in the rate determining step in COX catalysis [1, 110, 111]. As described earlier, there are two PGHS enzymes, PGHS-1 and PGHS-2. PGHS-2 is activated at about a ten-fold lower lipid hydroperoxide concentration than PGHS-1 [119, 64, 66]. The biological importance of this difference in the peroxide requirements of PGHS-1 and PGHS-2 remains to be resolved. In principle, this would permit PGHS-2 to operate under conditions where PGHS-1 is not activated [120]. It is known that PGHS-2 can function at low AA concentrations in NIH 3T3 cells when PGHS-1 is latent [106], and this could be due to the negative allosteric behavior of PGHS-1 [68, 16] which can be overcome by addition of peroxides [66].

Previous studies by other laboratories have indicated that primary and secondary alkyl hydroperoxides are better peroxidase substrates [74, 1, 110, 111], and the results of our POX assays have confirmed and extended this by providing more accurate measurements. The basis for the peroxide substrate specificity has been an enigma because although the POX site of PGHSs is relatively open to solvent [43, 121, 122] it exhibits a preference for alkyl hydroperoxides over small, hydrophilic molecules such as  $\text{H}_2\text{O}_2$ . Modeling studies including our own have suggested that alkyl groups of secondary hydroperoxides (i.e.  $\text{PGG}_2$  derivatives) can interact with

residues in the hydrophobic “dome” that overlies a portion of the distal surface of the heme group at the PGHS POX site [54, 55]. However, modification of these residues had relatively small effects on POX catalytic efficiency or on the rates of Compound I formation from 15-HPETE. These relatively small effects seen with some mutants having substitutions of dome residues can be attributed to differences in the rates of reduction of oxidized heme intermediates by guaiacol.

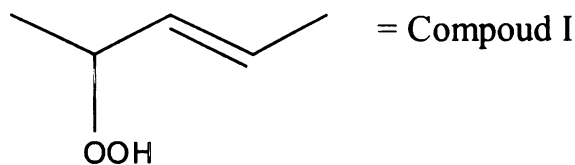
We examined the hypothesis that the hydroperoxide substrate specificity resides in the different reactivities of the O-O bonds of hydroperoxides toward heterolytic cleavage. It is surprising that the oxidant substrate specificity is not attributed to the chemical properties of the O-O bonds of hydroperoxides. Cukier and Seibold performed quantum mechanical (QM) calculations with different hydroperoxides in the gas phase to compare bond dissociation energies (BDE) of the peroxy group of different hydroperoxides (Table 2.10). The quantum chemical calculations were carried out by using the second-order Møller-Plesset perturbation method (MP2), as implemented in the Gaussian98 [123] software package. All the structures were geometry optimized and their vibrational frequencies calculated using the 6-311++G basis set, in which polarization and diffuse functions are included.

The calculations, in agreement with those of others [124, 125], demonstrated that a heterolytic O-O bond breakage required significantly higher energy activation than homolysis (e.g.  $\sim 360$  versus  $\sim 40$  kcal/mol). Studies clearly show that the enzyme active site, containing the proximal ligand of the heme-iron, the porphyrin redox properties, and the local protein structure (e.g. distal histidine and solvent water) can contribute to lowering the activation barrier for heterolytic cleavage [126, 127].

However, our experimental data suggested hydrophobic residues in the distal dome of heme do not significantly affect the interactions with lipid hydroperoxide substrates. The MP2 calculations indicate that no large difference ( $> 3$ - $13$  kcal/mol) exists between the BDEs of the small hydroperoxides and a larger carbon unit ( $C_5H_{10}O_2$ ) as shown in Table 2.10. Thus, presumably the hydroperoxide substrate specificity of PGHS POX is neither determined by key residues in the hydrophobic heme dome as previously thought, nor the intrinsic reactivity of hydroperoxides as QM calculations suggest.

Table 2.10: **Bond dissociation energies of different hydroperoxides.** Molecular orbital calculations were performed at the Møller-Plesset (MP2) level with the 6-311++G basis set to study the heterolytic and homolytic bond dissociation energies (BDE) of different hydroperoxides. The calculations were kindly provided by Drs. Cukier and Seibold. N/A, not available.

	Heterolytic O-O (kcal/mol)	Homolytic O-O (kcal/mol)
H <sub>2</sub> O <sub>2</sub>	377	46
MeOOH	374	43
EtOOH	370	45
Compound I	364	N/A



In order to understand the structural basis for the hydroperoxide substrate specificity, the impact of hydroperoxide binding to the POX active site need to be re-evaluated. Fig. 2.11 compares POX active sites of a crystal structure (1DIY) [44] and models with PGG<sub>2</sub> (Cukier and Seibold, unpublished data) or H<sub>2</sub>O<sub>2</sub> [128] simulated

by molecular dynamics (MD). There appears to be no change in the conformation of the active site of ovPGHS-1 with and without PGG<sub>2</sub> bound (Fig. 2.11A). MD simulation suggests that a peroxy-iron bond and a hydrogen bond with His207 of PGG<sub>2</sub> are formed as commonly seen in other peroxidases. Not surprisingly, MD simulation with PGG<sub>2</sub> also appears to show van der Waals interactions involving methylene groups adjoining the carbon bearing the peroxy group of PGG<sub>2</sub> and the protoporphyrin IX. However, the latter interactions are lacked for H<sub>2</sub>O<sub>2</sub> binding. We speculate that interactions between hydroperoxide substrate and the heme group other than a peroxy-iron bond are major contributors to PGHS POX specificity.

As alluded to previously, secondary alkyl hydroperoxides may adapt alternate conformations to bind the PGHS POX site via interactions between two lipid tails and a number of residues in the POX active site pocket [55]. This study indicated that removal of residues Lys211 and Lys212 in the far end of the POX active site (Fig. 2.12), e.g. K211A mutation, seemed to abolish PGE<sub>2</sub> formation by PGHS-transfected COS-1 cells. The same study using MD simulation also suggested that Lys211, Gln289 and Glu290 seemed to form a shallow groove that may accommodate a tail of PGG<sub>2</sub>, presumably, by the carboxyl end, and the  $\omega$ -end of fatty acid derived hydroperoxide appeared to bind the hydrophobic “dome” of the POX active site. We have shown that attenuation of potential hydrophobic interactions between the hydrophobic cluster (Val291, Leu294, Leu295, Leu408 and Phe409) and 15-HPETE was not sufficient to block the binding. In addition, it is not clear whether the protein was correctly folded, bound heme in the same way as the native enzyme, or how these mutations affected enzymatic reactions of PGHS in cells, e.g. whether the

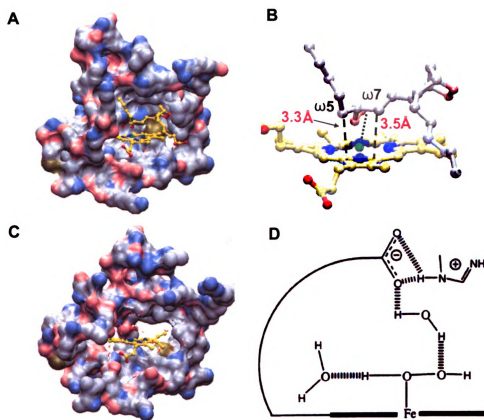


Figure 2.11: Molecular Dynamics Simulations with PGG<sub>2</sub> or H<sub>2</sub>O<sub>2</sub>. (A) A model of the POX site with PGG<sub>2</sub> (Cukier and Seibold, unpublished data). Carbons in surface model are shown in gray, nitrogens in light blue, and sulfurs in tan. Carbons in stick-ball models are shown in yellow, nitrogens in blue, oxygens in red and iron in green. (B) Interactions between PGG<sub>2</sub> and the heme group in the ovPGHS-1 POX active site. Structure coordinates are the same as used in (A). The peroxy-iron bond is formed, and the distances between the heme and the carbons adjacent to the carbon bearing the peroxy group are within reasonable van der Waals radii. In PGG<sub>2</sub> molecule, carbons are in gray and oxygens in light red. In the heme group, carbons are shown in yellow, oxygens in red, nitrogens in blue and iron in green. (C) Model of the POX site with H<sub>2</sub>O<sub>2</sub> [128]. H<sub>2</sub>O<sub>2</sub> is shown in a stick model and water molecules are in fine lines. Color designations are the same as described in (A). (D) A hydrogen bonding network in the MD simulation with H<sub>2</sub>O<sub>2</sub>. This figure is cited from [128]. Unit: Å. (Coordinates of MD simulations are kindly provided by Cukier and Seibold.) Images in this thesis/dissertation are presented in color.

K211A mutation disrupted the interactions of the reducing substrate to the active site which decreased the product formation. It will be valuable to perform pre-steady-state analysis with the mutation(s) (e.g. K211A) in the far end of the POX site which might be the determinant for the the binding of alkyl hydroperoxides to the PGHS POX.

MD simulations showed that substantial space existed in the POX active site in the MD simulation with  $\text{H}_2\text{O}_2$  which resulted in accommodation of a series of water molecules in the active site area (Fig. 2.11B) [128]. The distance between  $\epsilon$ -N of His207 and the heme iron increased from 5 Å without ligand (1DIY) to 8 Å with  $\text{H}_2\text{O}_2$  bound. In the POX active site with  $\text{H}_2\text{O}_2$  bound His207 appears to be out of hydrogen bonding distance from  $\text{H}_2\text{O}_2$  ( $\sim 6$  Å). Although water may mediate the deprotonation of  $\text{H}_2\text{O}_2$  through a proton transfer wire, His207-heme 7-propionate-water- $\text{H}_2\text{O}_2$  [128], the function of deprotonation may not be as efficient as via direct hydrogen bonding between His207 and  $\text{H}_2\text{O}_2$ . In addition, water can also be an unfavorable factor for  $\text{H}_2\text{O}_2$  binding in that it appears to have a higher affinity for ferric iron than  $\text{H}_2\text{O}_2$  [129], and  $\text{H}_2\text{O}_2$  must compete with water to form the peroxy-iron intermediate in the reaction.

For the case of  $\text{PGG}_2$ , it is possible that it may interact with active site residues and exclude water from the active site, easily forming a peroxy anion intermediate ( $\text{ROO}^- - \text{H}^+$ ). When PGHS had EtOOH or  $\text{PGG}_2$  docked, both compounds had non-polar interactions with local residues. So the pocket entrance was not as open (active site volume is occupied) and less, if any water gained access into interior for

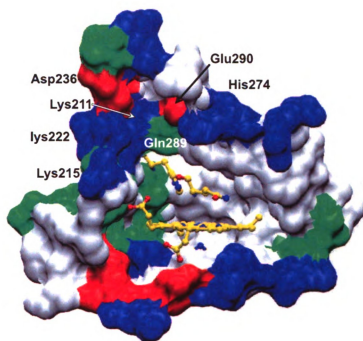


Figure 2.12: **Surface model of the POX active site.** The POX active site of ovPGHS-1 (1DIY) has a polar far end containing neutral (green), positive (blue) and negative (red) charged residues as indicated. The heme group, distal histidine and glutamine are shown in a stick-ball model. PDB code is 1DIY.

larger substrates. However,  $\text{H}_2\text{O}_2$  does not have these interactions and water gains admission and competes with  $\text{H}_2\text{O}_2$  substrate.

The physiological hydroperoxide initiator of the COX reaction is not known. Lipid peroxides can be formed both nonenzymatically from reactive oxygen species and polyunsaturated fatty acids in membrane lipids [18]. Oxidative stress induced by  $\text{H}_2\text{O}_2$  or *t*-BuOOH treatment of calf corneal fibroblasts increases the formation of  $\text{PGE}_2$  perhaps due to concomitant generation of lipid hydroperoxides that, in turn, stimulate PGHS COX activity [130]. Lipid peroxides can also be formed enzymatically through the actions of 5-, 12- and 15-lipoxygenases, which typically oxygenate free polyunsaturated fatty acids. Lipoxygenases are often found in the nuclear envelope and/or ER [131, 132] which is also the subcellular location of PGHSs [5, 7]. However, knock-out mice lacking platelet 12-lipoxygenase do not exhibit a platelet phenotype that would be expected were 12-lipoxygenase providing hydroperoxide for activation of PGHS-1 [133].

$\text{H}_2\text{O}_2$  is mostly found in the mitochondrial respiratory chain and there is no direct evidence showing  $\text{H}_2\text{O}_2$  exists in the lumen of the ER or nuclear envelope. And if present, the subcellular concentrations of  $\text{H}_2\text{O}_2$  are probably two orders of magnitude lower than in normally respiring mitochondria [134, 135].

One difficulty in identifying physiological reducing substrates for PGHS is that the redox state of the lumen of the ER and nuclear envelope where PGHS isoforms are found is oxidizing. Common reducing compounds are mostly found in the cytosol. The oxidative state of the ER determined as a GSH/GSSG ratio is 1:1-1:3, while the ratio is 100:1 in the cytosol [80]. Possible candidates for the reducing substrate

might be compounds that readily diffuse into the ER. For example, it is known that coenzyme Q can be detected in the ER and in subcellular membranes in addition to the inner membrane of mitochondria [81]. Reduced coenzyme Q is a good anti-oxidant and its phenolic structure suggests it may be used as a good reducing substrate for PGHS as mentioned by Marnett and coworkers [79]. Additionally, coenzyme Q is also capable of generating  $H_2O_2$  which triggers lipid peroxidation spontaneously [82]. Thus, coenzyme Q may function as the endogenous reducing reagent for PGHS.

# Chapter 3

## The Role of Q203 in PGHS

### Peroxidase Catalysis

#### 3.1 Introduction

The cyclooxygenase (COX) activity of prostaglandin endoperoxide H synthase (PGHS) is initiated by its peroxidase (POX) activity (Fig. 1.2) [1]. The PGHS POX active site contains a prosthetic group ferric protoporphyrin IX ( $\text{Fe}^{3+}$ -PPIX or heme *b*, Fig. 1.7). The reaction cycle of the PGHS POX is similar to classic heme peroxidases [28]. Resting enzyme cleaves the O-O bond of a hydroperoxide heterolytically, as most peroxidases do, and generates a corresponding alcohol and Compound I. The latter is an oxy-ferryl heme radical that is two oxidative states above the resting enzyme, with one electron from heme iron and one from the protoporphyrin. The reduction of the heme radical by Tyr385 produces a tyrosyl radical which is the initiator of the COX reaction.

The formation of Compound I of PGHS POX requires heterolytic cleavage of the O-O bond, which is believed to be facilitated by the heme group, along with distal histidine and glutamine residues [40]. His207 act as a general base and Gln203 stabilizes a transient state of  $\beta$ -oxygen (Fig. 3.1) [40, 136]. The role of Gln203, which is located four amino acids away from the distal histidine, has been thought to be critical for Compound I formation [40]. Elimination of the amide group of the Gln203 side chain (i.e. Q203V mutation) of muPGHS-2 resulted in an inactive peroxidase as shown by Marnett and coworkers [40]. Thus, it was proposed that Gln203 is an essential catalytic residue for the POX reaction, as well as the COX activity.

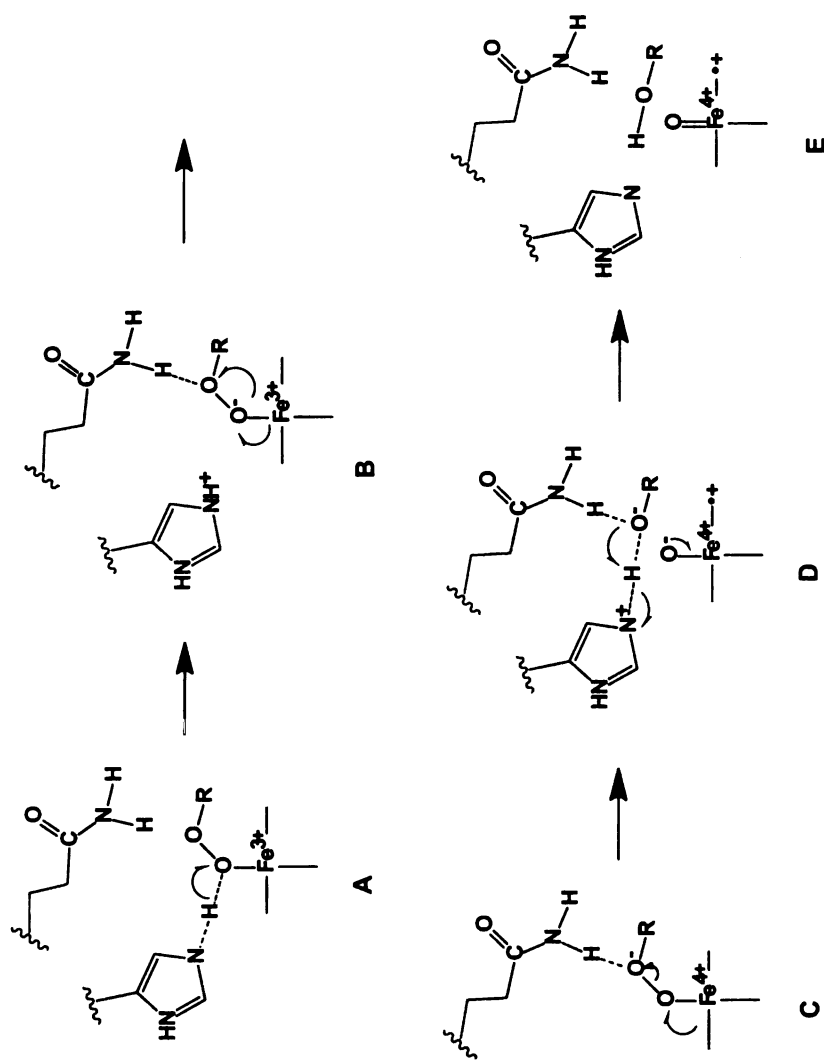


Figure 3.1: **Proposed mechanism for the formation of Compound I.** (A) His207 deprotonates the  $\alpha$ -oxygen of the hydroperoxide substrate (ROOH) and possesses a positive charge. (B) The  $\alpha$ -oxygen accepts one electron from the ferric ion, and it is delocalized to the  $\beta$ -oxygen which is stabilized by Gln203 via hydrogen bonds. The  $\beta$ -oxygen gains a negative charge. (C) The  $\alpha$ -oxygen obtains the second electron from the protoporphyrin group. The O-O bond breaks with the electron pair to the  $\beta$ -oxygen. (D) The  $\beta$ -oxygen forms a double-bond with the ferryl ion. On the other hand, the  $\beta$ -oxygen is hydrogen bound to His207. (E) The  $\beta$ -oxygen is protonated and leaves the POX active site as a corresponding alcohol. This diagram is modified from Ref. [136] and [40]

The distal glutamine is conserved in human peroxidases including PGHS, myeloperoxidase (MPO), lactoperoxidase (LPO), eosinophil peroxidase (EPO) and thyroid peroxidase (TPO) [137]. The similarities between the genes and the chromosomal locations of these mammalian proteins suggest that their sequences are highly conserved (>50%) and the genes are probably originated from the same ancestor [137]. PGHS shares only about 20% identical sequence with MPO, mostly within the region involving the POX active site. MPO, LPO, EPO and TPO are important for the cells in self-defense against microbes by raising levels of offensive oxidative molecules at the expense of H<sub>2</sub>O<sub>2</sub> in the peroxisome. These POXs are highly active to H<sub>2</sub>O<sub>2</sub> (e.g.  $k_1$  value for Compound I formation for MPO is about  $10^8 \text{ M}^{-1}\text{s}^{-1}$ ). But PGHS is much less active with H<sub>2</sub>O<sub>2</sub> ( $k_1$  is about  $10^4$ - $10^5 \text{ M}^{-1}\text{s}^{-1}$  for Compound I formation). The structural basis for the different H<sub>2</sub>O<sub>2</sub> catalytic efficiencies of PGHS and other POXs (e.g. MPO) is unknown. The axial histidines are essential for the POX catalysis; however, the roles of the distal glutamine in the POX active site for mammalian peroxidases have not been elucidated except for PGHS.

Plant/fungal/bacterial POXs [e.g. horseradish peroxidase (HRP) and cytochrome c peroxidase (CcP)] are also highly active to H<sub>2</sub>O<sub>2</sub>. Interestingly, the distal glutamine in PGHS POX is replaced by an arginine in fungal and plant peroxidases. Mutating the distal arginine of HRP to a leucine reduced the rate constant for Compound I formation ( $k_1=10^8 \text{ M}^{-1}\text{s}^{-1}$ ) by  $10^3$  fold [115, 91]. And the  $k_1$  value for CcP also decreased by 2 orders of magnitude when the distal arginine was mutated to leucine [90]. Previous work demonstrated that Gln203 in muPGHS-2 was essential for the catalysis for 15-HPETE but H<sub>2</sub>O<sub>2</sub> was not tested [40]. Our mutagenic and

kinetic studies addressed the catalytic roles of Gln203 mutant PGHSs with different hydroperoxides.

## 3.2 Materials and Methods

**Materials:** Materials for purifications and activity assays are described in Chapter 2 Materials and Methods. Hexanes, isopropanol and acetic acid were HPLC grade from Fisher Scientific.

**Mutagenesis, protein expression and purification:** A site-directed mutagenesis protocol was used as described in Chapter 2 Materials and Methods to mutate Gln203 in ovine (ov) PGHS-1, human (hu) PGHS-2 and murine (mu) PGHS-2. The primers are as follows:

Q203V ovPGHS-1, forward: 5'-GCC TTC TTT GCC GTA CAC TTC ACC CAT CAG-3'; backward: 5'-CTG ATG GGT GAA GTG TAC GGC AAA GAA GGC-3'.

Q203N ovPGHS-1, forward: 5'-GCC TTC TTT GCC AAC CAC TTC ACC CAT CAG-3'; backward: 5'-CTG ATG GGT GAA GTG GTT GGC AAA GAA GGC-3'.

Q203R ovPGHS-1, forward: 5'-GCC TTC TTT GCC CGA CAC TTC ACC CAT CAG-3'; backward: 5'-CTG ATG GGT GAA GTG TCG GGC AAA GAA GGC-3'.

Q203V huPGHS-2, forward: 5'-GCA TTC TTT GCC GTG CAC TTC ACG CAT CAG-3'; backward: 5'-CTG ATG CGT GAA GTG CAC GGC AAA GAA TGC-3'.

Q203V muPGHS-2, forward: 5'-GCA TTC TTT GCC GTG CAC TTC ACG CAT CAG-3'; backward: 5'-CTG ATG CGT GAA GTG CAC GGC AAA GAA TGC-3'.

The sequences of the plasmids containing PGHS genes were confirmed in the University of Michigan DNA Sequencing Core. Protein expression and purification were carried out as described in Chapter 2 Materials and Methods.

**POX and COX Activity assay:** Different species of purified Gln203 mutant proteins were subjected to the activity assays as described in Chapter 2 Materials and Methods.

**Identification of POX Spectral Intermediates and Kinetic Analysis:** Q203V ovPGHS-1 was re-constituted with hematin or mangano PPIX and subjected to stopped-flow UV-Vis spectroscopy while reacting with 15-hydroperoxyeicosatetraenoic acid (15-HPETE) or H<sub>2</sub>O<sub>2</sub> to identify potential intermediates as described in Chapter 2 Materials and Methods.

**Cyanide Binding Assay** Purified Gln203 mutant proteins were titrated by concentrated cyanide solution as described in Chapter 2 Materials and Methods.

**Analysis of 15-HPETE reaction in products:** A POX reaction was conducted in a 500  $\mu$ l reaction mixture containing 100 nM of native ovPGHS-1 or Q203V ovPGHS-1, 50  $\mu$ M hematin, and 4.5 mM phenol in 100 mM TrisHCl, pH 8.0, at room temperature. The reaction was initiated by adding 5  $\mu$ M 15-HPETE and

terminated at 2 min by adding 1.5 ml of a pre-cooled (4 °C) mixture of diethyl ether/methanol/0.2 M citric acid (30:4:1). 5-Phenyl-4-pentenyl-alcohol (PPA; 5 μM) was added as an internal control. The organic phase was shaken with 380 μl of a saturated NaCl solution at 4 °C to remove H<sub>2</sub>O. The upper organic layer was transferred to a clean tube and evaporated under N<sub>2</sub>O. The products were dissolved in 100 μl of hexane:isopropanol:acetic acid (987:12:1; running solution) [40] and resolved by HPLC on a Nucleosil Silica column (5 μm, 250×4.6 mm, Cobert Associates) mounted on a Shimadzu HPLC system equipped with a diode array detector. The bound products were eluted with running solution at a flow rate of 1 ml/min. 15-HPETE and 15-hydroxy-eicosatetraenoic (15-HETE) were monitored at 236 nm and 15-keto-eicosatetraenoic acid (15-KETE) at 279 nm. PPA was eluted after the 15-HPETE, 15-HETE and 15-KETE and had a strong UV absorption at 249 nm.

### **3.3 Results**

#### **3.3.1 The POX Activities of Gln203 Mutant OvPGHS-1s**

Three Gln203 mutant ovPGHS-1, Q203R, Q203N and Q203V, were constructed as described in Chapter 2. The arginine substitution resulted in an inactive enzyme when 15-HPETE or H<sub>2</sub>O<sub>2</sub> was used as substrates (Table 3.1). The ovPGHS-1 mutant Q203N with a conservative but smaller side chain retained about 20% and 7% of native peroxidase activity with 15-HPETE and H<sub>2</sub>O<sub>2</sub>, respectively. Eliminating the amide group of the Gln203 side chain was reported to eliminate the POX activity

of muPGHS-2 [40]. However, it is surprising that  $k_{cat}$  value of Q203V ovPGHS-1 with 15-HPETE was about 50% of that of native ovPGHS-1, and it also was active with  $H_2O_2$  as substrate. It is unclear why the Q203V muPGHS-2 mutant reported previously lacked activity [40].

**Table 3.1: Gln203 mutations in the PGHS distal active site altered guaiacol peroxidase activities** Mutant ovPGHS-1s were purified as described in Chapter 2 Materials and Methods. POX assays were performed using stopped flow measurements.  $k_{cat}$  and  $K_m$  values were calculated from the Michaelis-Menten equation (Equation 2.1). N/A, not applicable. Each value is the average of triplicate determinations.

Enzyme	15-HPETE			$H_2O_2$		
	$k_{cat}$ ( $s^{-1}$ )	$K_m$ ( $\mu M$ )	$k_{cat}/K_m$ ( $\mu M^{-1}s^{-1}$ )	$k_{cat}$ ( $s^{-1}$ )	$K_m$ (mM)	$k_{cat}/K_m$ ( $mM^{-1}s^{-1}$ )
Native	270±2.7	14±0.5	19	150±13	2.9±0.4	54
Q203V	135±2.0	42±2.2	3.2	37±4.7	17±3.1	2.3
Q203N	53±2.4	80±11	0.7	11±2.2	8.4±2.8	1.3
Q203R	0	N/A	N/A	0	N/A	N/A

### 3.3.2 The Formation of Compound I for Gln203 Mutant PGHSs

The intermediate Compound I was not formed with  $Fe^{3+}$ -PPIX Q203V ovPGHS-1 from either 15-HPETE or  $H_2O_2$ . However, when re-constituted with  $Mn^{3+}$ -PPIX, Q203V ovPGHS-1 produced intermediate species with a lower absorbance at 417 nm than other  $Mn^{3+}$ -PPIX ovPGHS-1 variants as discussed in Chapter 2, suggesting that Gln203 may play a role in Compound I formation. Nonetheless, the UV-vs spectra of  $Fe^{3+}$ - or  $Mn^{3+}$ -PPIX reconstituted Q203V ovPGHS-1 was the same as those of native enzyme at the resting state, implying that the heme binding environment was not altered by mutating Gln203 to valine. Kinetic traces of the reactions with  $Mn^{3+}$ -

PPIX Q203V ovPGHS-1 and varying concentrations of 15-HPETE also showed two phases similar to those shown in Fig. 2.8B, which suggested that the reaction had three species as follows: Mn-PGHS→Compound I→Compound II/Intermediate II. Fitting these traces to a two-consecutive-step model yielded first order rate constants  $k_{1(obs)}$  and  $k_{2(obs)}$  for the formation of Compound I and Compound II/Intermediate II complex, respectively. The second-order rate constants  $k_1$  and  $k_2$  were calculated as described in Chapter 2. Mn<sup>3+</sup>-PPIX Q203V ovPGHS-1 did not have any spectral change with H<sub>2</sub>O<sub>2</sub>.  $k_1$  value for the formation of Compound I of Mn-PPIX Q203V ovPGHS-1 with 15-HPETE was only slightly lower than that of native enzyme (Table 3.2), suggesting that the Q203V substitution had trivial effect on Compound I formation.

**Table 3.2: Rate constants for Compound I Formation from Q203V Mn<sup>3+</sup>-PPIX ovPGHS-1.** Kinetic traces collected at different 15-HPETE concentrations were fitted to two-exponential equations to obtain  $k_{1(obs)}$  and  $k_{2(obs)}$ . Second-order rate constants were calculated as described in Chapter 2.

Enzyme	15-HPETE		H <sub>2</sub> O <sub>2</sub>	
	$k_1$ ( $10^5$ M <sup>-1</sup> s <sup>-1</sup> )	$k_2$ (s <sup>-1</sup> )	$k_1$ (M <sup>-1</sup> s <sup>-1</sup> )	$k_2$ (s <sup>-1</sup> )
native	9.3±1.1	5.3±0.0049	510±59	3.6±1.1
Q203V	3.5±0.85	8.1±0.53	N/D	N/D

### 3.3.3 Cyanide Binding to the Active Site

The integrity of the POX active site in Gln203 mutant ovPGHS-1s was further investigated by testing the affinity of the enzyme for CN<sup>-</sup>. The Soret peaks of Gln203 mutant ovPGHS-1s are the same as that of the native enzyme, but they become red-shifted to 420 nm at a saturating concentration of CN<sup>-</sup>, instead of 424 nm for the

native and other mutant ovPGHS-1 with hydrophobic residue substitutions described in Chapter 2. This suggested that valine and arginine substitutions of Gln203 did not affect heme association but disturbed the electronic environment of the distal ligand binding site. As shown in Table 3.3 dissociation constants ( $K_d$ ) for the binding of  $CN^-$  to the heme group of native and Gln203 mutant PGHSs were similar. Hence, the interference of the distal ligand binding site by Gln203 mutations had no significant effect.

**Table 3.3: Effect of Gln203 on  $CN^-$  binding to the heme group of ovPGHS-1.** Native and mutant ovPGHS-1 (1-2 M) reconstituted with 0.8 mol heme/monomer were titrated with NaCN and the effects were examined spectrophotometrically. Shifts in the Soret absorbance peak from 411 to 424 nm (420 nm for Gln203 mutants) were observed. Plotting maximum absorbance changes at 430 nm as a function of cyanide concentration identified a saturable value and permitted calculation of  $K_d$  values.

Protein	$K_{d,CN^-}$ (mM)
native	$0.41 \pm 0.04$
Q203V	$1.01 \pm 0.05$
Q203R	$0.83 \pm 0.08$

### 3.3.4 Product Analysis of Guaiacol Peroxidase Assays

Kinetic analysis suggested that Q203V ovPGHS-1 was able to form a Compound I-like species and activate COX activity. This was confirmed by analysis of the products formed from 15-HPETE [40]. Hydroperoxides can undergo homolytic or heterolytic cleavage of the O-O bond. The type of cleavage is determined by the heme environment [138, 40]. Free  $Fe^{3+}$ -PPIX only catalyzes homolytic cleavage and at low rates. Addition of a fifth heme ligand in peroxidases dramatically increases the turnover numbers and the proportion of heterolysis rises depending on the distal

ligands. 15-HPETE can undergo heterolytic or homolytic cleavage leading to the alcohol (15-HETE) or ketone (15-KETE), respectively. PGHS-1 is reported to catalyze 95% heterolytic cleavage of the O-O bond of 15-HPETE, while PGHS-2 catalyzes 60% heterolytic cleavage [40].

Shown in Fig. 3.2 are normal phase HPLC chromatograms of difference profiles for products generated by native and Q203V ovPGHS-1 with 15-HPETE and guaiacol when the proteins were reconstituted with heme (0.5 heme/monomer). For both enzymes 15-HETE was the major lipid product from 15-HPETE. There was little or no detectable 15-KETE, although another species eluted at 11.6 minutes, having doublet peaks at around 280 nm. This species may be a lipid derivative containing three conjugated double bonds, but its identification was not pursued. There was a small amount of 15-HPETE remaining in the reaction mixture when heme-reconstituted enzyme and lipid hydroperoxide concentrations were 50 nM and 5  $\mu$ M, respectively. These results showing equal amounts of 15-HETE formation by native and Q203V ovPGHS-1 support the conclusion that Gln203 is not essential for heterolytic cleavage of hydroperoxide substrates by PGHSs.

### **3.3.5 COX Activation Influenced by Q203V Substitution**

Q203V ovPGHS-1 appeared to be fully functional with regard to its specific COX activity (Table 3.4). Comparing with the native enzyme, there is no obvious longer lag time to activate the COX reaction of Q203V ovPGHS-1 using AA as the COX substrate. This is consistent with our observations that Q203V Mn-ovPGHS-1 yielded

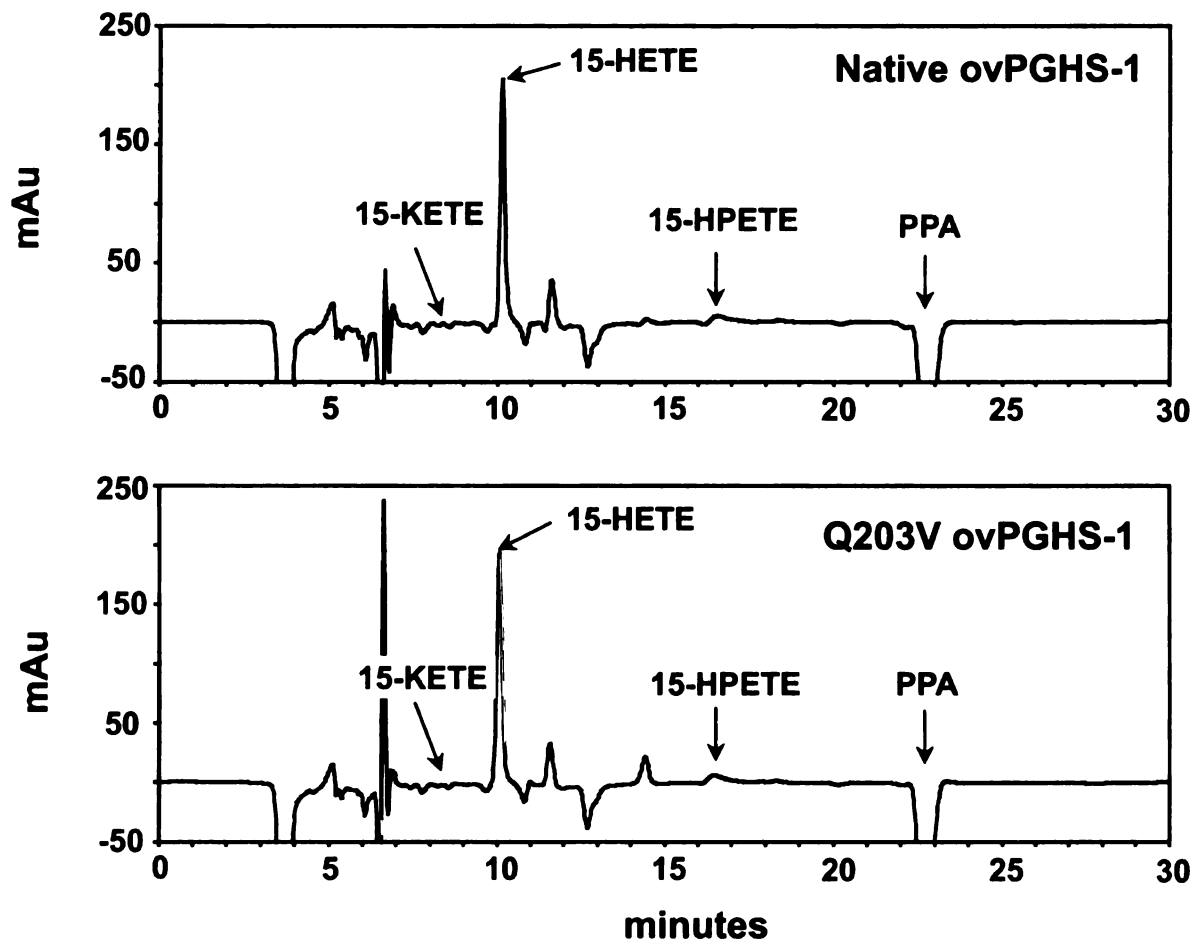


Figure 3.2: **Gln203 is not essential for heterolytic cleavage of the O-O bond of 15-HPETE by  $\text{Fe}^{3+}$ -PPIX ovPGHS-1.** POX assay mixtures were extracted as described in Methods and Materials, and separated on a HPLC silica column ( $5\ \mu\text{m}$ ,  $250\times 4.6\ \text{mm}$ , Cobert Associates). The chromatograms represent difference spectra after subtracting values for two controls, 15-HPETE plus heme alone for the non-enzymatic reaction and  $\text{Fe}^{3+}$ -PPIX ovPGHS alone. The arrows indicated the elution times of chromatographic standard, 15-HPETE, 15-HETE, 15-KETE, and PPA.

Compound I as efficiently as the native enzyme. Q203V mutation of two other PGHS species, huPGHS-2 and muPGHS-2, also exhibited reasonable COX activities (31 and 39  $\mu\text{mol O}_2/\text{min}/\text{mg}$  for specific COX activities of huPGHS-2 and muPGHS-2, respectively). Again, there is no appropriate interpretation for the inactive Q203V muPGHS-2 COX reported previously.

**Table 3.4: Lag times and specific COX activities of Gln203 mutant  $\text{Fe}^{3+}$ -PPIX ovPGHS-1s** PGHSs used in this set of experiments were all ovine species and were averaged from multiple protein preparations. The COX assays were carried out as described in Chapter 2 Materials and Methods. N/A, not applicable.

Enzyme	Lag Time (s)	Specific COX Activity ( $\mu\text{mol O}_2/\text{min}/\text{mg}$ )
native	10	$34 \pm 15$
Q203V	11	$32 \pm 17$
Q203R	N/A	0

### 3.4 Discussion

Glutamine in the distal “dome” of the heme active site is conserved in mammalian peroxidases [93, 137]. Its counterpart in plant/fungal/bacterial POXs is an arginine which has been shown to be critical for catalysis with  $\text{H}_2\text{O}_2$  and Compound I formation [139]. However, our data, consistent with previous observations with muPGHS-2, confirmed that a distal arginine was not suitable for the particular situation of PGHSs.

In my experiments with all three species of PGHSs, Q203V substitution did not abolish catalytic activities. We do not have an appropriate interpretation for the discrepancy that  $\text{Fe}^{3+}$ -PPIX Q203V ovPGHS-1 did not form spectral Compound I from hydroperoxides in the same way as native enzyme did, but the  $k_1$  value from

intermediate formation of  $\text{Mn}^{3+}$ -PPIX Q203V ovPGHS-1 with 15-HPETE was comparable with that of native ovPGHS-1 (Table 3.2), and calculations for  $k_1$  were also consistent with the observations that the COX of Q203V ovPGHS-1 had the same behavior as native enzyme (Table 3.4).

It is interesting that the Q203V mutation had a more profound influence on the POX activity with  $\text{H}_2\text{O}_2$  than with 15-HPETE. Q203V ovPGHS-1, using either  $\text{Fe}^{3+}$  or  $\text{Mn}^{3+}$  form, showed no spectral change with  $\text{H}_2\text{O}_2$ , suggesting that there was no Compound I formation. This mutant enzyme also had only 20% POX activity of the native enzyme with  $\text{H}_2\text{O}_2$ , but retained 50% with 15-HPETE. Furthermore, Q203V ovPGHS-1 had the same COX activity with AA as native enzyme (Table 3.4), suggesting that Q203V PGHS can be activated by alkyl hydroperoxide. In contrast, we presume that the COX activity of Q203V ovPGHS-1 will not be activated by  $\text{H}_2\text{O}_2$  because a spectral intermediate of Q203V ovPGHS-1 was never formed from  $\text{H}_2\text{O}_2$ .

Molecular dynamics simulations suggest that native ovPGHS-1, with  $\text{H}_2\text{O}_2$  as a substrate, had an expanded POX site which accommodated more water molecules than the situation without substrate (Fig. 2.11B) [128]. Q203V substitution in the PGHS POX site creates an even larger space for competing water molecules, which, in turn, results in lower POX activity. It is also assumed that a smaller side chain like alanine at position 203 will completely quench the PGHS POX activity with  $\text{H}_2\text{O}_2$  and guaiacol by allowing for entry of more water. Thus, we hypothesize that Gln203 is required for the binding of  $\text{H}_2\text{O}_2$  in such a way that it excludes water as a competitor for the sixth coordination of the heme iron in the PGHS POX site [129].

Our studies on the distal “dome” of the PGHS POX suggest that while the distal Gln203 is not essential for binding alkyl hydroperoxides, it may be critical for interactions with small, polar hydroperoxide substrates such as H<sub>2</sub>O<sub>2</sub>.

# Chapter 4

## Cross-talk between POX and COX Active Sites of PGHS Homodimer

### 4.1 Introduction

Prostaglandin endoperoxide H synthases (PGHSs) function as homodimers with each monomer having spatially distinct cyclooxygenase (COX) and peroxidase (POX) sites (Fig. 4.1A) [1, 140, 111, 141]. PGHS COX converts arachidonic acid (AA) to prostaglandin G<sub>2</sub> (PGG<sub>2</sub>), and the POX reduces PGG<sub>2</sub> to prostaglandin H<sub>2</sub> (PGH<sub>2</sub>) (Fig. 1.1). The activation of COX reaction requires a Tyr385 radical generated by the heme-dependent catalysis of POX (Fig. 1.2). Non-steroidal anti-inflammatory drugs (NSAIDs) are PGHS COX inhibitors.

Like many oligomerized enzymes [142, 143, 144, 145], PGHS activities are manipulated by cross-talk between the active sites. The tryptic susceptibility of a peptide sequence (residues 272-283 of ovine PGHS-1) on the PGHS-1 peroxidase active site

[146] is prevented by treatment with PGHS COX inhibitor flurbiprofen. A negative allosteric effect is also observed between the monomers. Complete inhibition of PGHS by NSAIDs appears to require only one binding site [147, 148, 149, 150]. A recent investigation by Smith and coworkers revealed that AA or NSAIDs binding to one monomer of PGHS caused residue rearrangements involving the dimerization interface of PGHS-2 (Yuan, unpublished data) and reduced the affinity of the other monomer [151], strongly supporting the hypothesis that there is cross-talk between the two COX sites of the partnering monomers.

Although allosteric regulation is also seen in many heme proteins [152, 153, 154], it is difficult to predict whether POXs are allosteric sites from the structure (Fig. 1.4). However, a possible interaction between the two POX sites may occur via tyrosyl radical dynamics. All the radicals formed during the POX reactions are identified to reside on tyrosines among which Tyr385 is essential for COX activation [155, 156, 71, 72, 157, 158]. Radical migration is suggested between Tyr385 and Tyr504 (in the proximal POX site) when a COX inhibitor is bound to PGHS-2 [159]. And the formation of Tyr385 radical appeared to be facilitated by Tyr348 [158]. There are seven tyrosines in the dimerization interface of muPGHS-2 (Tyr65, 130, 134, 136, 147, 373 and 544). In the present studies, I tested the possibility of radical migration in huPGHS-2 to determine if there was cross-talk between the POX and COX sites of partnering monomers. A model with a defective POX in one monomer and a dysfunctional COX in the other monomer was constructed as a G533A/Q203R huPGHS-2 heterodimer (Fig. 4.1B). COX activity assays were carried out and confirmed COX activation by the POX of the same monomer.

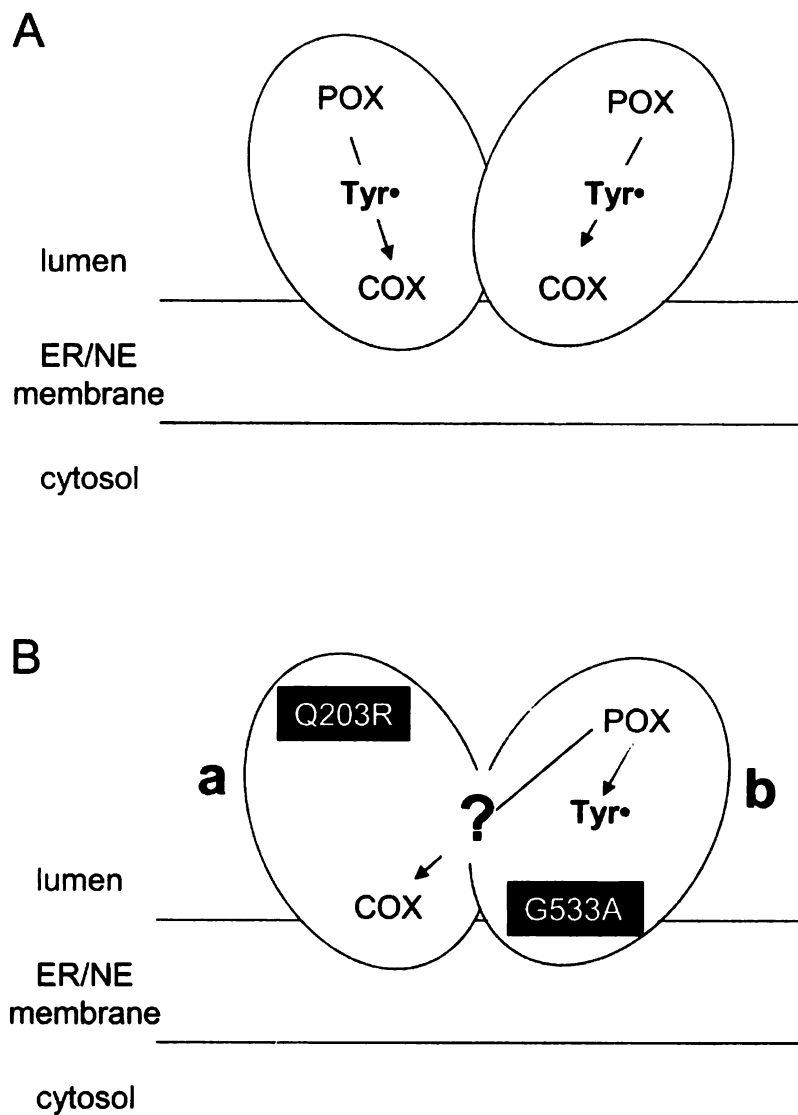


Figure 4.1: **Models of PGHS-2 homodimer and heterodimer.** (A) PGHS-2 homodimer with a POX and a COX site in each monomer. COX activation requires Tyr385 radical formed by the POX reaction. (B) G533A/Q203R PGHS-2 heterodimer. Monomer a has a Q203R mutation which quenches both POX and COX activity (Chapter 2). Monomer b is defective for the COX reaction [151].

## 4.2 Materials and Methods

**Materials:** Materials for purifications and activity assays are described in Chapter 2 Materials and Methods.

**Mutagenesis, protein expression and purification:** The site-directed mutagenesis protocol was used as described in Chapter 2 Materials and Methods for creating the G533A/G533A and Q203R/Q203R huPGHS-2 homodimers. Native/native, G533A/G533A and Q203R/Q203R huPGHS-2 homodimers are all tagged with hexahistidine (His<sub>6</sub>) polypeptides at their N-termini. The primers are as follows:

G533A/G533A, forward: 5'-C TCC TTG AAA GCA CTT ATG GGT AAT G-3'; backward: 5'-C ATT ACC CAT AAG TGC TTT CAA GGA G-3'.

Q203R/Q203R, forward: 5'- GCA TTC TTT GCC CGG CAC TTC ACG CAT CAG-3'; backward: 5'-CTG ATG CGT GAA GTG CCG GGC AAA GAA TGC-3'.

A G533A/Q203R huPGHS-2 heterodimer was constructed and expressed using procedures described previously (Fig. 4.2) [151]. The pFastBac vector containing a FLAG-tagged-native huPGHS-2 gene was a kind gift of Dr. C. Yuan. Mutated FLAG-tagged-G533A huPGHS-2 cDNA was cleaved from the pFastBac vector with Stu I and Kpn I and inserted downstream of Promoter p10 in pFastBac Dual vector that had been treated Sma I and Kpn I (Fig. 4.2). Mutated His<sub>6</sub>-tagged-Q203R huPGHS-2 was cloned into Promoter PH of pFastBac Dual using the same strategy except that the EcoR I and Hind III were used to digest the DNAs. The correct orientation and positions of the inserts were confirmed by restriction digestion and DNA sequencing (the University of Michigan DNA Sequencing Core). The heterodimer was expressed

in the baculovirus system as described above and purified by a combination of Ni-NTA and anti-FLAG agarose chromatography [160]. The purity was determined by SDS-PAGE and the identity was confirmed by western blot analysis using anti-His<sub>6</sub> and anti-FLAG antibodies (Sigma).

**Western Blot:** Purified proteins were separated electrophoretically by SDS-polyacrylamide gel electrophoresis (NuPAGE 10% polyacrylamide Bis-Tris, Invitrogen, Carlsbad, CA) and transferred to nitrocellulose. Rabbit antibody. Anti-His<sub>6</sub> and anti-FLAG antibodies were from Sigma. Anti-rabbit and anti-murine antibodies were obtained from Bio-Rad. The detection system used the Super Signal West Pico chemiluminescence kit (Pierce, Rockford, IL)

**POX and COX Activity assay:** Purified huPGHS-2 homodimers and heterodimer were subjected to the activity assays as described in Chapter 2 Materials and Methods.

## 4.3 Results

### 4.3.1 Construct, Expression and Purification of HuPGHS-2 Homodimers and Heterodimer

A FLAG-tagged G533A/hexa-histidine (His<sub>6</sub>)-tagged-Q203R huPGHS-2 heterodimer was prepared using sequential Ni-NTA and anti-FLAG affinity chromatography. His<sub>6</sub>-G533A huPGHS-2 and His<sub>6</sub>-Q203R huPGHS-2 homodimers were prepared by Ni-NTA chromatography. All of the proteins were more than 95% pure as determined

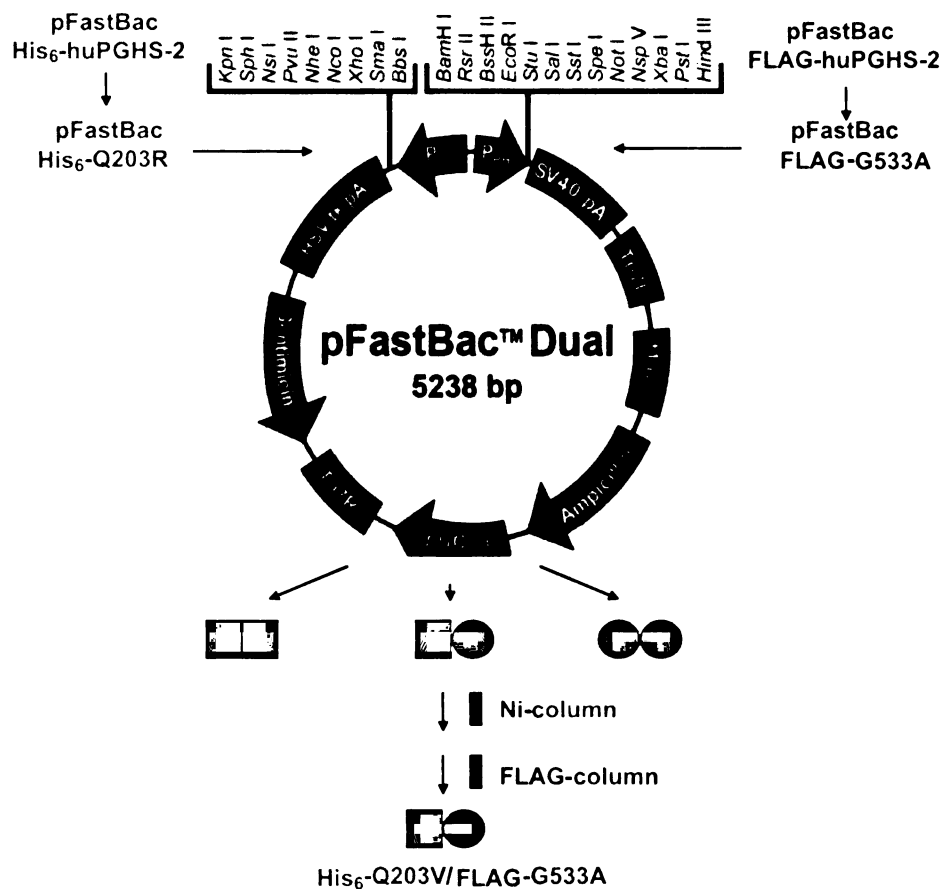


Figure 4.2: **Construct of PGHS-2 heterodimer and protein purification strategy.** FLAG- or His<sub>6</sub>-tagged mutant huPGHS-2 genes were cloned to different promoters of pFastBac™ Dual vector. Proteins were expressed in baculovirus expression system as three populations, His<sub>6</sub>-Q203R/His<sub>6</sub>-Q203R (green squares), FLAG-G533A/FLAG-G533A (blue circles) homodimers and His<sub>6</sub>-Q203R/FLAG-G533A heterodimer. Affinity chromatography using Ni- and anti-FLAG columns yielded a homogenous his-Q203R/FLAG-G533A heterodimer fraction. The plasmid map is from [www.invitrogen.com](http://www.invitrogen.com).

by SDS-PAGE. As expected, all of the proteins were recognized by the antibodies against the hexa-histidine tag and PGHS-2, while only the heterodimer was reactive to the anti-FLAG antibody [151].

### **4.3.2 POX Activities of HuPGHS-2 Homodimers and Heterodimer**

As reported previously, the POX activity of the G533A/G533A huPGHS-2 homodimer was about the same as that of native/native PGHS-2 (Fig. 4.4) [151]. Moreover, as observed earlier with Q203R ovPGHS-1 (Table 3.1), the Q203R/Q203R huPGHS-2 homodimer lacked POX activity. The G533A/Q203R huPGHS-2 heterodimer, lacking POX activity in one monomer, showed somewhat less (20-30%) than half of the POX activity of the native homodimer that we expected previously. Although, there are other explanations, we suspect that the mutant monomers may not interact as well as complimentary monomers.

### **4.3.3 COX Activities of HuPGHS-2 Homodimers and Heterodimer**

Importantly, the G533A/Q203R huPGHS-2 heterodimer exhibited no COX activity. This was also true when exogenous 15-HPETE was added to optimize COX activation. Thus, the POX site of the G533A monomer is unable to activate the COX site of the Q203R monomer. This result suggests there is no cross-talk between POX and COX sites of partner monomers.

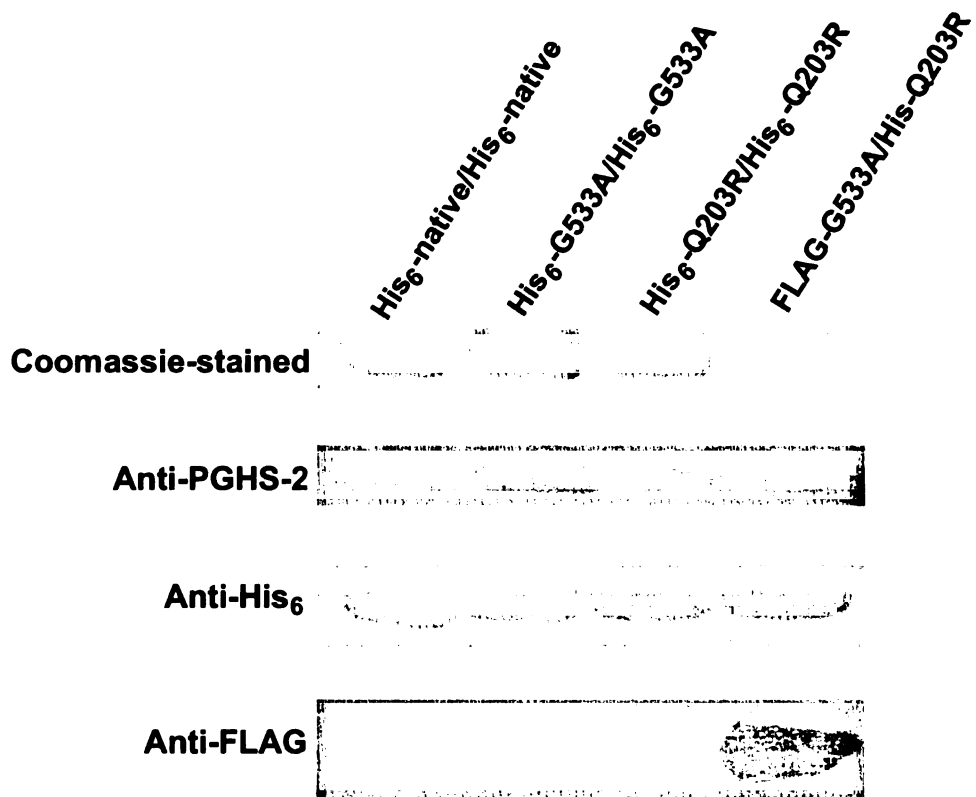


Figure 4.3: **Expression and identification of PGHS-2 homodimers and heterodimer.** His-tagged native/native, G533A/G533A, Q203R/G533A and FLAG-G533A/his-Q203R huPGHS-2s were expressed and purified as described in Materials and Methods. The purity was confirmed by Coomassie-stained SDS-PAGE and western blots.

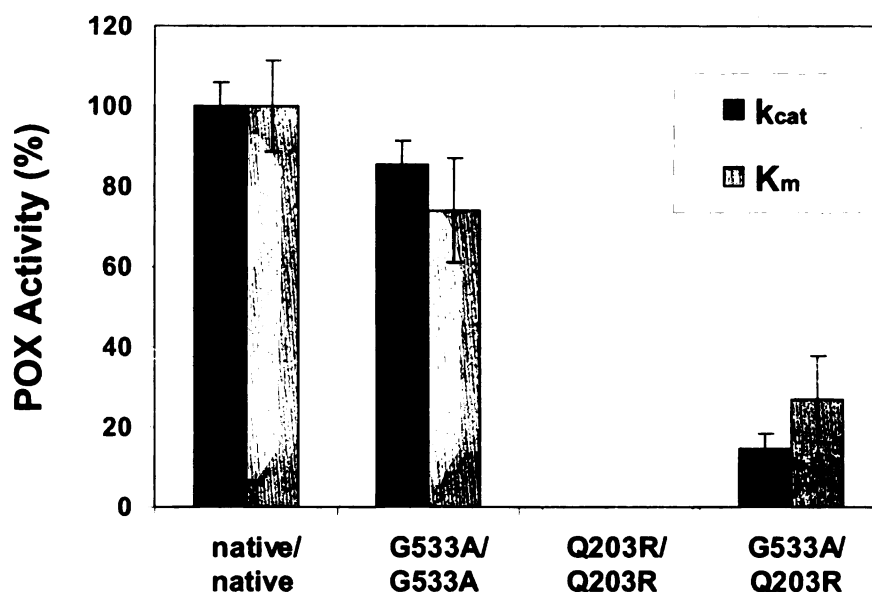


Figure 4.4: Normalized POX activities of native/native, G533A/G533A, Q203R/Q203R and G533A/Q203R huPGHS-2s. 100  $\mu$ l reaction buffer (100 mM TrisHCl, pH 8.0 at 4  $^{\circ}$ C) contained 38 nM PGHS monomers, 4.5 mM guaiacol and 15-HPETE of different concentrations (4, 8, 16, 32, 64 and 128 mM). The initial rates of guaiacol oxidation were achieved by measuring the linear increase of UV absorbance ( $\lambda=436$  nm). Rate-concentration simulations using the Michaelis-Menten equation yielded  $k_{cat}$  of 250  $s^{-1}$  and  $K_m$  of 88  $\mu$ M for the native enzyme.

## 4.4 Discussion

Radical migration has been of interest in the context of the PGHS reaction mechanism. Radicals may migrate within or between the macromolecules proteins including PGHS-1 [72], DNAs or lipids [161, 162]. For example, electrons can be transferred from a human myoglobin monomer to a tyrosyl radical in another nearby monomer [163]. However, the present work clearly shows that there is no electron transfer between the two monomers of PGHS dimers that lead to COX activation. COX activity requires initiation by the radical generated from the POX reaction in the same

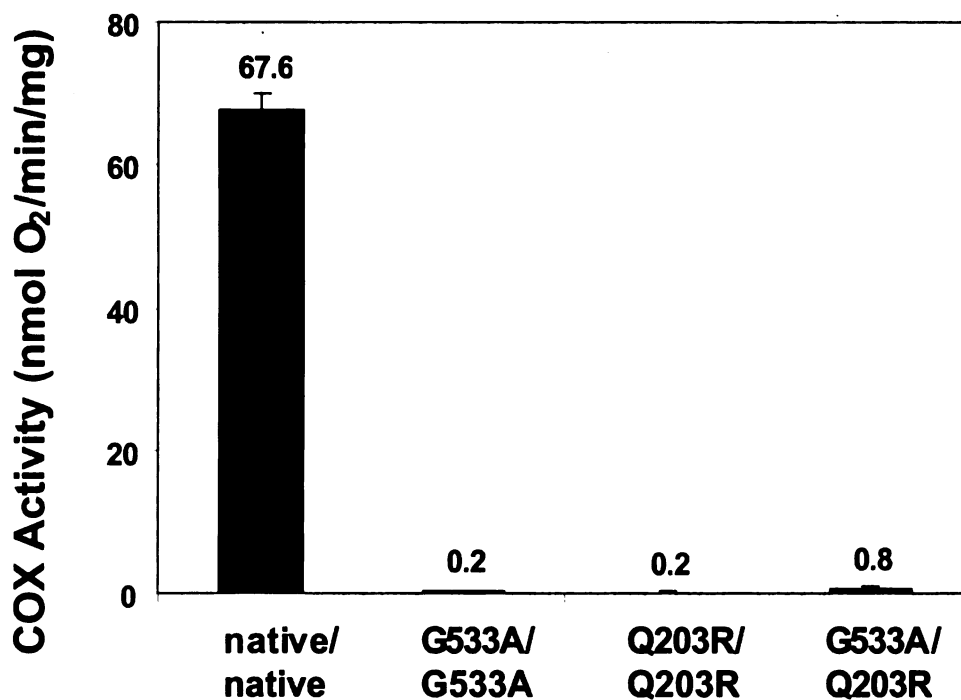


Figure 4.5: Specific COX activities of huPGHS-2 enzymes. 3 ml reaction buffer (100 mM TrisHCl, pH 8.0 at 4 °C) contained 5  $\mu$ g PGHS monomers, 1 mM phenol and 100  $\mu$ M AA. O<sub>2</sub> consumption was monitored by an O<sub>2</sub> electrode probe and initial rates were calculated using DasyLab.

monomer. Funk and coworkers have suggested that a PGHS-2 lacking COX activity may dimerize with a PGHS-1 monomer and stimulate PGHS-2 COX activity [164].

Based on our studies, this seems unlikely.

## Chapter 5

# Conclusions and Future Directions

COX activity assays using purified ovPGHS-1 or recombinant proteins have affirmed that PGHS prefers lipid hydroperoxides to  $\text{H}_2\text{O}_2$ , which is present at higher concentrations in cells. We assessed the impact of distal residues in the heme POX active site on hydroperoxide substrate utilization. When large hydrophobic residues comprising the distal dome were mutated to smaller residues (e.g. alanine), Compound I formation from 15-HPETE was unaffected (Fig. 2.5 and 2.7). Substitution with an acidic residue (L294D) also had no impact on Compound I formation. These results indicate that the hydrophobic dome does not significantly influence lipid hydroperoxide association or heterolysis. The intrinsic bond dissociation energies of heterolytic O-O bond cleavage in different hydroperoxides appeared similar (Table 2.10). Molecular Dynamics simulations indicated that binding of  $\text{H}_2\text{O}_2$  but not  $\text{PGG}_2$  allowed more water molecules to compete for the binding to the heme iron. In short, hydroperoxide substrate specificity is not determined by hydrophobic interactions of peroxides with the hydrophobic dome or different chemical properties of different hydroperoxides. In-

stead, the essential interactions for hydroperoxide binding are peroxy-iron bond and hydrogen bond involving His207, and long carbon chains appear to enhance binding of alkyl hydroperoxides to the PGHS POX active site perhaps by interacting with the heme.

H<sub>2</sub>O<sub>2</sub> appears more sensitive to the residue at position 203 in the PGHS heme active site than alkyl hydroperoxides. We hypothesize that the association of H<sub>2</sub>O<sub>2</sub> to the POX site requires a distal Gln203 to exclude competing water molecules near the sixth coordinate position of the heme iron. It is not clear whether the heterolytic cleavage of O-O bond in H<sub>2</sub>O<sub>2</sub> also requires facilitation by Gln203 in the native PGHS. The existence and importance of a hydrogen bond between Gln203 and H<sub>2</sub>O<sub>2</sub> can be tested by measuring the POX activity of a Q203L mutant PGHS with H<sub>2</sub>O<sub>2</sub> as well as investigating Compound I formation. Moreover, the activity level of H<sub>2</sub>O<sub>2</sub> seems also manipulated by the distance to the distal His207 in the PGHS POX active site as suggested by molecular dynamics simulations (Chapter 2). It is implied that a distal histidine in an appropriate proximity to H<sub>2</sub>O<sub>2</sub> may increase PGHS POX activity with this polar, small hydroperoxide substrate.

Our mutagenic analysis suggests that the hydrophobic dome residues of PGHS POX are not critical for Compound I formation; however, there are some effects on POX specific activities with guaiacol presumably due to differences in the activity of guaiacol to reduce oxidized heme intermediates. PGHS POX has a big cavern which may accommodate bulky phenolic reductants. Presumably, the reduction of organic compounds is carried out on the surface of the heme, instead of the edge groups as observed in peroxidases with narrow POX active sites such as HRP. Potential

positions for the reduction of PGHS can be the axial oxygen of higher oxidative species, or coordinating nitrogen atoms of the heme iron.

# Bibliography

1. W. L. Smith, D. L. DeWitt, and R. M. Garavito. Cyclooxygenases: structural, cellular, and molecular biology. *Annu Rev Biochem*, 69:145–82, 2000.
2. C. D. Funk. Prostaglandins and leukotrienes: advances in eicosanoid biology. *Science*, 294(5548):1871–1875, 2001.
3. R. Langenbach, S. G. Morham, H. F. Tiano, C. D. Loftin, B. I. Ghanayem, P. C. Chulada, J. F. Mahler, C. A. Lee, E. H. Goulding, K. D. Kluckman, H. S. Kim, and O. Smithies. Prostaglandin synthase 1 gene disruption in mice reduces arachidonic acid-induced inflammation and indomethacin-induced gastric ulceration. *Cell*, 83(3):483–492, 1995.
4. A. R. Brash. Arachidonic acid as a bioactive molecule. *J Clin Invest*, 107(11):1339–1345, 2001.
5. T. E. Rollins and W. L. Smith. Subcellular localization of prostaglandin-forming cyclooxygenase in swiss mouse 3t3 fibroblasts by electron microscopic immunocytochemistry. *J Biol Chem*, 255(10):4872–4875, 1980.
6. W. L. Smith and T. E. Rollins. Characteristics of rabbit anti-pgh synthase antibodies and use in immunocytochemistry. *Methods Enzymol*, 86:213–222, 1982.
7. A. G. Spencer, J. W. Woods, T. Arakawa, II Singer, and W. L. Smith. Subcellular localization of prostaglandin endoperoxide h synthases-1 and -2 by immunoelectron microscopy. *J Biol Chem*, 273(16):9886–93, 1998.
8. W. L. Smith, R. L. Huslig, T. E. Rollins, and R. L. Fogwell. Uterine prostaglandin-forming cyclooxygenase: relationship to luteolysis and subcellular localization. *Adv Prostaglandin Thromboxane Res*, 8:1345–1349, 1980.
9. J. C. Otto, D. L. DeWitt, and W. L. Smith. N-glycosylation of prostaglandin endoperoxide synthases-1 and -2 and their orientations in the endoplasmic reticulum. *J Biol Chem*, 268(24):18234–42, 1993.
10. Tadashi Tanabe and Norimitsu Tohnai. Cyclooxygenase isozymes and their gene structures and expression. *Prostaglandins Other Lipid Mediat*, 68-69:95–114, 2002.

11. Yeon-Joo Kang, Uri R. Mbonye, Cynthia J. DeLong, Masayuki Wada, and William L. Smith. Regulation of intracellular cyclooxygenase levels by gene transcription and protein degradation. *Prog Lipid Res.*, page Epub ahead of print, 2007.
12. W. L. Smith and R. Langenbach. Why there are two cyclooxygenase isozymes. *J Clin Invest*, 107(12):1491–1495, 2001.
13. M. Hemler and W. E. Lands. Purification of the cyclooxygenase that forms prostaglandins. demonstration of two forms of iron in the holoenzyme. *Journal of Biological Chemistry*, 251(18):5575–9, 1976.
14. T. Miyamoto, N. Ogino, S. Yamamoto, and O. Hayaishi. Purification of prostaglandin endoperoxide synthetase from bovine vesicular gland microsomes. *J Biol Chem*, 251(9):2629–36, 1976.
15. F. J. Van der Ouderaa, M. Buytenhek, D. H. Nugteren, and D. A. Van Dorp. Purification and characterisation of prostaglandin endoperoxide synthetase from sheep vesicular glands. *Biochim Biophys Acta*, 487(2):315–31, 1977.
16. M. Shitashige, I. Morita, and S. Murota. Different substrate utilization between prostaglandin endoperoxide synthase-1 and -2 in nih3t3 fibroblasts. *Biochim Biophys Acta*, 1389(1):57–66, 1998.
17. M. Liminga and E. Oliw. Qualitative and quantitative analysis of lipoxygenase products in bovine corneal epithelium by liquid chromatography-mass spectrometry with an ion trap. *Lipids*, 35(2):225–32, 2000.
18. A. W. Girotti. Lipid hydroperoxide generation, turnover, and effector action in biological systems. *J Lipid Res*, 39(8):1529–1542, 1998.
19. M. J. Smith. Aspirin and prostaglandins: some recent developments. *Agents Actions*, 8(4):427–429, 1978.
20. W. L. Smith and D. L. Dewitt. Prostaglandin endoperoxide synthases-1 and -2. *Adv Immunol*, 62:167–215, 1996.
21. T. S. Brannon, A. J. North, L. B. Wells, and P. W. Shaul. Prostacyclin synthesis in ovine pulmonary artery is developmentally regulated by changes in cyclooxygenase-1 gene expression. *J Clin Invest*, 93(5):2230–2235, 1994.
22. Jan M Schwab, Rudi Beschorner, Richard Meyermann, Fatma Gzalan, and Hermann J Schluesener. Persistent accumulation of cyclooxygenase-1-expressing microglial cells and macrophages and transient upregulation by endothelium in human brain injury. *J Neurosurg*, 96(5):892–899, 2002.
23. J. M. Schwab, K. Brechtel, T. D. Nguyen, and H. J. Schluesener. Persistent accumulation of cyclooxygenase-1 (cox-1) expressing microglia/macrophages and upregulation by endothelium following spinal cord injury. *J Neuroimmunol*, 111(1-2):122–130, 2000.

24. Uri R Mbonye, Masayuki Wada, Caroline J Rieke, Hui-Yuan Tang, David L Dewitt, and William L Smith. The 19 amino acid cassette of cyclooxygenase-2 mediates entry of the protein into the er-associated degradation system. *J Biol Chem*, 2006.
25. C. D. Breder, D. Dewitt, and R. P. Kraig. Characterization of inducible cyclooxygenase in rat brain. *J Comp Neurol*, 355(2):296-315, 1995.
26. S. G. Morham, R. Langenbach, C. D. Loftin, H. F. Tiano, N. Vouloumanos, J. C. Jennette, J. F. Mahler, K. D. Kluckman, A. Ledford, C. A. Lee, and O. Smithies. Prostaglandin synthase 2 gene disruption causes severe renal pathology in the mouse. *Cell*, 83(3):473-482, 1995.
27. W. L. Smith and W. E. Lands. Oxygenation of polyunsaturated fatty acids during prostaglandin biosynthesis by sheep vesicular gland. *Biochemistry*, 11(17):3276-3285, 1972.
28. R. Dietz, W. Nastainczyk, and H. H. Ruf. Higher oxidation states of prostaglandin h synthase. rapid electronic spectroscopy detected two spectral intermediates during the peroxidase reaction with prostaglandin g2. *European Journal of Biochemistry*, 171(1-2):321-8, 1988.
29. R. Karthein, R. Dietz, W. Nastainczyk, and H. H. Ruf. Higher oxidation states of prostaglandin h synthase. epr study of a transient tyrosyl radical in the enzyme during the peroxidase reaction. *European Journal of Biochemistry*, 171(1-2):313-20, 1988.
30. C. E. Schulz, R. Rutter, J. T. Sage, P. G. Debrunner, and L. P. Hager. Mssbauer and electron paramagnetic resonance studies of horseradish peroxidase and its catalytic intermediates. *Biochemistry*, 23(20):4743-4754, 1984.
31. P. Ortiz de Montellano. *Cytochrome P450: Structure, Mechanism and Biochemistry*. Plenum Press, New York, 1995.
32. W. R. Patterson, T. L. Poulos, and D. B. Goodin. Identification of a porphyrin pi cation radical in ascorbate peroxidase compound i. *Biochemistry*, 34(13):4342-5, 1995.
33. M. J. Benecky, J. E. Frew, N. Scowen, P. Jones, and B. M. Hoffman. Epr and endor detection of compound i from micrococcus lysodeikticus catalase. *Biochemistry*, 32(44):11929-33, 1993.
34. J. E. Erman, L. B. Vitello, J. M. Mauro, and J. Kraut. Detection of an oxyferryl porphyrin pi-cation-radical intermediate in the reaction between hydrogen peroxide and a mutant yeast cytochrome c peroxidase. evidence for tryptophan-191 involvement in the radical site of compound i. *Biochemistry*, 28(20):7992-5, 1989.

35. A. L. Houseman, P. E. Doan, D. B. Goodin, and B. M. Hoffman. Comprehensive explanation of the anomalous epr spectra of wild-type and mutant cytochrome c peroxidase compound es. *Biochemistry*, 32(16):4430–43, 1993.
36. M. Hamberg and B. Samuelsson. On the mechanism of the biosynthesis of prostaglandins e-1 and f-1-alpha. *Journal of Biological Chemistry*, 242(22):5336–43, 1967.
37. I. Song, T. M. Ball, and W. L. Smith. Different suicide inactivation processes for the peroxidase and cyclooxygenase activities of prostaglandin endoperoxide h synthase-1. *Biochem Biophys Res Commun*, 289(4):869–875, 2001.
38. P. R. Ortiz de Montellano, S. I. Ozaki, S. L. Newmyer, V. P. Miller, and C. Har-  
mann. Structural determinants of the catalytic activities of peroxidases. *Biochem Soc Trans*, 23(2):223–227, 1995.
39. J. H. Dawson. Probing structure-function relations in heme-containing oxyge-  
nases and peroxidases. *Science*, 240(4851):433–439, 1988.
40. L. M. Landino, B. C. Crews, J. K. Gierse, S. D. Hauser, and L. J. Marnett. Mutational analysis of the role of the distal histidine and glutamine residues of prostaglandin-endoperoxide synthase-2 in peroxidase catalysis, hydroperoxide reduction, and cyclooxygenase activation. *J Biol Chem*, 272(34):21565–74, 1997.
41. G. Wu, C. Wei, R. J. Kulmacz, Y. Osawa, and A. L. Tsai. A mechanistic study of self-inactivation of the peroxidase activity in prostaglandin h synthase-1. *Journal of Biological Chemistry*, 274(14):9231–7, 1999.
42. W. Shi, C. W. Hoganson, M. Espe, C. J. Bender, G. T. Babcock, G. Palmer, R. J. Kulmacz, and A. Tsai. Electron paramagnetic resonance and electron nuclear double resonance spectroscopic identification and characterization of the tyrosyl radicals in prostaglandin h synthase 1. *Biochemistry*, 39(14):4112–21, 2000.
43. D. Picot, P. J. Loll, and R. M. Garavito. The x-ray crystal structure of the membrane protein prostaglandin h2 synthase-1. *Nature*, 367(6460):243–9, 1994.
44. M. G. Malkowski, S. L. Ginell, W. L. Smith, and R. M. Garavito. The productive conformation of arachidonic acid bound to prostaglandin synthase. *Science*, 289(5486):1933–7, 2000.
45. T. E. Eling, W. C. Glasgow, J. F. Curtis, W. C. Hubbard, and J A Han-  
dler. Studies on the reduction of endogenously generated prostaglandin g2 by prostaglandin h synthase. *J Biol Chem*, 266(19):12348–12355, 1991.
46. J. K. Gierse, J. J. McDonald, S. D. Hauser, S. H. Rangwala, C. M. Koboldt, and K. Seibert. A single amino acid difference between cyclocxygenase-1 (cox-1) and -2 (cox-2) reverses the selectivity of cox-2 specific inhibitors. *J Biol Chem*, 271(26):15810–15814, 1996.

47. T. J. Fiedler, C. A. Davey, and R. E. Fenna. X-ray crystal structure and characterization of halide-binding sites of human myeloperoxidase at 1.8 Å resolution. *J Biol Chem*, 275(16):11964–11971, 2000.
48. Kre Meno, Simon Jennings, Andrew T Smith, Anette Henriksen, and Michael Gajhede. Structural analysis of the two horseradish peroxidase catalytic residue variants h42e and r38s/h42e: implications for the catalytic cycle. *Acta Crystallogr D Biol Crystallogr*, 58(Pt 10 Pt 2):1803–1812, 2002.
49. Tiffany P Barrows, B. Bhaskar, and Thomas L Poulos. Electrostatic control of the tryptophan radical in cytochrome c peroxidase. *Biochemistry*, 43(27):8826–8834, 2004.
50. Arthur E Kummerle, Gilberto M Sperandio da Silva, Carlos M R Sant'Anna, Eliezer J Barreiro, and Carlos A M Fraga. A proposed molecular basis for the selective resveratrol inhibition of the pghs-1 peroxidase activity. *Bioorg Med Chem*, 13(21):5981–5985, 2005.
51. P. R. Ortiz de Montellano. Catalytic sites of hemoprotein peroxidases. *Annu Rev Pharmacol Toxicol*, 32:89–107, 1992.
52. G. Smulevich. Understanding heme cavity structure of peroxidases: comparison of electronic absorption and resonance raman spectra with crystallographic results. *Biospectroscopy*, 4(5 Suppl):S3–17, 1998.
53. Y. Mino, H. Wariishi, N. J. Blackburn, T. M. Loehr, and M. H. Gold. Spectral characterization of manganese peroxidase, an extracellular heme enzyme from the lignin-degrading basidiomycete, *phanerochaete chrysosporium*. *J Biol Chem*, 263(15):7029–7036, 1988.
54. S. A. Seibold, J. F. Cerda, A. M. Mulichak, I. Song, R. M. Garavito, T. Arakawa, W. L. Smith, and G. T. Babcock. Peroxidase activity in prostaglandin endoperoxide synthase-1 occurs with a neutral histidine proximal heme ligand. *Biochemistry*, 39(22):6616–6624, 2000.
55. Anthony J Chubb, Desmond J Fitzgerald, Kevin B Nolan, and Edelmiro Mo-man. The productive conformation of prostaglandin g2 at the peroxidase site of prostaglandin endoperoxide synthase: docking, molecular dynamics, and site-directed mutagenesis studies. *Biochemistry*, 45(3):811–820, 2006.
56. J. A. Mancini, D. Riendeau, J. P. Falgoutyret, P. J. Vickers, and G. P. O'Neill. Arginine 120 of prostaglandin g/h synthase-1 is required for the inhibition by nonsteroidal anti-inflammatory drugs containing a carboxylic acid moiety. *J Biol Chem*, 270(49):29372–29377, 1995.
57. D. K. Bhattacharyya, M. Lecomte, C. J. Rieke, M. Garavito, and W. L. Smith. Involvement of arginine 120, glutamate 524, and tyrosine 355 in the binding of arachidonate and 2-phenylpropionic acid inhibitors to the cyclooxygenase

- active site of ovine prostaglandin endoperoxide h synthase-1. *J Biol Chem*, 271(4):2179–2184, 1996.
58. G. M. Greig, D. A. Francis, J. P. Falguyret, M. Ouellet, M. D. Percival, P. Roy, C. Bayly, J. A. Mancini, and G. P. O'Neill. The interaction of arginine 106 of human prostaglandin g/h synthase-2 with inhibitors is not a universal component of inhibition mediated by nonsteroidal anti-inflammatory drugs. *Mol Pharmacol*, 52(5):829–838, 1997.
  59. C. J. Rieke, A. M. Mulichak, R. M. Garavito, and W. L. Smith. The role of arginine 120 of human prostaglandin endoperoxide h synthase-2 in the interaction with fatty acid substrates and inhibitors. *J Biol Chem*, 274(24):17109–17114, 1999.
  60. E. D. Thuresson, K. M. Lakkides, C. J. Rieke, Y. Sun, B. A. Wingerd, R. Miccielli, A. M. Mulichak, M. G. Malkowski, R. M. Garavito, and W. L. Smith. Prostaglandin endoperoxide h synthase-1: the functions of cyclooxygenase active site residues in the binding, positioning, and oxygenation of arachidonic acid. *J Biol Chem*, 276(13):10347–10357, 2001.
  61. Lawrence J. Marnett and Krishna Rao Maddipati. *Prostaglandin H synthase*, chapter 13, pages 293–334. CRC Press, 1991.
  62. M. E. Hemler, H. W. Cook, and W. E. Lands. Prostaglandin biosynthesis can be triggered by lipid peroxides. *Archives of Biochemistry & Biophysics*, 193(2):340–5, 1979.
  63. M. E. Hemler, G. Graff, and W. E. Lands. Accelerative autoactivation of prostaglandin biosynthesis by pgg<sub>2</sub>. *Biochemical & Biophysical Research Communications*. 85(4):1325–31, 1978.
  64. R. J. Kulmacz and L. H. Wang. Comparison of hydroperoxide initiator requirements for the cyclooxygenase activities of prostaglandin h synthase-1 and -2. *Journal of Biological Chemistry*, 270(41):24019–23, 1995.
  65. R. J. Kulmacz and W. E. Lands. Quantitative similarities in the several actions of cyanide on prostaglandin h synthase. *Prostaglandins*, 29(2):175–90, 1985.
  66. W. Chen, T. R. Pawelek, and R. J. Kulmacz. Hydroperoxide dependence and cooperative cyclooxygenase kinetics in prostaglandin h synthase-1 and -2. *Journal of Biological Chemistry*, 274(29):20301–6, 1999.
  67. O. Y. So, L. E. Scarafia, A. Y. Mak, O. H. Callan, and D. C. Swinney. The dynamics of prostaglandin h synthases. studies with prostaglandin h synthase 2 y355f unmask mechanisms of time-dependent inhibition and allosteric activation. *J Biol Chem*, 273(10):5801–5807, 1998.

68. D. C. Swinney, A. Y. Mak, J. Barnett, and C. S. Ramesha. Differential allosteric regulation of prostaglandin h synthase 1 and 2 by arachidonic acid. *J Biol Chem*, 272(19):12393–12398, 1997.
69. B. R. Culp, B. G. Titus, and W. E. Lands. Inhibition of prostaglandin biosynthesis by eicosapentaenoic acid. *Prostaglandins & Medicine*, 3(5):269–78, 1979.
70. R. W. Egan, P. H. Gale, G. C. Beveridge, G. B. Phillips, and L. J. Marnett. Radical scavenging as the mechanism for stimulation of prostaglandin cyclooxygenase and depression of inflammation by lipoic acid and sodium iodide. *Prostaglandins*, 16(6):861–869, 1978.
71. A. Tsai, L. C. Hsi, R. J. Kulmacz, G. Palmer, and W. L. Smith. Characterization of the tyrosyl radicals in ovine prostaglandin h synthase-1 by isotope replacement and site-directed mutagenesis. *J Biol Chem*, 269(7):5085–91, 1994.
72. L. C. Hsi, C. W. Hoganson, G. T. Babcock, R. M. Garavito, and W. L. Smith. An examination of the source of the tyrosyl radical in ovine prostaglandin endoperoxide synthase-1. *Biochem Biophys Res Commun*, 207(2):652–60, 1995.
73. Stefano Fiorucci, Eleonora Distrutti, Octavio Menezes de Lima, Mario Romano, Andrea Mencarelli, Miriam Barbanti, Ernesto Palazzini, Antonio Morelli, and John L Wallace. Relative contribution of acetylated cyclo-oxygenase (cox)-2 and 5-lipoxygenase (lox) in regulating gastric mucosal integrity and adaptation to aspirin. *FASEB J*, 17(9):1171–1173, 2003.
74. S. Ohki, N. Ogino, S. Yamamoto, and O. Hayaishi. Prostaglandin hydroperoxidase, an integral part of prostaglandin endoperoxide synthetase from bovine vesicular gland microsomes. *J Biol Chem*, 254(3):829–36, 1979.
75. G. Lu, A. L. Tsai, H. E. Van Wart, and R. J. Kulmacz. Comparison of the peroxidase reaction kinetics of prostaglandin h synthase-1 and -2. *Journal of Biological Chemistry*, 274(23):16162–7, 1999.
76. A. Tsai, C. Wei, H. K. Baek, R. J. Kulmacz, and H. E. Van Wart. Comparison of peroxidase reaction mechanisms of prostaglandin h synthase-1 containing heme and mangano protoporphyrin ix. *Journal of Biological Chemistry*, 272(14):8885–94, 1997.
77. M. Bakovic and H. B. Dunford. Reactions of prostaglandin endoperoxide synthase and its compound i with hydroperoxides. *J Biol Chem*, 271(4):2048–56, 1996.
78. D. C. Goodwin, L. M. Landino, and L. J. Marnett. Reactions of prostaglandin endoperoxide synthase with nitric oxide and peroxyxynitrite. *Drug Metab Rev*, 31(1):273–294, 1999.

79. C. M. Markey, A. Alward, P. E. Weller, and L. J. Marnett. Quantitative studies of hydroperoxide reduction by prostaglandin h synthase. reducing substrate specificity and the relationship of peroxidase to cyclooxygenase activities. *J Biol Chem*, 262(13):6266–6279, 1987.
80. C. Hwang, A. J. Sinskey, and H. F. Lodish. Oxidized redox state of glutathione in the endoplasmic reticulum. *Science*, 257(5076):1496–502, 1992.
81. A. Szkopinska. Ubiquinone. biosynthesis of quinone ring and its isoprenoid side chain. intracellular localization. *Acta Biochim Pol*, 47(2):469–80, 2000.
82. A. W. Linnane and H. Eastwood. Cellular redox regulation and prooxidant signaling systems: a new perspective on the free radical theory of aging. *Ann N Y Acad Sci*, 1067:47–55, 2006.
83. M. Sundaramoorthy, K. Kishi, M. H. Gold, and T. L. Poulos. The crystal structure of manganese peroxidase from phanerochaete chrysosporium at 2.06- $\text{\AA}$  resolution. *J Biol Chem*, 269(52):32759–32767, 1994.
84. X. Yi, M. Mroczko, K. M. Manoj, X. Wang, and L. P. Hager. Replacement of the proximal heme thiolate ligand in chloroperoxidase with a histidine residue. *Proc Natl Acad Sci U S A*, 96(22):12412–12417, 1999.
85. P. R. Ortiz de Montellano. Arylhydrazines as probes of hemoprotein structure and function. *Biochimie*, 77(7-8):581–593, 1995.
86. M. A. Ator, S. K. David, and P. R. Ortiz de Montellano. Stabilized isoporphyrin intermediates in the inactivation of horseradish peroxidase by alkylhydrazines. *J Biol Chem*, 264(16):9250–9257, 1989.
87. G. D. DePillis, B. P. Sishta, A. G. Mauk, and P. R. Ortiz de Montellano. Small substrates and cytochrome c are oxidized at different sites of cytochrome c peroxidase. *J Biol Chem*, 266(29):19334–19341, 1991.
88. J. Zeng and R. E. Fenna. X-ray crystal structure of canine myeloperoxidase at 3  $\text{\AA}$  resolution. *J Mol Biol*, 226(1):185–207, 1992.
89. A. Jacquet, L. Garcia-Quintana, V. Deleersnyder, R. Fenna, A. Bollen, and N. Moguilevsky. Site-directed mutagenesis of human myeloperoxidase: further identification of residues involved in catalytic activity and heme interaction. *Biochem Biophys Res Commun*, 202(1):73–81, 1994.
90. L. B. Vitello, J. E. Erman, M. A. Miller, J. Wang, and J. Kraut. Effect of arginine-48 replacement on the reaction between cytochrome c peroxidase and hydrogen peroxide. *Biochemistry*, 32(37):9807–9818, 1993.
91. J. N. Rodriguez-Lopez, A. T. Smith, and R. N. Thorneley. Role of arginine 38 in horseradish peroxidase. a critical residue for substrate binding and catalysis. *J Biol Chem*, 271(8):4023–4030, 1996.

92. Karin Khnel, Wulf Blankenfeldt, James Turner, and Ilme Schlichting. Crystal structures of chloroperoxidase with its bound substrates and complexed with formate, acetate, and nitrate. *J Biol Chem*, 281(33):23990–23998, 2006.
93. Paul G Furtmüller, Martina Zederbauer, Walter Jantschko, Jutta Helm, Martin Bogner, Christa Jakopitsch, and Christian Obinger. Active site structure and catalytic mechanisms of human peroxidases. *Arch Biochem Biophys*, 445(2):199–213, 2006.
94. K. T. Yue, K. L. Taylor, J. M. Kinkade, R. B. Sinclair, and L. S. Powers. X-ray absorption and resonance raman spectroscopy of human myeloperoxidase at neutral and acid pH. *Biochim Biophys Acta*, 1338(2):282–294, 1997.
95. I. M. Kooter, N. Moguilevsky, A. Bollen, L. A. van der Veen, C. Otto, H. L. Dekker, and R. Wever. The sulfonium ion linkage in myeloperoxidase. direct spectroscopic detection by isotopic labeling and effect of mutation. *J Biol Chem*, 274(38):26794–26802, 1999.
96. Martina Zederbauer, Walter Jantschko, Karin Neugschwandtner, Christa Jakopitsch, Nicole Moguilevsky, Christian Obinger, and Paul Georg Furtmüller. Role of the covalent glutamic acid 242-heme linkage in the formation and reactivity of redox intermediates of human myeloperoxidase. *Biochemistry*, 44(17):6482–6491, 2005.
97. I. M. Kooter, N. Moguilevsky, A. Bollen, N. M. Sijtsma, C. Otto, H. L. Dekker, and R. Wever. Characterization of the asp94 and glu242 mutants in myeloperoxidase, the residues linking the heme group via ester bonds. *Eur J Biochem*, 264(1):211–217, 1999.
98. Liusheng Huang, Grzegorz Wojciechowski, and Paul R Ortiz de Montellano. Role of heme-protein covalent bonds in mammalian peroxidases. protection of the heme by a single engineered heme-protein link in horseradish peroxidase. *J Biol Chem*, 281(28):18983–18988, 2006.
99. W. L. Smith, T. E. Rollins, and D. L. DeWitt. Subcellular localization of prostaglandin forming enzymes using conventional and monoclonal antibodies. *Prog Lipid Res*, 20:103–110, 1981.
100. J. C. Otto and W. L. Smith. The orientation of prostaglandin endoperoxide synthase-1 in the endoplasmic reticulum of transiently transfected cos-1 cells. *Adv Prostaglandin Thromboxane Leukot Res*, 23:29–34, 1995.
101. J. E. Huyett, S. B. Choudhury, D. M. Eichhorn, P. A. Bryngelson, M. J. Maroney, and B. M. Hoffman. Pulsed endor and esem study of [bis(maleonitriledithiolato)nickel](-): An investigation into the ligand electronic structure. *Inorg Chem*, 37(6):1361–1367, 1998.

102. M. Sivaraja, D. B. Goodin, M. Smith, and B. M. Hoffman. Identification by endor of trp191 as the free-radical site in cytochrome c peroxidase compound es. *Science*, 245(4919):738–40, 1989.
103. M. Hamberg and B. Samuelsson. Oxygenation of unsaturated fatty acids by the vesicular gland of sheep. *Journal of Biological Chemistry*, 242(22):5344–54, 1967.
104. L. M. Landino and L. J. Marnett. Mechanism of hydroperoxide reduction by mangano-prostaglandin endoperoxide synthase. *Biochemistry*, 35(8):2637–43, 1996.
105. S. Strieder, K. Schaible, H. J. Scherer, R. Dietz, and H. H. Ruf. Prostaglandin endoperoxide synthase substituted with manganese protoporphyrin ix. formation of a higher oxidation state and its relation to cyclooxygenase reaction. *Journal of Biological Chemistry*, 267(20):13870–8, 1992.
106. R. V. Reddy, M. M. Eldeib, and C. S. Reddy. Inhibition of adenylate cyclase in perfusion mouse palate by secalonic acid d. *J Toxicol Environ Health*, 41(2):175–185, 1994.
107. Graff. Preparation of 15-l-hydroperoxy-5.8.11.13-eicosatetraenoic acid 9215 (hpete). In *Methods in Enzymology*, volume 86, pages 386–392. 1982.
108. J. Putter. *Methods of Enzymatic Analysis*. Verlag Chemie, Weinheim, 1975.
109. J. A. DeGray, G. Lassmann, J. F. Curtis, T. A. Kennedy, L. J. Marnett, T. E. Eling, and R. P. Mason. Spectral analysis of the protein-derived tyrosyl radicals from prostaglandin h synthase. *J Biol Chem*, 267(33):23583–23588. 1992.
110. R. J. Kulmacz, W. A. van der Donk, and A. L. Tsai. Comparison of the properties of prostaglandin h synthase-1 and -2. *Progress in Lipid Research*, 42(5):377–404, 2003.
111. Carol A Rouzer and Lawrence J Marnett. Structural and functional differences between cyclooxygenases: fatty acid oxygenases with a critical role in cell signaling. *Biochem Biophys Res Commun*, 338(1):34–44, 2005.
112. G. Wu, J. L. Vuletich, R. J. Kulmacz, Y. Osawa, and A. L. Tsai. Peroxidase self-inactivation in prostaglandin h synthase-1 pretreated with cyclooxygenase inhibitors or substituted with mangano protoporphyrin ix. *Journal of Biological Chemistry*, 276(23):19879–88, 2001.
113. G. Wu, R. J. Kulmacz, and A. L. Tsai. Cyclooxygenase inactivation kinetics during reaction of prostaglandin h synthase-1 with peroxide. *Biochemistry*, 42(46):13772–7, 2003.

114. R. J. Kulmacz. Prostaglandin h synthase and hydroperoxides: peroxidase reaction and inactivation kinetics. *Archives of Biochemistry & Biophysics*, 249(2):273–85, 1986.
115. J. N. Rodriguez-Lopez, J. Hernandez-Ruiz, F. Garcia-Canovas, R. N. Thorneley, M. Acosta, and M. B. Arnao. The inactivation and catalytic pathways of horseradish peroxidase with m-chloroperoxybenzoic acid. a spectrophotometric and transient kinetic study. *J Biol Chem*, 272(9):5469–76, 1997.
116. T. Spolitak, J. H. Dawson, and D. P. Ballou. Reaction of ferric cytochrome p450cam with peracids: kinetic characterization of intermediates on the reaction pathway. *J Biol Chem*, 280(21):20300–9, 2005.
117. M. E. Hemler and W. E. Lands. Evidence for a peroxide-initiated free radical mechanism of prostaglandin biosynthesis. *J Biol Chem*, 255(13):6253–6261, 1980.
118. R. J. Kulmacz and W. E. Lands. Requirements for hydroperoxide by the cyclooxygenase and peroxidase activities of prostaglandin h synthase. *Prostaglandins*, 25(4):531–40, 1983.
119. J. H. Capdevila, J. D. Morrow, Y. Y. Belosludtsev, D. R. Beauchamp, R. N. DuBois, and J. R. Falck. The catalytic outcomes of the constitutive and the mitogen inducible isoforms of prostaglandin h2 synthase are markedly affected by glutathione and glutathione peroxidase(s). *Biochemistry*, 34(10):3325–37, 1995.
120. R. J. Kulmacz. Regulation of cyclooxygenase catalysis by hydroperoxides. *Biochem Biophys Res Commun*, 338(1):25–33, 2005.
121. R. G. Kurumbail, A. M. Stevens, J. K. Gierse, J. J. McDonald, R. A. Stegeman, J. Y. Pak, D. Gildehaus, J. M. Miyashiro, T. D. Penning, K. Seibert, P. C. Isakson, and W. C. Stallings. Structural basis for selective inhibition of cyclooxygenase-2 by anti-inflammatory agents.[erratum appears in nature 1997 feb 6;385(6616):555]. *Nature*, 384(6610):644–8, 1996.
122. C. Luong, A. Miller, J. Barnett, J. Chow, C. Ramesha, and M. F. Browner. Flexibility of the nsaid binding site in the structure of human cyclooxygenase-2. *Nature Structural Biology*, 3(11):927–33, 1996.
123. M. J. Frisch, G. W. Trucks, H. B. Schlegel, G. E. Scuseria, M. A. Robb, J. R. Cheeseman, J. A. Montgomery, T. Vreven J., K. N. K., J. C. Burant, J. M. Millam, S. S. Iyenga, J. Tomasi, V. Barone, B. Mennucci, M. Cossi, G. Scalmani, N. Rega, G. A. Petersson, H. Nakatsuji, M. Hada, M. Ehara, K. Toyota, R. Fukuda, J. Hasegawa, M. Ishida, T. Nakajima, Y. Honda, O. Kitao, H. Nakai, M. Klene, X. Li, J. E. Knox, H. P. Hratchian, J. B. Cross, V. Bakken, C. Adamo, J. Jaramillo, R. Gomperts, R. E. Stratmann, O. Yazyev, A. J. A., R. Cammi, C. Pomelli, J. W. Ochterski, P. Y. Ayala, K. Morokuma, G. A. Voth,

- P. Salvador, J. J. Dannenberg, V. G. Zakrzewski, S. Dapprich, A. D. Daniels, M. C. Strain, O. Farkas, D. K. Malick, A. D. Rabuck, K. Raghavachari, J. B. Foresman, J. V. Ortiz, Q. Cui, A. G. Babou, S. Clifford, J. Cioslowski, B. B. Stefanov, G. Liu, A. L., P. Piskorz, I. Komaromi, R. L. Martin, D. J. Fox, T. Keith, M. A. Al-Laham, C. Y. Peng, A. Nanayakkara, M. Challacombe, P. M. W. Gill, B. Johnson, W. Chen, M. W. Wong, C. Gonzalez, and Pople J. A. Technical report, Gaussian Inc.,
124. Robert D. Bach, Ming-Der Su, and H. Bernhard Schlegel. Oxidation of amines and sulfides with hydrogen peroxide and alkyl hydrogen peroxide. the nature of the oxygen-transfer step. *J. Am. Chem. Soc.*, 116:5379–5391, 1994.
  125. D. Cremer. *The Chemistry of Peroxides*, chapter 1. Wiley Interscience: New York, 1983.
  126. Ilya G. Denisov, Thomas M. Makris, Stephen G Sligar, and Ilme Schlichting. Structure and chemistry of cytochrome p450. *Chem. Rev.*, 105:2253–2277, 2005.
  127. Nicolai Lehnert, Kiyoshi Fujisawa, and Edward I. Solomon. Electronic structure and reactivity of high-spin iron-alkyl- and pterinperoxo complexes. *Inorganic Chemistry*, 42(2):469–481.
  128. R. I. Cukier and S. A. Seibold. Molecular dynamics simulations of prostaglandin endoperoxide synthase-1. role of water and the mechanism of compound i formation from hydrogen peroxide. *J. Phys. Chem.*, 106:12031, 2002.
  129. J. R. Collins, P. Du, and G. H. Loew. Molecular dynamics simulations of the resting and hydrogen peroxide-bound states of cytochrome c peroxidase. *Biochemistry*, 31(45):11166–11174, 1992.
  130. L. Taylor, M. Menconi, M. H. Leibowitz, and P. Polgar. The effect of ascorbate, hydroperoxides, and bradykinin on prostaglandin production by corneal and lens cells. *Invest Ophthalmol Vis Sci*, 23(3):378–82, 1982.
  131. H. Hussain, L. P. Shornick, V. R. Shannon, J. D. Wilson, C. D. Funk, A. P. Pentland, and M. J. Holtzman. Epidermis contains platelet-type 12-lipoxygenase that is overexpressed in germinal layer keratinocytes in psoriasis. *Am J Physiol*, 266(1 Pt 1):C243–C253, 1994.
  132. R. Brinckmann, K. Schurr, D. Heydeck, T. Rosenbach, G. Kolde, and H. Kuhn. Membrane translocation of 15-lipoxygenase in hematopoietic cells is calcium-dependent and activates the oxygenase activity of the enzyme. *Blood*, 91(1):64–74, 1998.
  133. E. N. Johnson, L. F. Brass, and C. D. Funk. Increased platelet sensitivity to adp in mice lacking platelet-type 12-lipoxygenase. *Proc Natl Acad Sci U S A*, 95(6):3100–3105, 1998.

134. K. Staniek and H. Nohl. Are mitochondria a permanent source of reactive oxygen species? *Biochim Biophys Acta*, 1460(2-3):268–75, 2000.
135. J. St-Pierre, J. A. Buckingham, S. J. Roebuck, and M. D. Brand. Topology of superoxide production from different sites in the mitochondrial electron transport chain. *J Biol Chem*, 277(47):44784–90, 2002.
136. Alexander N P Hiner, Emma L Raven, Roger N F Thorneley, Francisco Garcia-Cnovas, and Jos Neptuno Rodriguez-Lpez. Mechanisms of compound i formation in heme peroxidases. *J Inorg Biochem*, 91(1):27–34, 2002.
137. P. J. O'Brien. Peroxidases. *Chem Biol Interact*, 129(1-2):113–139, 2000.
138. F. Achard, M. Gilbert, C. Benistant, S. Ben Slama, D. L. DeWitt, W. L. Smith, M. Lagarde, S. Adachi, S. Nagano, K. Ishimori, Y. Watanabe, I. Morishima, T. Egawa, T. Kitagawa, and R. Makino. Roles of proximal ligand in heme proteins: replacement of proximal histidine of human myoglobin with cysteine and tyrosine by site-directed mutagenesis as models for p-450, chlooperoxidase, and catalase. *Biochem Biophys Res Commun*, 32(1):241–52, 1993.
139. P. R. Ortiz de Montellano, S.-I. Ozaki, S.L. Newmyer, V. P. Miller, and C hartmann. Plant peroxidases, structure and molecular biology. *Biochemical Society Transactions*, 23:223–227, 1995.
140. Wilfred A van der Donk, Ah-Lim Tsai, and Richard J Kulmacz. The cyclooxygenase reaction mechanism. *Biochemistry*, 41(52):15451–15458, 2002.
141. G. Xiao, W. Chen, and R. J. Kulmacz. Comparison of structural stabilities of prostaglandin h synthase-1 and -2. *Journal of Biological Chemistry*, 273(12):6801–11, 1998.
142. S. Ochoa. Regulation of protein synthesis. *Eur J Cell Biol*, 19(2):95–101, 1979.
143. T. Izard and A. Geerlof. The crystal structure of a novel bacterial adenylyltransferase reveals half of sites reactivity. *EMBO J*, 18(8):2021–2030, 1999.
144. M. F. Hoylaerts, T. Manes, and J. L. Milln. Mammalian alkaline phosphatases are allosteric enzymes. *J Biol Chem*, 272(36):22781–22787, 1997.
145. Victor Guallar, Andrzej A Jarzecki, Richard A Friesner, and Thomas G Spiro. Modeling of ligation-induced helix/loop displacements in myoglobin: toward an understanding of hemoglobin allostery. *J Am Chem Soc*, 128(16):5427–5435, 2006.
146. J. C. Otto and W. L. Smith. The orientation of prostaglandin endoperoxide synthases-1 and -2 in the endoplasmic reticulum. *J Biol Chem*, 269(31):19868–75, 1994.

147. R. J. Kulmacz and W. E. Lands. Stoichiometry and kinetics of the interaction of prostaglandin h synthase with anti-inflammatory agents. *Journal of Biological Chemistry*, 260(23):12572–8, 1985.
148. M. Rosenstock, A. Danon, and G. Rimon. Pghs-2 inhibitors, ns-398 and dup-697, attenuate the inhibition of pghs-1 by aspirin and indomethacin without altering its activity. *Biochim Biophys Acta*, 1440(1):127–137, 1999.
149. M. Rosenstock, A. Danon, M. Rubin, and G. Rimon. Prostaglandin h synthase-2 inhibitors interfere with prostaglandin h synthase-1 inhibition by nonsteroidal anti-inflammatory drugs. *Eur J Pharmacol*, 412(1):101–108, 2001.
150. Tali Burde and Gilad Rimon. On the interaction of specific prostaglandin h synthase-2 inhibitors with prostaglandin h synthase-1. *Eur J Pharmacol*, 453(2-3):167–173, 2002.
151. C. Yuan, C. J. Rieke, G. Rimon, B. A. Wingerd, and W. L. Smith. Partnering between monomers of cyclooxygenase-2 homodimers. *Proc Natl Acad Sci U S A*, 103(16):6142–7, 2006.
152. Jed N Lampe and William M Atkins. Time-resolved fluorescence studies of heterotropic ligand binding to cytochrome p450 3a4. *Biochemistry*, 45(40):12204–12215, 2006.
153. Andrea Bellelli, Maurizio Brunori, Adriana Erica Miele, Gianna Panetta, and Beatrice Vallone. The allosteric properties of hemoglobin: insights from natural and site directed mutants. *Curr Protein Pept Sci*, 7(1):17–45, 2006.
154. C. H Kang, S. Ferguson-Miller, and E. Margoliash. Steady state kinetics and binding of eukaryotic cytochromes c with yeast cytochrome c peroxidase. *J Biol Chem*, 252(3):919–926, 1977.
155. R. Karthein, W. Nastainczyk, and H. H. Ruf. Epr study of ferric native prostaglandin h synthase and its ferrous no derivative. *European Journal of Biochemistry*, 166(1):173–80, 1987.
156. T. Shimokawa, R. J. Kulmacz, D. L. DeWitt, and W. L. Smith. Tyrosine 385 of prostaglandin endoperoxide synthase is required for cyclooxygenase catalysis. *J Biol Chem*, 265(33):20073–6, 1990.
157. Michael R Gunther, Bradley E Sturgeon, and Ronald P Mason. Nitric oxide trapping of the tyrosyl radical-chemistry and biochemistry. *Toxicology*, 177(1):1–9, 2002.
158. C. E. Rogge, B. Ho, W. Liu, R. J. Kulmacz, and A. L. Tsai. Role of tyr348 in tyr385 radical dynamics and cyclooxygenase inhibitor interactions in prostaglandin h synthase-2. *Biochemistry*, 45(2):523–32, 2006.

159. C. E. Rogge, W. Liu, G. Wu, L. H. Wang, R. J. Kulmacz, and A. L. Tsai. Identification of tyr504 as an alternative tyrosyl radical site in human prostaglandin h synthase-2. *Biochemistry*, 43(6):1560–8, 2004.
160. T. Smith, J. Leippardt, and D. DeWitt. Purification and characterization of the human recombinant histidine-tagged prostaglandin endoperoxide h synthases-1 and -2. *Arch Biochem Biophys*, 375(1):195–200, 2000.
161. Dimitri A Svistunenko. Reaction of haem containing proteins and enzymes with hydroperoxides: the radical view. *Biochim Biophys Acta*, 1707(1):127–155, 2005.
162. S. O. Kelley and J. K. Barton. Radical migration through the dna helix: chemistry at a distance. *Met Ions Biol Syst*, 36:211–249, 1999.
163. P. K. Witting and A. G. Mauk. Reaction of human myoglobin and h<sub>2</sub>o<sub>2</sub>. electron transfer between tyrosine 103 phenoxyl radical and cysteine 110 yields a protein-thiyl radical. *J Biol Chem*, 276(19):16540–16547, 2001.
164. Ying Yu, Jinjin Fan, Xin-Sheng Chen, Dairong Wang, Andres J Klein-Szanto, Robert L Campbell, Garret A FitzGerald, and Colin D Funk. Genetic model of selective cox2 inhibition reveals novel heterodimer signaling. *Nat Med*, 12(6):699–704, 2006.

MICHIGAN STATE UNIVERSITY LIBRARIES



3 1293 02845 8978